2014-01-01

Geophysical Model Of The Cu-Mo Porphyry Ore Deposit At Copper Flat Mine, Hillsboro, Sierra County, New Mexico

Adrian Emmanuel Gutierrez
University of Texas at El Paso, aegutierrez@miners.utep.edu

GEOPHYSICAL MODEL OF THE CU-MO PORPHYRY ORE DEPOSIT AT COPPER FLAT MINE, HILLSBORO, SIERRA COUNTY, NEW MEXICO

ADRIÁN EMMANUEL GUTIÉRREZ GUTIÉRREZ

Department of Geological Sciences

APPROVED:

Philip C. Goodell, Ph.D., Chair

Rodrigo A. Romero, Ph.D.

Aaron A. Velasco, Ph.D.

Bess Sirmon-Taylor, Ph.D.
Interim Dean of the Graduate School

Dedication

I would like to dedicate this thesis to my mother for always being there for me.

GEOPHYSICAL MODEL OF THE CU-MO PORPHYRY ORE DEPOSIT AT COPPER FLAT MINE, HILLSBORO, SIERRA COUNTY, NEW MEXICO

by

ADRIÁN EMMANUEL GUTIÉRREZ GUTIÉRREZ, B.S.

THESIS

Presented to the Faculty of the Graduate School of

The University of Texas at El Paso

in Partial Fulfillment

of the Requirements

for the Degree of

MASTER OF SCIENCE

Department of Geological Sciences

THE UNIVERSITY OF TEXAS AT EL PASO

August 2014

Acknowledgements

I would like to thank Victor "Yogi" Avila and Guillermo Vargas for all their help with the acquisition of data, without your help this thesis would not be possible. To Alex, Christine, Oscar, Ray, and the rest crew at Copper Flat for all their help and friendship. To Martin Sandoval for all his help during this past year, without your help I would not have graduated. Teira Solis, for all your help as a guru in illustration. To Christine Sanchez for being my editor and drinking buddy all this year, thanks. To Ibrahim, Humberto, and everyone else that has made these years as fun as they have been. To Laura for introducing me to the world geophysics, even if they say it is the dark side, I really like it. To Dr. Romero who jumped in on short notice to be part of my committee. To Dr. Velasco and Dr. Chavez for their input in the project. Finally, to Phil Goodell for all his support and mentorship over the years, especially for introducing me to the world of mining, which is my professional path, thank you, you got an A!

Abstract

A 3D gravity model of the Copper Flat Mine was performed as part of the exploration of new resources in at the mine. The project is located in the Las Animas Mining District in Sierra County, New Mexico. The mine has been producing ore since 1877 and is currently owned by the New Mexico Copper Corporation, which plans o bringing the closed copper mine back into production with innovation and a sustainable approach to mining development. The Project is located on the Eastern side of the Arizona-Sonora-New Mexico porphyry copper Belt of Cretaceous age. Copper Flat is predominantly a Cretaceous age stratovolcano composed mostly of quartz monzonite. The quartz monzonite was intruded by a block of andesite alter which a series of latite dikes creating veining along the topography where the majority of the deposit. The Copper Flat deposit is mineralized along a breccia pipe where the breccia is the result of auto-brecciation due to the pore pressure. There have been a number of geophysical studies conducted at the site. The most recent survey was a gravity profile on the area. The purpose of the new study is the reinterpretation of the IP Survey and emphasizes the practical use of the gravity geophysical method in evaluating the validity of the previous survey results. The primary method used to identify the deposit is gravity in which four Talwani models were created in order to created a 3D model of the ore body. The Talwani models have numerical integration approaches that were used to divide every model into polygons. The profiles were sectioned into polygons; each polygon was assigning a specific density depending on the body being drawn. Three different gridding techniques with three different filtering methods were used producing ten maps prior to the modeling, these maps were created to establish the best map to fit the models. The calculation of the polygons used an exact formula instead of the numerical integration of the profile made with a Talwani approach. A least squared comparison between the calculated and observed gravity is used to determine the best fitting gravity vectors and the best susceptibility for the assemblage of polygonal prisms. The survey is expected to identify the geophysical anomalies found at the Copper Flat deposit in order to identify the

alteration that surrounds that part of the ore body. The understanding of the anomalies needs to be reevaluated in order to have a sharper model of Copper Flat, and to understand the relations of the different structures that shaped this copper porphyry deposit.

Table of Contents

List of Figures

List of Illustrations

List of Tables

Chapter 1: Introduction

A geophysical survey on the Copper Flat Mine (CF) near Hillsboro, New Mexico, was conducted through the summer of 2012 on site. The survey consisted of over one hundred gravity points collected to create geophysical models of the copper/molybdenum deposit of the mine. These models were created to further understand the present nature of the deposit as well as helping to pinpoint any anomalies that might exist within the deposit. The purpose of this study is to create a new geophysical model using gravity data that can be compared with previous geophysical models done in the area in order to understand the anomalies found in the deposit. The project is located in south central New Mexico near the town of Hillsboro.

1.1 LOCATION

The Copper Flat mine is located in Sierra County, New Mexico, 30 kilometers southwest the town of Truth or Consequences, NM. It is 24 kilometers west of the Rio Grande River and about 185 kilometers north from El Paso, Texas by road and 250 kilometers south from Albuquerque, NM, as illustrated in figure 1.1. The Copper Flat property is referenced as sitting on latitude 32°57'40"N and 107°32'08"W. The terrain is composed of a central valley surrounded by a steep mountainous relief including the Animas, Black, and Empire peaks (Quantec, 2011). The Elephant Butte and Caballo lakes are east of the property along Interstate 25, which is the main highway to get to the property from any major city. Access to the mine site from Truth or Consequences, NM, is by 39 kilometers of paved highway, Interstate 25 and New Mexico Route 152, and 5 kilometers of weather gravel road. This gravel road is historically called the "Gold Dust" dirt road.

As a location reference point for the property, one is located in the Hillsboro 15' USGS quadrangle, North of the New Mexico highway 152. The communities of Hillsboro and Caballo are located at the edges of the property. The terrain and major topographical features are shown in figure 1.2.

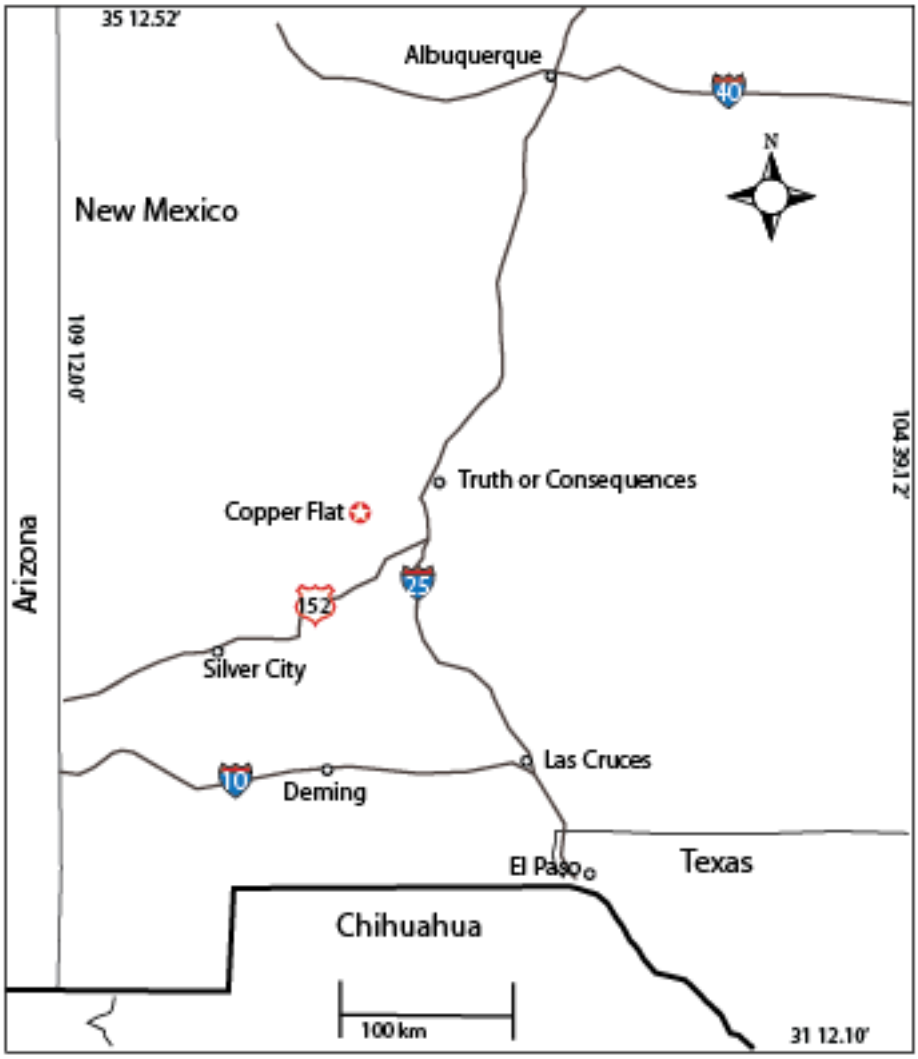

Figure 1.1: Location Map of Copper Flat.

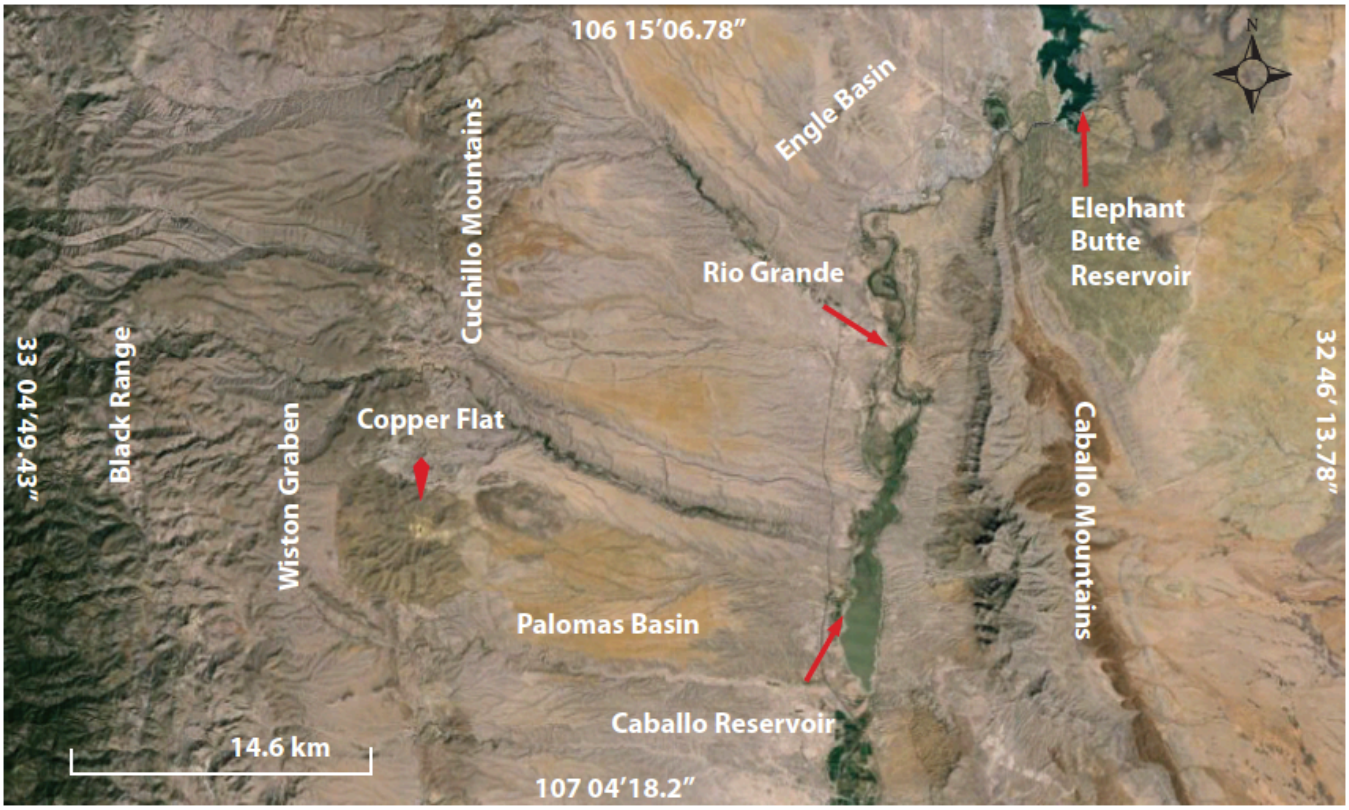

Figure 1.2: Topography of the Copper Flat Region (satellite image).

1.2 History of the Copper Flat Mine

The Hillsboro Mining District, part of the Animas Mining District, has been active since 1877 when the first recorded production occurred. There has been gold and silver production valued at US$8.5 million, primarily from underground and placer operations in the area (Dunn, 1984). The town Gold Dust was founded in 1881 as a base camp for prospectors in the area. A copper deposit was recognized early, giving place to the small-scale Stenberg copper mine (Harley, 1934). The copper mine was operated between 1911 and 1931; other mining works occurred after the closure of Stenberg and all the small-scale mining ceased in 1941 (Segerstrom et al., 1975).

Prior to 1952, various owners held the Copper Flat property. Newmont Mining Company explored the district for copper in 1952 followed by Inspiration Development Company, Bear Creek

Mining Company and Hilltop Mining (Dunn, 1982). These three companies held the property from 1952 to 1974. This was considered to be the evaluation period of the property (Dunn et al., 1992).

Illustration 1.1: Copper Flat during the Quintana days in 1983. Photography historical archive of Copper Flat owned by NMCC.

In 1974 Quintana Minerals Corporation acquired the property from the Inspiration Development Company. Starting in 1974 until 1982, Quintana Minerals Corporation carried out an exploration, pre-feasibility, and feasibility campaign at the site. Quintana Minerals Corporation mined the property for three months in 1982 producing 3357 tons of copper, 64374 grams of gold, and 1.5 tons of silver (Raugust, 2003). Due to a significant drop on copper prices, Quintana ceased the operation on the property. The mining claims were leased to Hydro Resources in 1987, which held the rights until 1989 when Rio Gold held the property. Rio Gold created Copper Flat Mining Corporation and in association with Hydro Resources formed the Cooper Flat Partnership, which held all rights until 1993. Gold

Express acquired Copper Flat from Rio Gold with the intent of placing the property into production employing the 1982 design parameter (SRK, 2010).

In 1994, Alta Gold auctioned the project and were the owners until 1999 when the company filed for bankruptcy. Afterwards, Hydro Resources in association with Copper Flat and GCM companies purchased the property along with all rights for it in 2001. Later, Themac Resources Company and the New Mexico Copper Corporation (NMCC) acquired an exclusive option over the Copper Flat property in 2009. During the summers of 2010 and 2011, a drilling campaign for the pre-feasibility of the mine was conducted. Subsequently, in May 2011 NMCC acquired 100% of the Copper Flat project. In February 2012 a final exploration and drilling program was announced (Themac, 2012). Due to the dropped of prices in copper the mining project has been put on hold since the summer of 2013 (Themac, 2013).

Chapter 2: Geology of Copper Flat

The mine is located in southern New Mexico along the west edge of the Rio Grande Rift. This rift has a physiographic expression called the Rio Grande Valley. The rifting occurs from southern Colorado all the way the northern part of Mexico. The stratigraphy of the area is noted in the uplift of the Rio Grande Valley. Copper Flat is in the central mountains province in the transition zone between the Colorado Plateau and the Basin and Range province (Titley, 1982).

2.1 REGIONAL GEOLOGY

Regionally, Copper Flat lies on the edge of the Cretaceous aged, Arizona-Sonora-New Mexico porphyry copper belt (McLemore et al., 2000). There is a significant difference on the age of each deposit: Copper Flat (74.93 m.y.), Chino (59 m.y.), and Tyrone (56.2 m.y.). Figure 2.1 shows a distinct lineament known as the Santa Rita lineament in southwestern New Mexico and continuing into adjacent Arizona. Copper Flat is one of the oldest and known porphyry deposits in the Southwest, and is the easternmost of such deposits in the United States according to Hedlund, 1974.

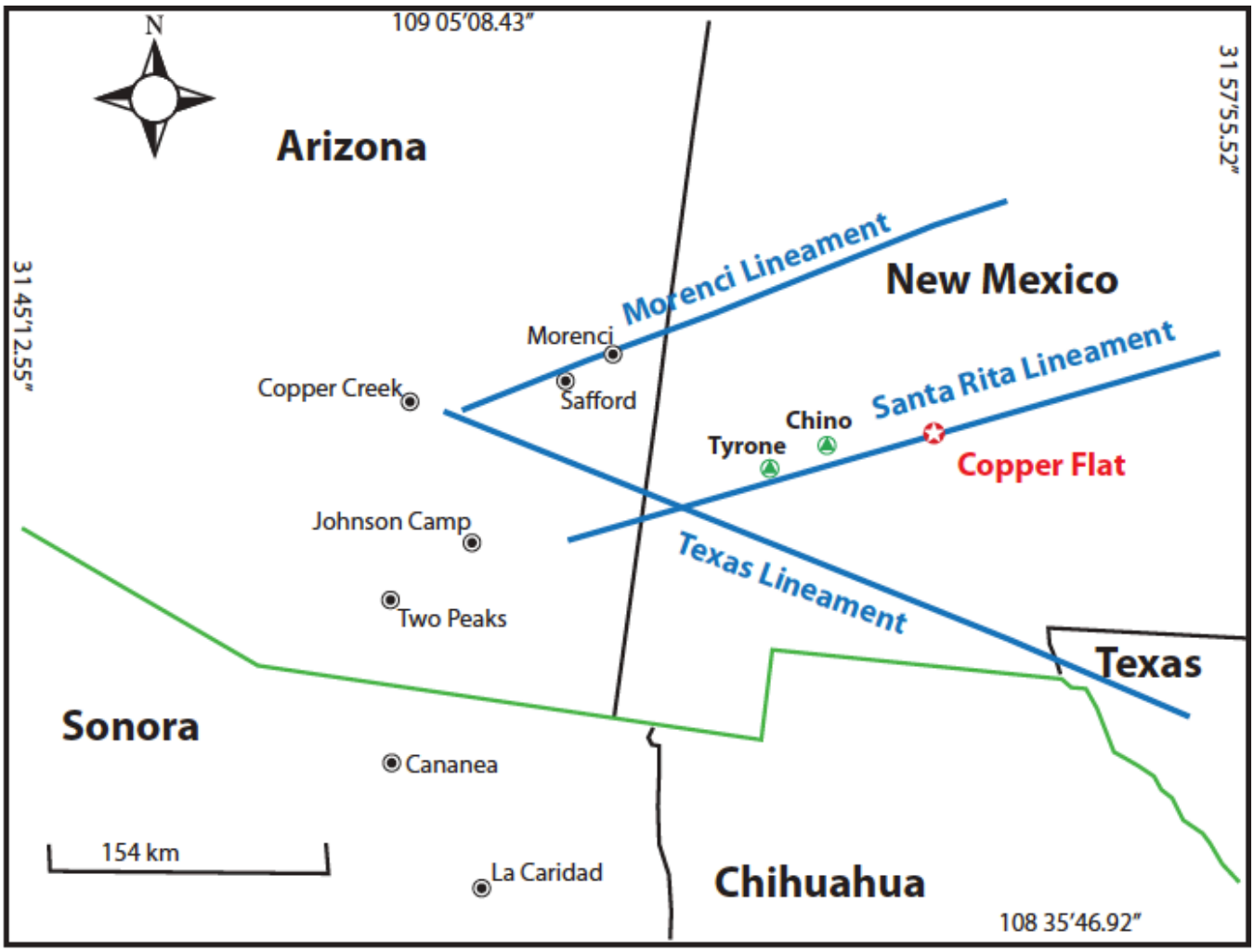

Figure 2.1: Santa Rita lineament figure modified from McLemore et. al., 2001.

Mineral deposits in this region lie on the North American creaton within about 350 km of the Laramide western margin of the craton (Titley, 1994). The three major physiographic regions, seen in Figure 2.2, known in the area are the Basin and Range Province, Rio Grande Rift, and the Colorado Plateau. The mineral deposits in the area have evolved above a combination of granite, volcanic, and clastic Proterozoic basement section of Paleozoic platform strata and a Mesozoic section dominated by clastic and volcanic rocks of local derivation (Titley, 1982).

The Cretaceous in this area was marked by the Laramide orogeny, being active 75-60 millions yeas ago. This orogeny is normally associated with all the porphyry copper deposits in the Santa Rita

lineament, the copper porphyry deposits being a product of magmas generated during the subduction of the Farallon plate beneath the American Plate. Copper Flat is located on the Sonora slab segment of the Farallon plate (Keith et al., 1995). The orogenic activity during the Cretaceous was followed by volcanism that resulted in the formation of calderas in the area and the deposition of ash-flow tuffs where Copper Flat is located that has no relation with the mineral deposit. The opening of the Rio Grande rift is often associated with volcanic and deformation of southern New Mexico (Clarkson, 1984). The Regional geology of the deposit can be seen in the Figure 2.2 below.

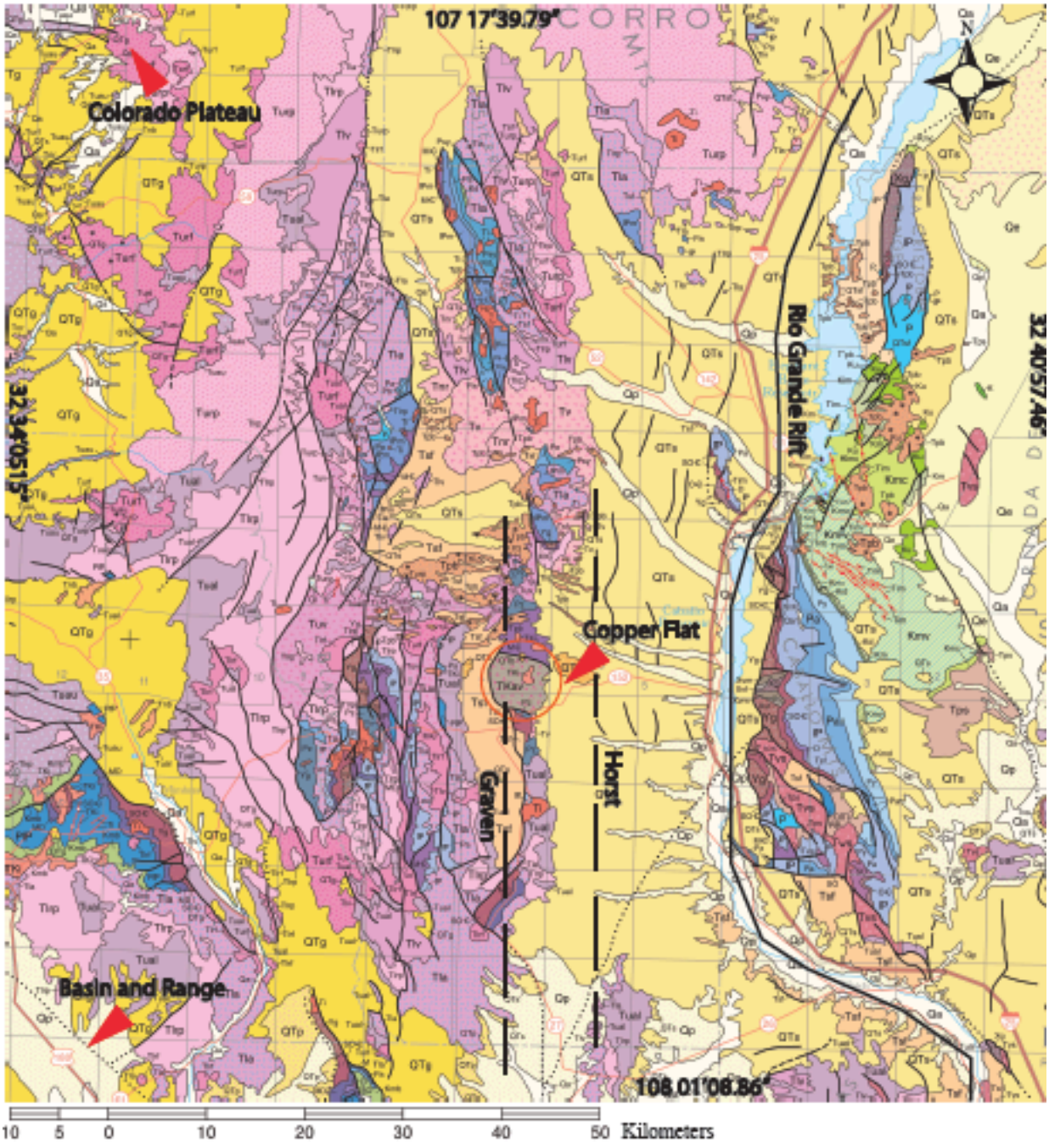

Figure 2.2: New Mexico Geologic Map modified from NMBGMR 2006.

2.2 LOCAL GEOLOGY

Copper Flat is located in the Animas Mining District also known as the Hillsboro Mining District. The geology of the district was predominantly formed of Cretaceous andesite flows, breccias, and volcanoclastic rocks that were erupted from an andesite volcano (McLemore, 2001). On the western edge of the Rio Grande Rift, a low range formed by the Animas Hills horst is present. This horst has faults that bound it and are related to the tectonic activity of the Miocene-age Rio Grande rift (Dunn, 1982). The Copper Flat volcanic/intrusive complex has been interpreted as an eroded strato-volcano based on the presence of agglomerates and flow band textures in some of the andesites (Richards, 2003). The geology of the deposit can be seen in Figure 2.3. Although, the Rio Grande Rift is close to Copper Flat there is no evidence that can relate the two; therefore, the ore was deposited prior to rifting which in turn did not affect the composition of the ore.

In the Animas Hills there is an andesite that has been eroded to a topographic low; the andesite is a fault contact with the Santa Fe Group sediments deposited in the ancestral Rio Grande Rift (SRK, 2010). Drilling in the area indicates that the Santa Fe Group sediments in the area are at least 610 meters thick (Dunn, 1982). The remainder of the terrain is marked mainly by vertical displacement along faulting; there is no data regarding the thickness of the andesite, however, estimation suggests the thickness to be at least 900 meters from the surface. The thickness of the andesite and the radial fault pattern suggest a deeply eroded Cretaceous age complex (Dunn, 1982).

Two quartz monzonite stocks, the Warm Springs Quartz Monzonite (WSQM) and the Copper Flat Quartz Monzonite (CFQM) intruded the volcanic complex at the Animas Mining District. The CFQM stock has been dated by argon 40-argon 39 techniques to be 74.93 million years old (McLemore, 2000). At least 30 dikes radiate out from the quartz monzonite as seen in Figure 2.3. The WSQM was emplaced after the period of mineralization, but is related to other igneous rocks near the deposit and was dated to be 73.4 million years old (Hedlund, 1974).

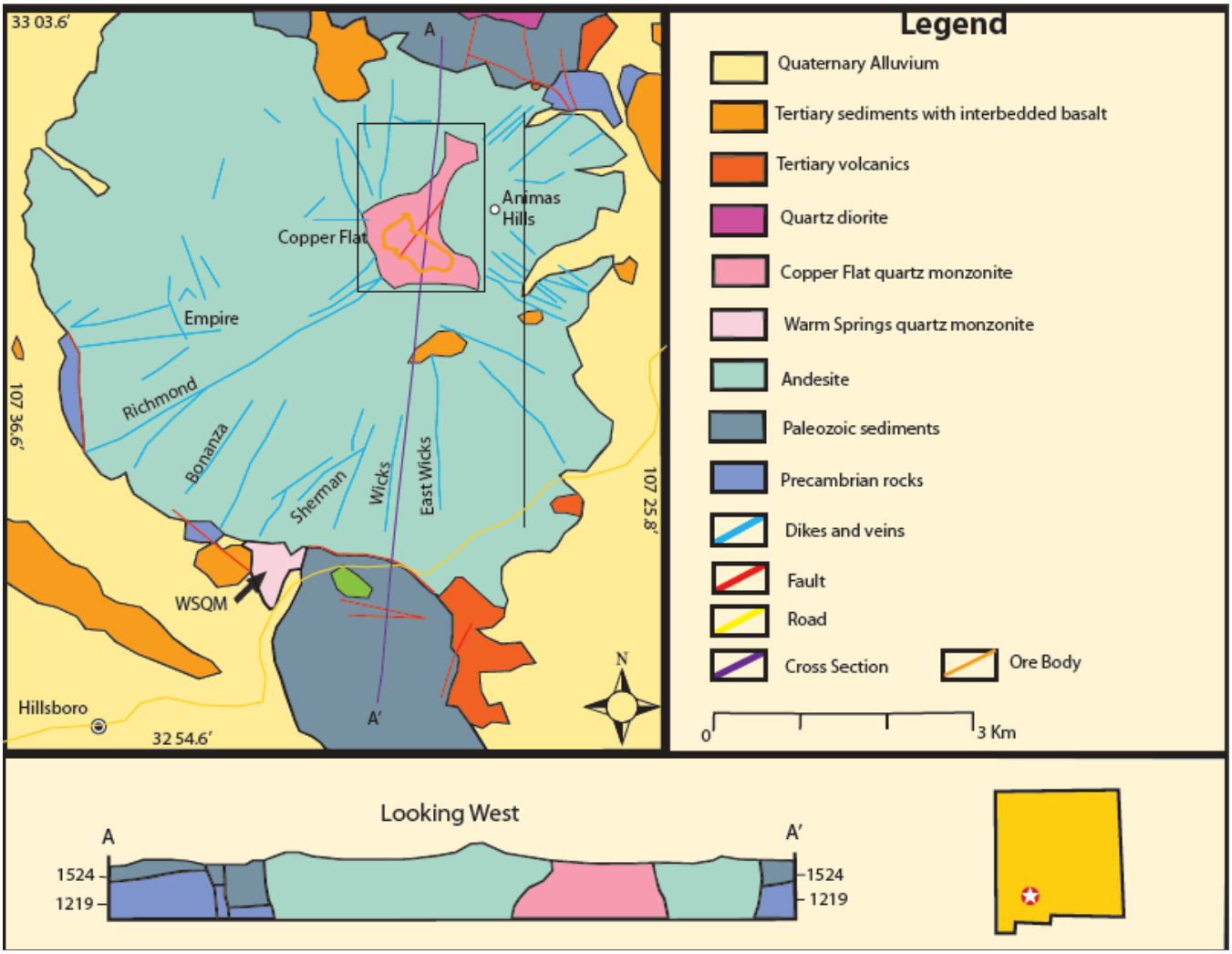

Figure 2.3: Generalized geologic map of Hillsboro mining district modified from McLemore, 2000.

The dikes are normally oriented NE and NW and represent a late stage differentiation of the CFQM stock; these dikes are as much as 38 meters wide to 1,575m long (Hedlund, 1985). The coloration of such dikes tends to be from grey to tan, typically porphyritic and holocrystalline. The most common dikes in the area are aphanitic latite and porphyritic latite with large orthoclase phenocrysts. The dikes contain quartz, potassium feldspar, plagioclase, biotite, magnetite, hornblend, pyrite, apatite, and rutile (McLemore, 2000). The latite dikes, unlike the andesite and CFQM that were cut and altered by them, do not alter the WSQM as seen in figure 2.3. The fault-bounded andesites of the district sharply define the Copper Flat volcanic/intrusive complex against the Santa Fe Group Quaternary sediments (SRK, 2010).

2.3 GEOLOGY OF THE DEPOSIT

The copper deposit is restricted entirely to a small quartz monzonite stock (CFQM) that has intruded andesitic rocks (Quintana, 1980). As seen in Figure 3.2 the deposit is in a small alluvium covered depression, Copper Flat, in the center of the stock and includes a large body of breccia only a portion of which displays definite rotated fragments (Dunn, 1984). The alluvium over the deposit is from 2-10 meters thick, covering the majority of the breccia pipe. The specific geology of the deposit plays an important part in the geophysical response expected for each rock. Table 2.1 displays the geology of the deposit. The information of the rocks is taken from Fowler et. al (1982), Hedlund (1974), McLemore et.al. (2000), and SRK (2001). The illustrations show below are part of the core photo log for the Copper Flat Drilling Project.

Table 2.1: Generalized geology of the deposit

Name	Age	Mineralogy	Gravity Response
Quartz Breccia	73.4	quartz, biotite, potassium feldspar, pyrite and chalcopyrite	Negative
Feldspar Breccia	73.4	quartz, biotite, potassium feldspar, pyrite and chalcopyrite	Negative
Biotite Breccia	73.4	quartz, biotite, potassium feldspar, pyrite, chalcopyrite, magnetite, molybdenite, fluorite, anhydrite, and calcite	Negative
Crackle Breccia	73.4	quartz, biotite, potassium feldspar, pyrite and chalcopyrite	Negative
Warm Springs Qtz Monzonite	73.4	potassium feldspar, plagioclase, hornblende, biotite	Positive/Negative
Copper Flat Quartz Monzonite	74.93	potassium feldspar, plagioclase, hornblende, biotite, magnetite apatite, zircon and rutile	Positive/Negative
Latite Dikes	75.1	quartz, potassium feldspar, plagioclase, biotite, magnetite, hornblend, pyrite, apatite, and rutile	Positive
Andesite	75.4	plagioclase, orthoclase, hornblende, and magnetite	Positive

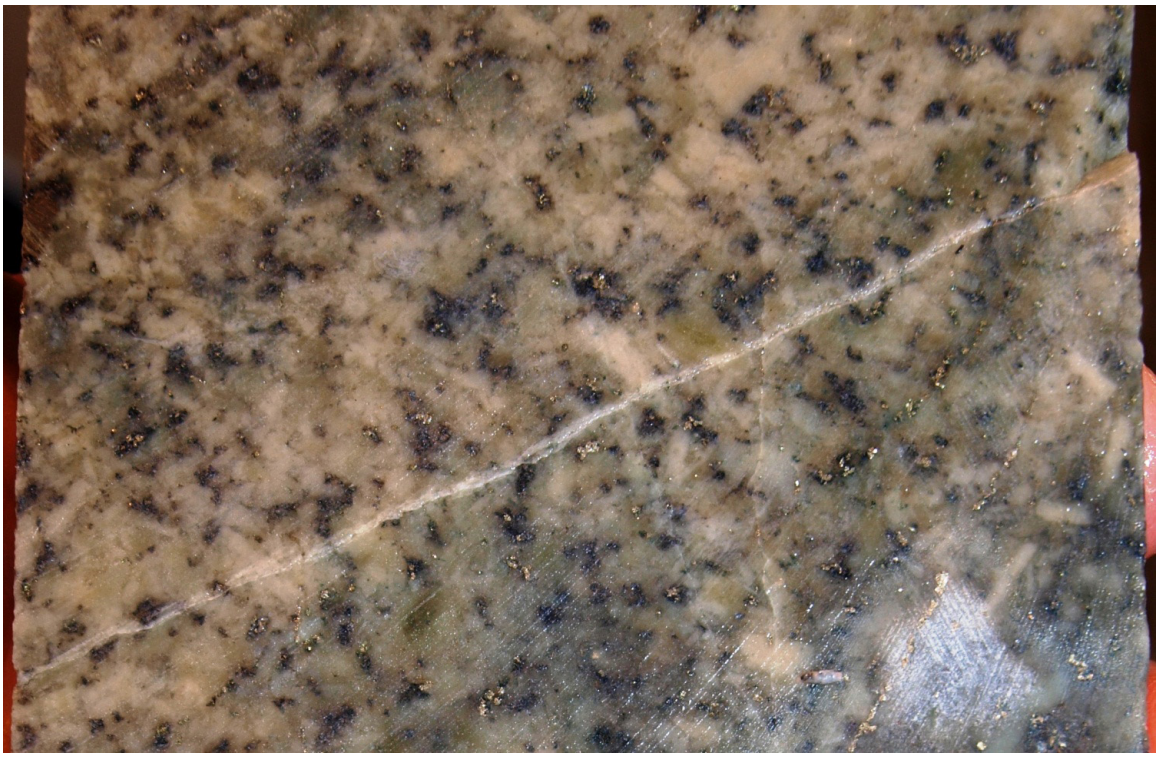

Illustration 2.1: Copper Flat Quartz Monzonite from drill hole CF-11-03.

The andesite is composed of volcanic flows, flow breccias and volcanoclastic rocks (Verdel, 2001). It is composed of plagioclase, orthoclase, hornblende, and magnetite with lesser amounts of biotite, clinopyroxene, quartz, rutile, apatite and zircon (McLemore, 1999). The andesite also contains epidote and is propylitically altered near the CFQM and the polymetallic veins (Fowler, 1982). The andesite at the southern part of the Copper Flat quartz monzonite is a shallow intrusive phase and is coarse-grained. Magnetite is a common association with the mafic phenocrysts, and accessory apatite is found in nearly every thin section (Dunn, 1984). The andesite is on the outward side of the copper deposit there will be no further discussion of it.

Illustration 2.2: Magnetite present in quartz monzonite from CF-11-07.

The majority of the CFQM stock is porphyritic, with phenocrysts that can be as large as 5 centimeters long. The composition of the rock is almost equally proportionate between andesine and orthoclase; there are zones in which feldspar can be 50% of the rock composition. Andesine occurs as small phenocrysts. Sphene crystals are present in the CFQM (Dunn, 1984). Mafic minerals in the deposit are normally associated with magnetite having apatite as an accessory mineral.

Chapter 3: Relevant Geology of the Deposit

3.1 BRECCIAS

A breccia is a coarse-grained clastic rock, composed of angular broken rock fragments held together by a mineral cement of fine-grained matrix originated as a result of explosive igneous processes, collapse of rock material, or faulting (AGI, 1987). The breccias are interpreted as the result of auto-brecciation due to pore pressure created by hydrothermal fluids that were greater than the confining pressure. That is, part of the occurrence of the crackle breccia is at the edges of the mineralized zone where the energy dissipated, and three types of breccias (quartz, feldspar and biotite) are defined by their main phases. Rotation of the brecciated clasts, which is commonly incomplete, makes those parts not necessarily true breccias by definition. Most of the literature about Copper Flat mentions only two types of breccia. These two sub-divisions do not correspond to the divisions between the breccia with rotated and non-rotated fragments (Dunn, 1984). During the summer of 2011 the geologist of the project decided to divide the breccia into four members. The four different breccias in the deposit according to these divisions are: crackle, biotite, feldspar, and quartz breccias.

The ore body is 366 meters long, 183 meters wide, and extends at least 518 meters below the surface (Quintana, 1980). The majority of the ore body is covered by alluvium, which makes for a difficult determination of what the mineralization is from the surface. The richest mineralization of the ore body is surrounding the CFQM, while the eastern part of the Quartz-Feldspar breccia sits outside the main mineralized zone. The breccias are important to the mine project since it hosts one-half of the copper that will be produced. On the other hand, it only comprises of about one-third of the total resource tonnage (Dunn, 1984). The copper mineralization that is only found on the CFQM stock consists almost entirely of chalcopyrite (Quintana, 1980).

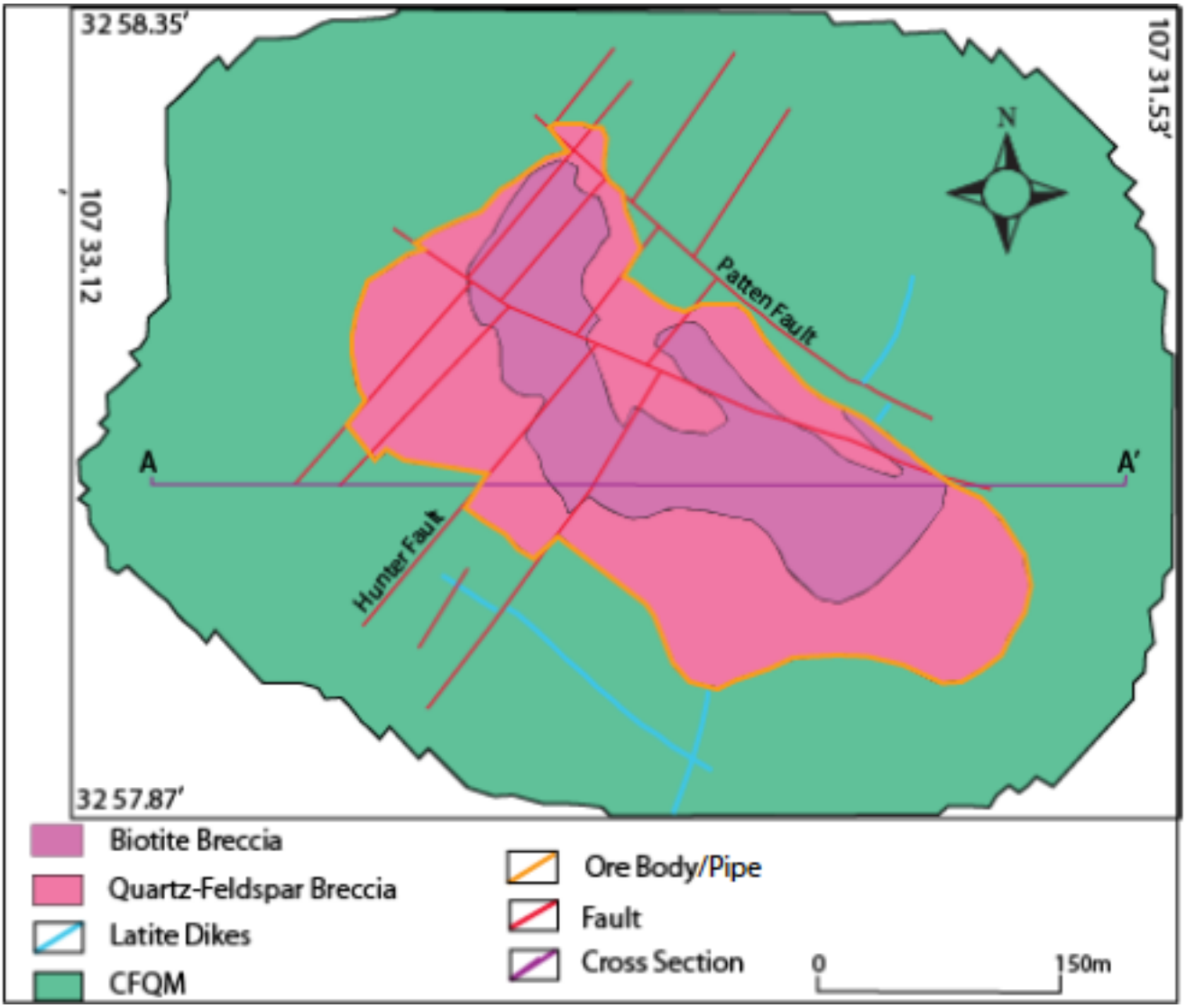

Figure 3.1: Brecciation zone diagram modified from Dunn, 1984.

The ore body zone within the CFQM features numerous, randomly oriented, irregular veins that are thicker and coarser-grained than the narrow fractured-controlled veinlets in the surrounding stock (SRK, 2010). The northwestern Biotite Breccia section is a hydrothermal matrix that cemented some angular rotated fragments. The extent of the breccia with rotated fragments is a rough determination coming from the drill core sample data (Dunn, 1984). The extent of the two breccias can be seen in Figure 3.1.

Figure 3.1 has a cross-section (A-A') present in the Figure 3.2. The importance of Figure 3.2 is that it shows the extent of the ore deposit below the surface. This cross-section is at the south of the rotated fragment zone. Part of the ore body is covered by the overlying CFQM but there are some zones in which the breccia reaches the surface beneath the alluvium. The figure below suggests that the top of the pipe/ore body has not been uncovered by erosion (Dunn, 1984).

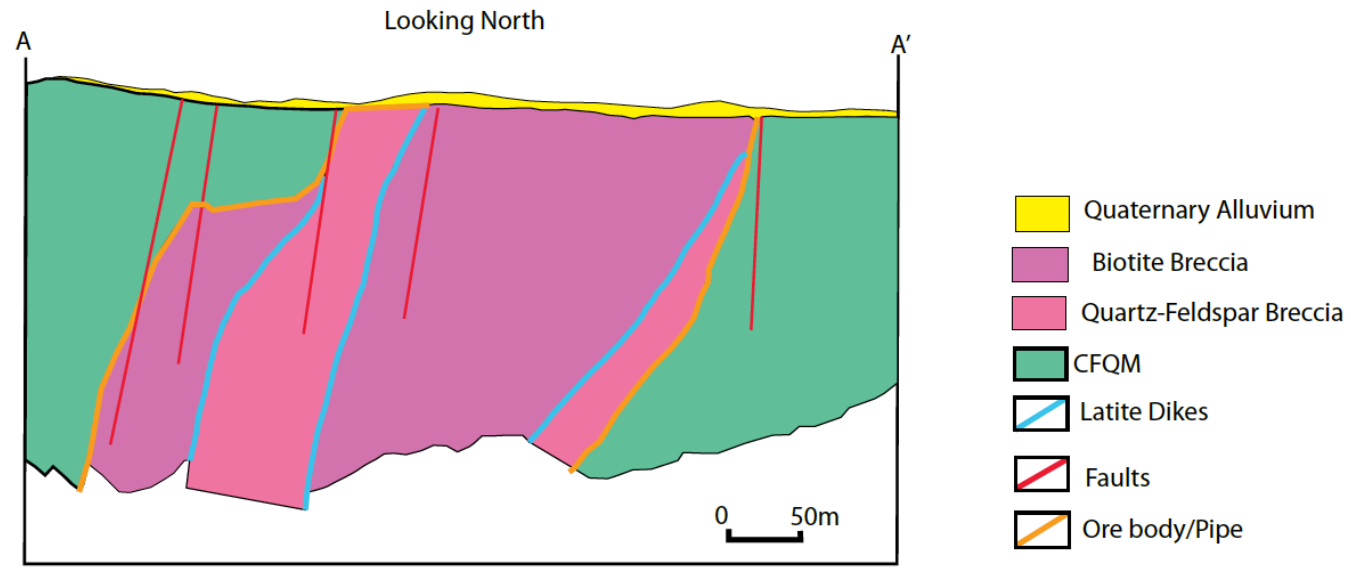

Figure 3.2: Crossection A-A' modified from Dunn 1984.

The post-mineral rotation of the pipe has caused a steep plunge at the southwest part of the breccia. A limited number of latitudes taken on the andesites show 20° dips to the east (Dunn, 1982). Taking these dip measurements into consideration, the altitudes could be the result of movement of the breccia from a vertical position. The majority of the fragments on the breccia are mineralized quartz monzonite. Some latite dikes can be projected into the breccia zone making them abundant in the matrix of the breccia where the rays of the dikes are exposed in the quartz monzonite. There is andesite present in the breccia, although, it is only confined to areas where there was a partial contact with intrusive CFQM. No other rock types are recognized as fragments in the breccia (Dunn, 1984).

The main minerals in the breccia are quartz, biotite, potassium feldspar, pyrite and chalcopyrite. The breccia has other mineral such as magnetite, molybdenite, fluorite, anhydrite, and calcite. Apatite is a common accessory mineral. No tourmaline is found in the breccia matrix or in the surrounding veins (McLemore, 2000). Much of the quartz-feldspar matrix has a pegmatite texture (SRK, 2010). The breccia fragments are rimmed with either biotite or potassium feldspar and the quartz and sulfide minerals have generally formed in the center of the matrix (Dunn, 1984).

The biotite breccia, Illustration 3.1, is the most important rock in the deposit. For one, it is associated with high-grade chalcopyrite mineralization. Second, the biotite crystals have grown nearly perpendicular to the breccia-arrangement contact. Third, magnetite commonly occurrs in this type and is associated with the changes of magnetization of the deposit.

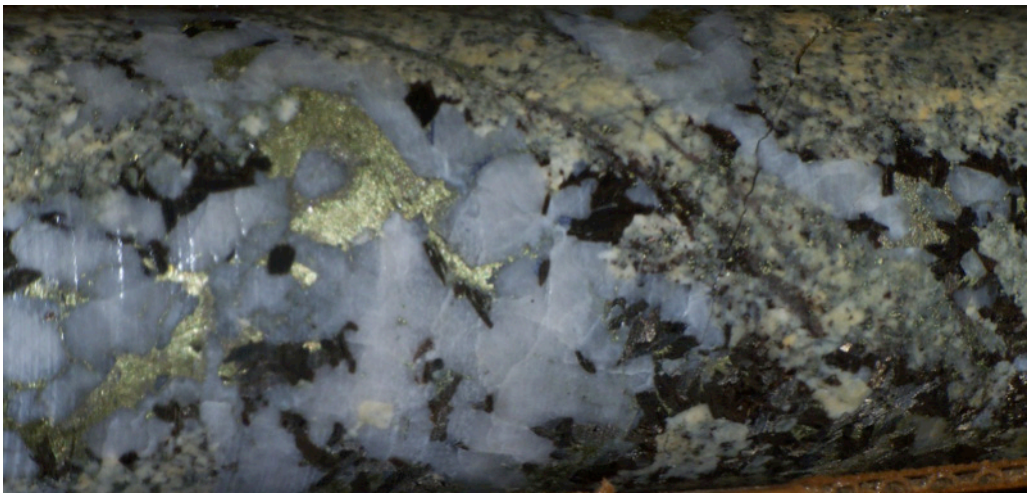

Illustration 3.1: Biotite breccia photo from core CF-11-01, 8 centimeter is the diameter of the core on the y-axis.

The quartz and feldspar breccia types, Illustration 3.2, are related to each other, however, in previous documentation they are not considered separate but one breccia called the quartz-feldspar breccia. The separation or identification of these two divisions is based on the ratio of quartz versus

feldspar content found in the rock. The grades in these two divisions are more variable than in the other breccia divisions. Chalcopyrite is positively related to the quartz content in the breccia, but is found in less quantity than in the biotite breccia division. Most of the copper content is disseminated in the biotite breccia. The matrix in the eastern waste portion of the breccia consists primarily of pegmatitic potassium feldspar with subordinate amounts of quartz and pyrite and only rarely chalcopyrite (Dunn, 1984).

Illustration 3.2: Quartz/Feldspar breccia from core CF-11-11, 8 centimeters is the diameter of the core on the x-axis.

The crackle breccia division, Illustration 3.3, as its name suggests, is easily breakable. This breccia normally has a large occurrence of thin veins and fractures, making it the weakest of the types within the deposit. This sub-division of the breccia has limited documentation and discussion. The identification of this type of breccia was along the fault gauge zone of the core.

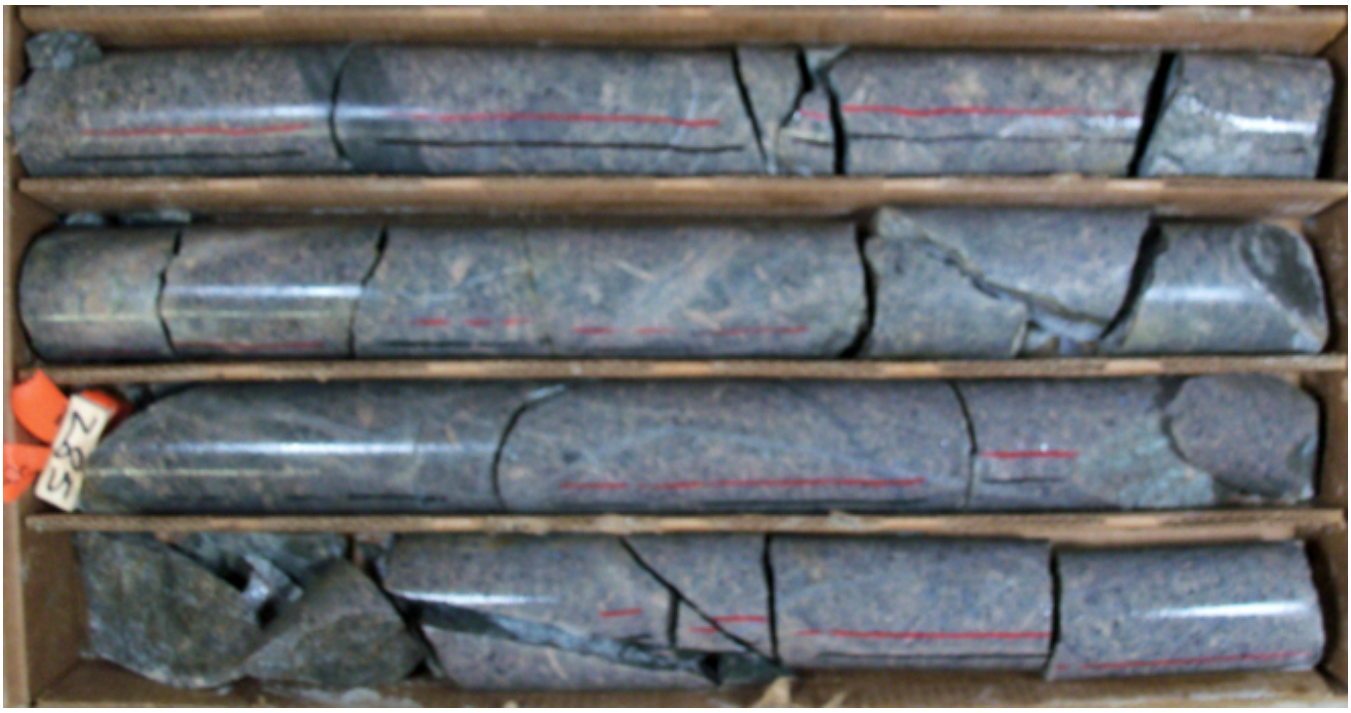

Illustration 3.3: Crackle breccia from core CF-11-05, 8 centimeters is the diameter of the core in the y-axis.

3.2 ALTERATION IN COPPER FLAT

Copper mineralization occurs within a potassic alteration zone with extensive outer phyllic, argillic and propylitic alteration zones (Quantec, 2010). Hydrothermal alteration assemblages are significant in the Animas Mining District. Taking this into consideration, the model for hydrothermal alteration in porphyry copper deposits developed by Lowell and Guilbert (1970) can apply to Copper Flat. A modified version of this model is presented as Figure 3.3. In this model, alteration progresses outward from a central core of potassic alteration to a phyllic alteration zone, then to an argillic zone, and finally to a propylitic alteration zone along the periphery (Verdel, 2001). Three types of alteration

mineral assemblages are recognized in the Copper Flat porphyry copper deposit: biotite-potassic, potassic, and sericitic alteration (Fowler, 1982).

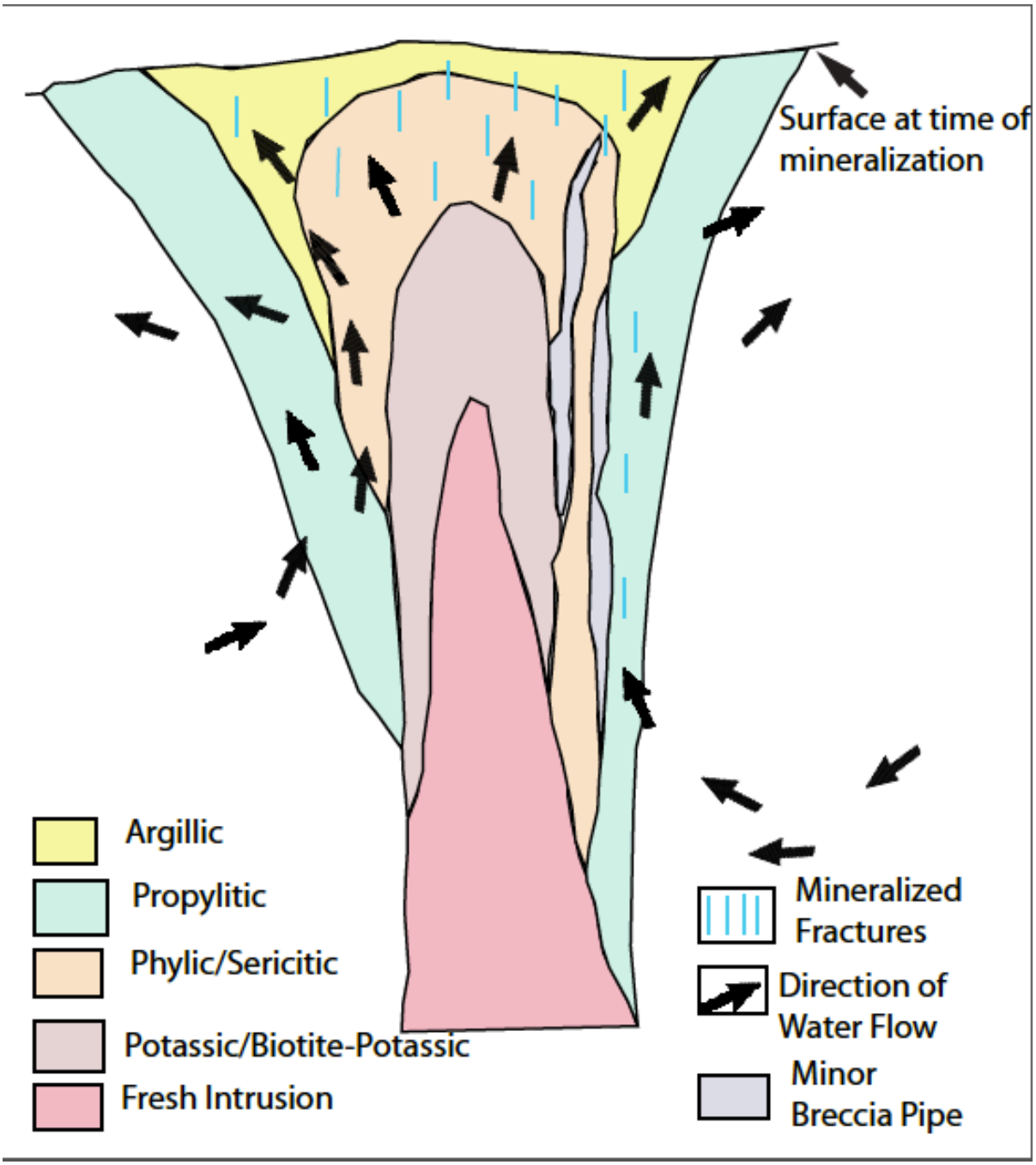

Figure 3.3: Porphyry copper alteration model of Copper Flat from Hollister 1978.

Potassic alteration is peripheral to the deposit and is characterized by large potassium feldspar phenocrysts and rimming of the plagioclase by potassium feldspar, chlorite, quartz, and pyrite (Fowler, 1982). Biotite-potassic alteration coincides with the highest copper grades in the deposit, and is characterized by hydrothermal biotite, potassium feldspar, quartz, and pyrite occurring in veinlets and as a replacement of monzonite (McLemore, 2000). Sericitic alteration is the outermost alteration zone of the deposit and is characterized by the replacement of the biotite and feldspar by sericite (Raugust, 2003). The ore body is located between the biotite-potassic/potassic and the phylic alteration zones.

3.3 FAULTS

The Copper Flat porphyry deposit has three major faults present in the area as shown in figure 3.4. The Hunter fault is the most predominant of all the fault. It strikes northeast and parallels the majority of the faults in the project. The other two structural trends are the west-northwest striking faults, marked by the Patten and Greer faults, and east-northeast striking faults marked by the Olympia and Llewellyn faults (SRK, 2010). All of the fault structures are dipping nearly vertical, the Hunter fault system dips 80°W, and both the Olympia and Llewellyn fault systems dip between 80°S and 90° (Dunn, 1984).

The three fault systems outline the Copper Flat stock. To the southeast and northwest the contacts are the Olympia and Llewellyn faults, seen in Figure 3.4, which are almost parallel to the stock. The Greer fault is at the south of the stock and the fault is sub-parallel to the deposit. It has not been possible to determine whether there was movement on the fault systems prior to the emplacement of the stock or whether these were simply well defined fracture systems (Dunn, 1984).s

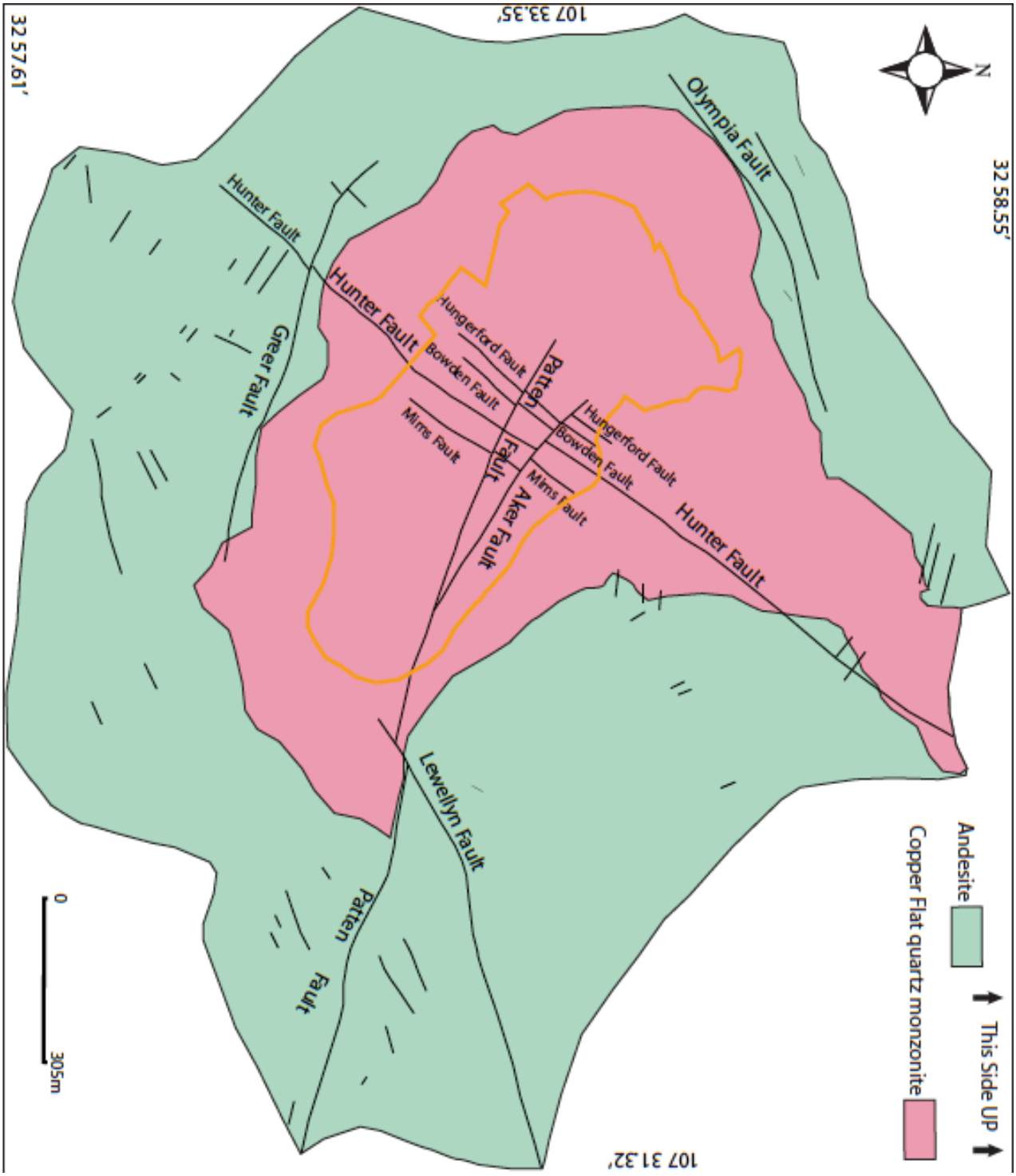

Figure 3.4: Copper Flat Faults modified from Dunn Geologic Map 1976.

Chapter 4: Geophysical Investigations

There have been various geophysical surveys conducted at Copper Flat. All the surveys made prior to Quintana days are missing or lost due to the change of ownership on the property. No physical record of this surveys have been found but mentions of this surveys have been mention in some of the literature on the property. Quantec Geoscience LTD conducted the most recent survey at the site during early 2011. This survey was accomplished by the use of the Titan-24 electrical survey system that performs three electrical methods simultaneously. The three methods performed were Induced Polarization (IP), Direct Current (DC), and Magnotellurics (MT).

4.1 Previous geophysical work at Copper Flat

The survey performed by Quantec consisted of five lines along the Copper Flat area. Figure 4.1 illustrates the location of the lines done for the survey Cooper Flat. Two of the lines were oriented north at 12°NE and the remainder of the three lines were in the EW direction at 98°NE (Quantec, 2011). The five lines used during this survey had a total length of 22 kilometers.

The Quantec survey had two main objectives. The first objective was to detect low resistivity structures and polarizable structures that could be related to disseminated chalcopyrite or pyrite at depths between 500 to 600 meters. The second objective was to map and detect phyllic and argillic alteration zones that may host porphyry copper mineralization according to the preliminary report done by Quantec (2011).

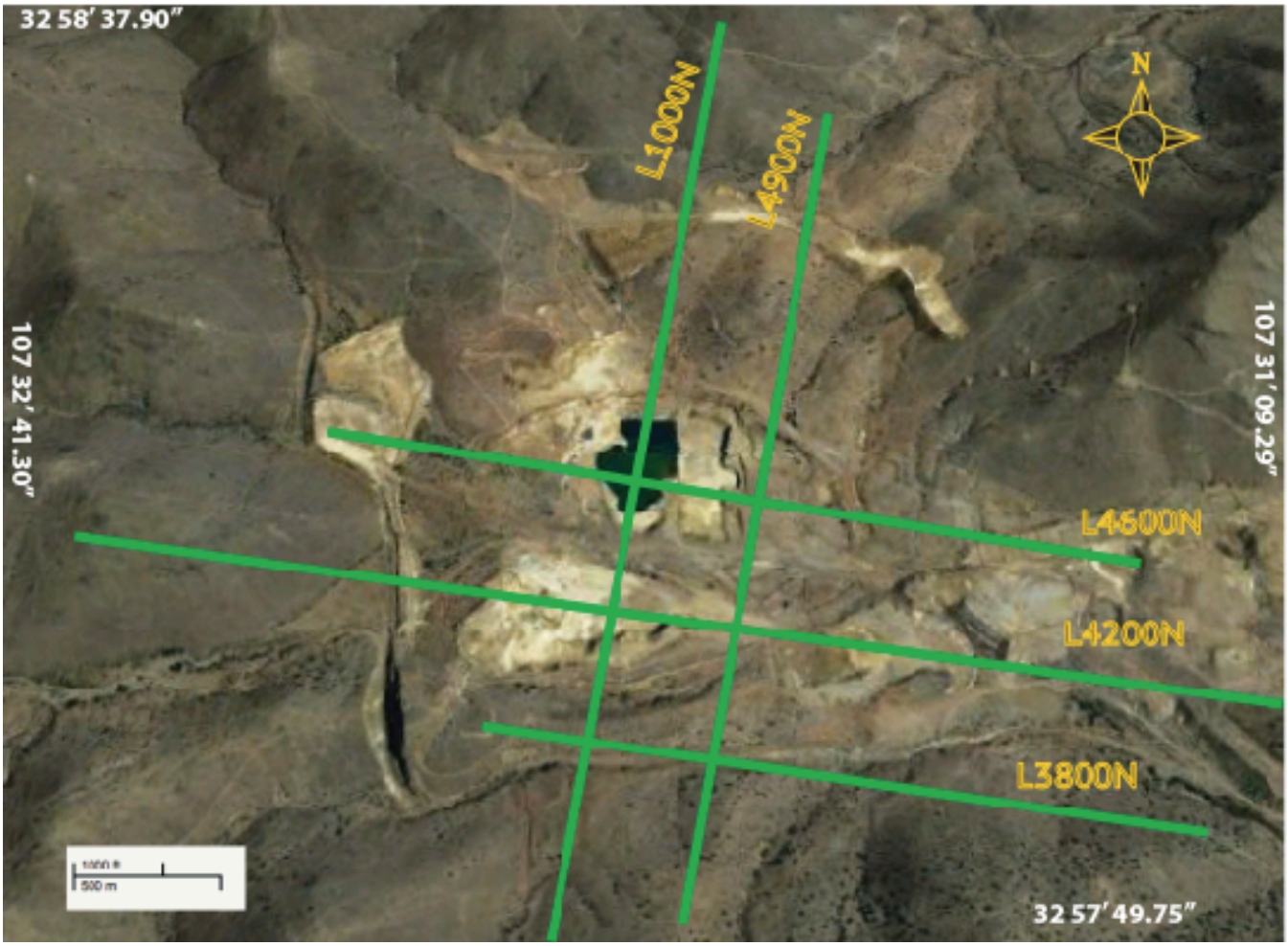

Figure 4.1: Survey lines performed by Quantec, 2011.

The DC and MT methods are used to resolve the resistivity distribution of the surface by measuring the electric potential (DC) and the variation of natural occurring magnetic and electric fields (MT) (Quantec, 2011). Metallic mineralization reacts to resistivity, but porosity in the rock can control the mineralization making it an indicator of alteration on the rock. The induced polarization method (IP) is used to measure the chargeability at the surface or electrical capacitance. Where there is some chargeability near the surface, some disseminated or massive sulphide mineralization is indicated by the process. Chargeability reacts with clay-type minerals, a number of sulphides, and graphite making it a preferred tool for base-metal exploration.

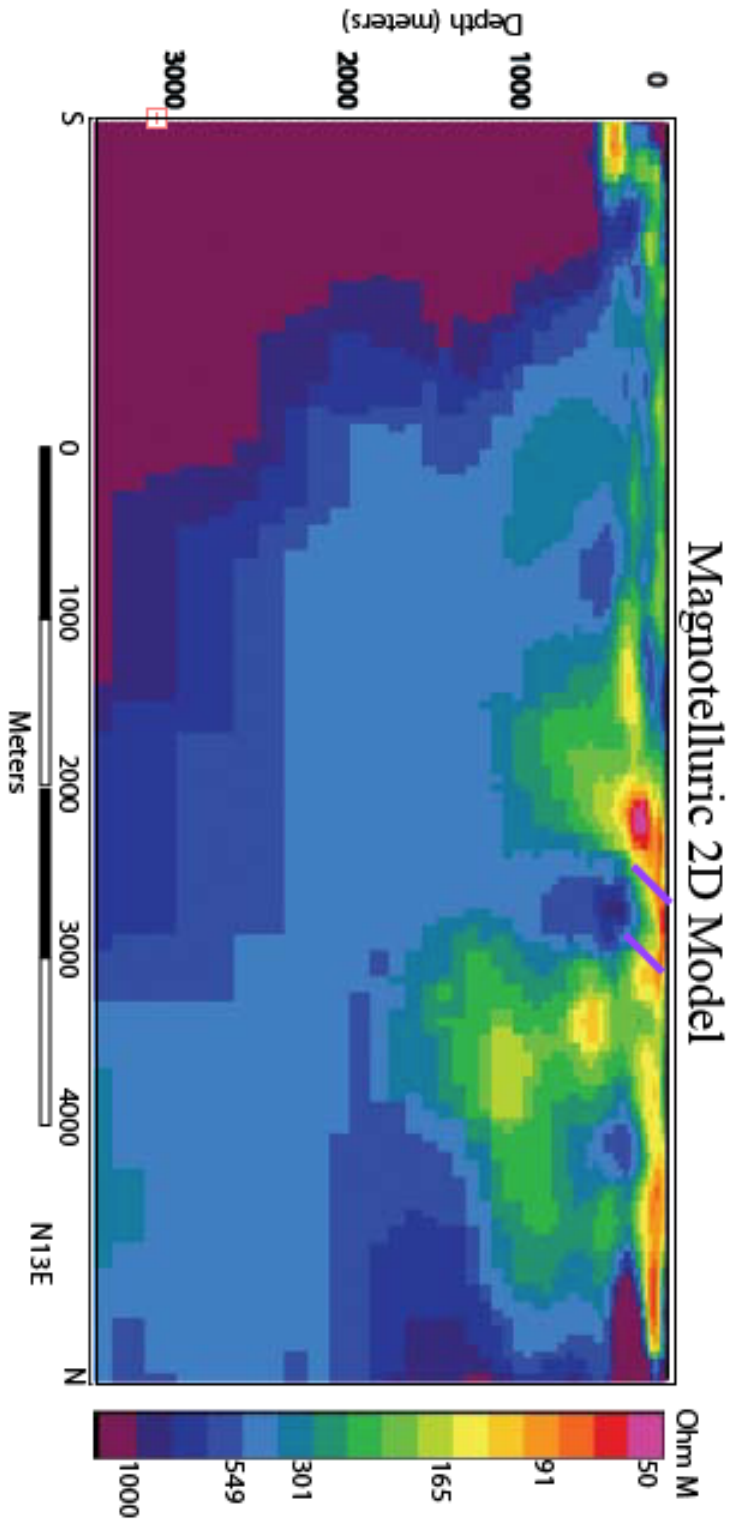

Figure 4.2: MT model from Quantec. The purple lines are the limits of the ore body.

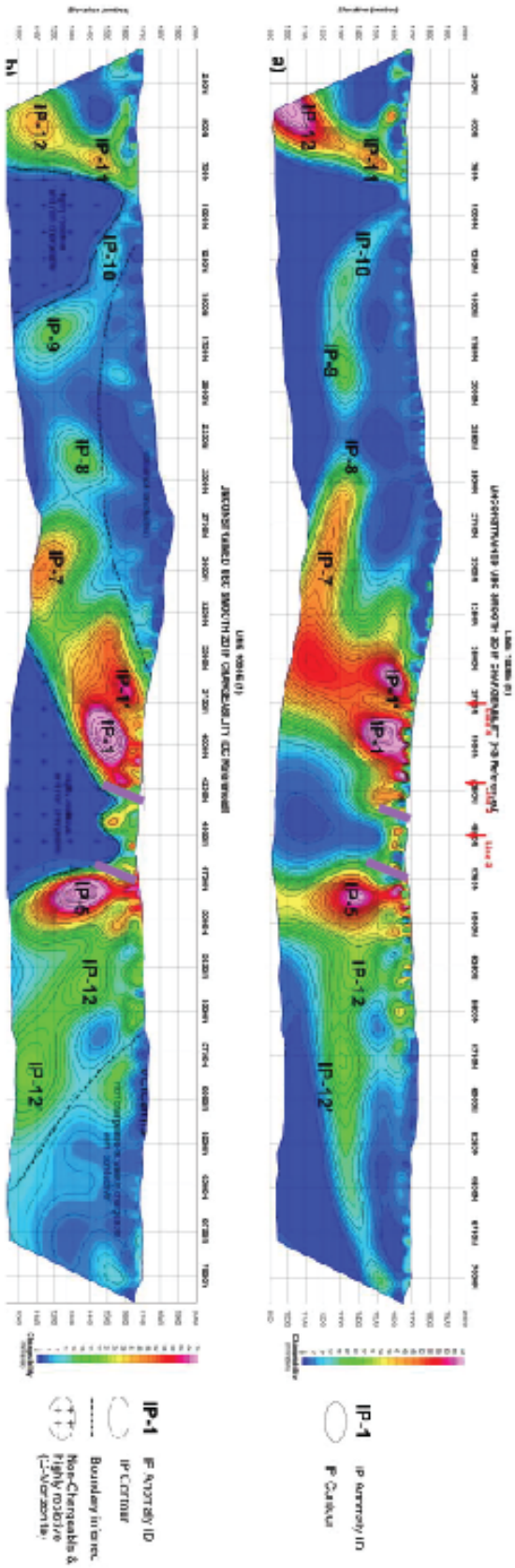

Figure 4.3 illustrates the IP models done at the deposit. The purple lines are the limits of the ore body.

The Quantec survey revealed several shallow, strong IP anomalies, label IP-1 and IP-5 in Figure 4.3, within a zone of 1 kilometer diameter approximately and coincident with highly conductivity. This anomalous feature is thought to be associated with alteration and therefore is regarded as a potential target for disseminated sulphides and porphyry copper deposits (Quantec, 2011). The inversion model performed by Quantec with the magnotelluric data confirmed the result obtained by the DC survey, suggesting a steeply dipping and highly conductive within survey area. The model of the MT interpretation can be seen above in Figure 4.2. The results of this survey resulted in a series of drill hole suggestions for THEMAC resources to explore the possibility of mineralized zone in the deposit.

The most recent geophysical study in the area involved using IP to locate geophysical anomalies in the deposit (Figure 4.3). However, the structure was not well defined by that survey because of poor signal penetration. For that reason, I collected gravity data to further explore the anomalies that had been identified previously with the Quantec survey to determine whether the mineralization could be confirmed. Figure 4.4 has the performed lines that would be done for the study in order to obtain a gravity model.

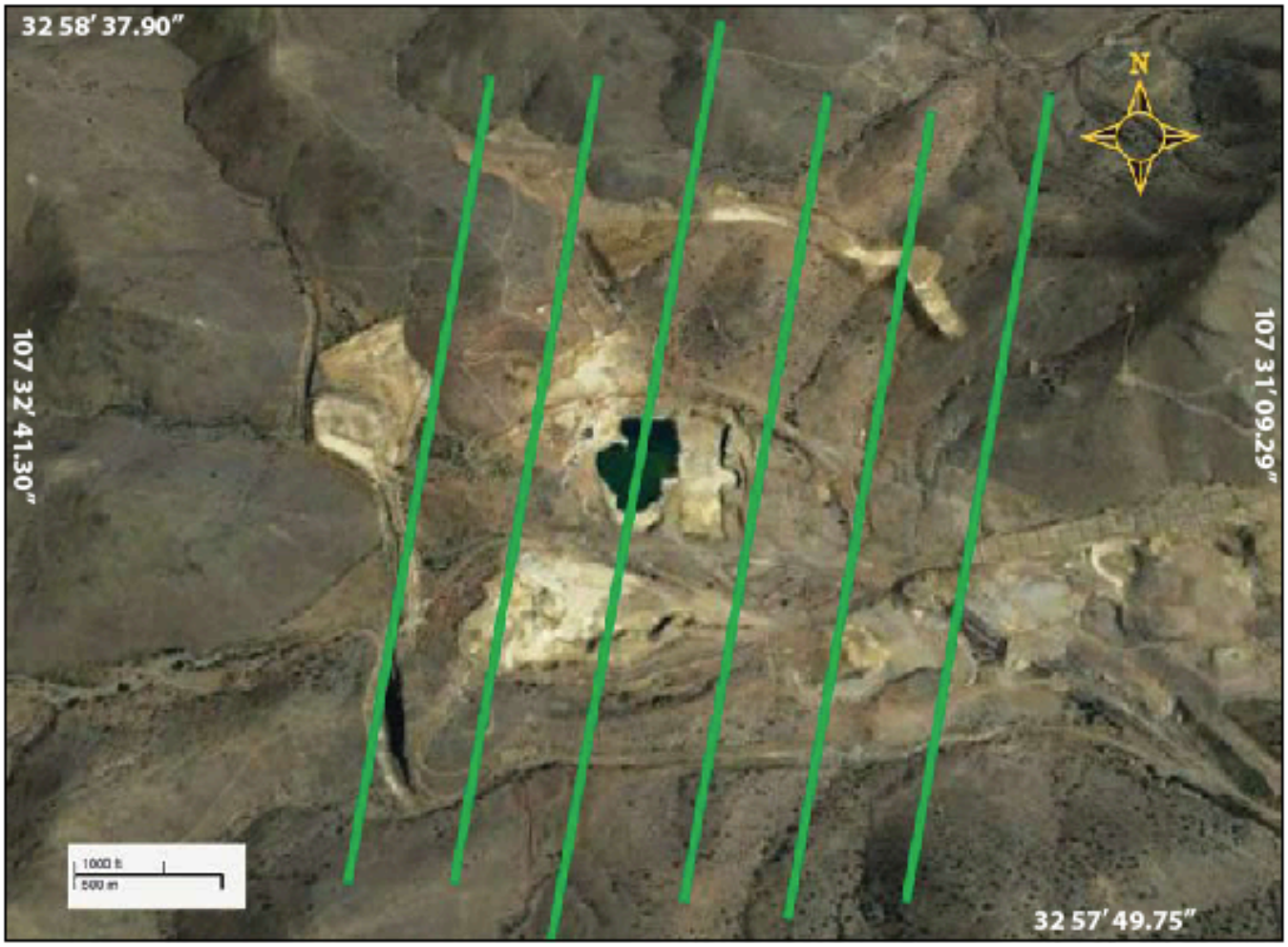

Figure 4.4: Gravity lines for survey. Some additional points were taken outside the gravity lines.

Chapter 5: Data Acquisition and Analysis

The geological structure as well as the offset in the deposit generates a density contrast that should be detected in a gravity survey. Prior to the gravity data collection, the survey area was gridded to allow the design of a survey focused on areas of greatest interest where the data collection would be most closely spaced. The collection of gravity data was performed with a LaCoste and Romberg gravimeter. The precise elevations for the survey were obtained by taking the second gravity reading of the loop at a known drill hole location in the pit of the mine where the location is precisely known. The monument location was determined by the use of a database made by the NMCC during their drilling campaigns as well as GPS locations measured at the site.

The survey was conducted during late August of 2012. A gravity base station located next to the postal office in downtown Truth or Consequences, New Mexico, was used because it was the closest absolute gravity monument to the mine site. A description of the benchmark used for the absolute gravity can be located in Appendix I. The gravity data was collected in three parts during two days in three loops. Data was taken in loopss with the first reading taken at the base station, then a series of the reading were taken along a zone of the grid, and the last reading was taken again at the base station. The loops were completed in about 6-8 hours in order to correct the drift and tidal effects of the instrument. The spacing of the readings was 100 meters, approximately, except in the areas of interest where the gravity measurements taken every approximately of 50 meters. A total of 130 gravity stations were measured during this survey.

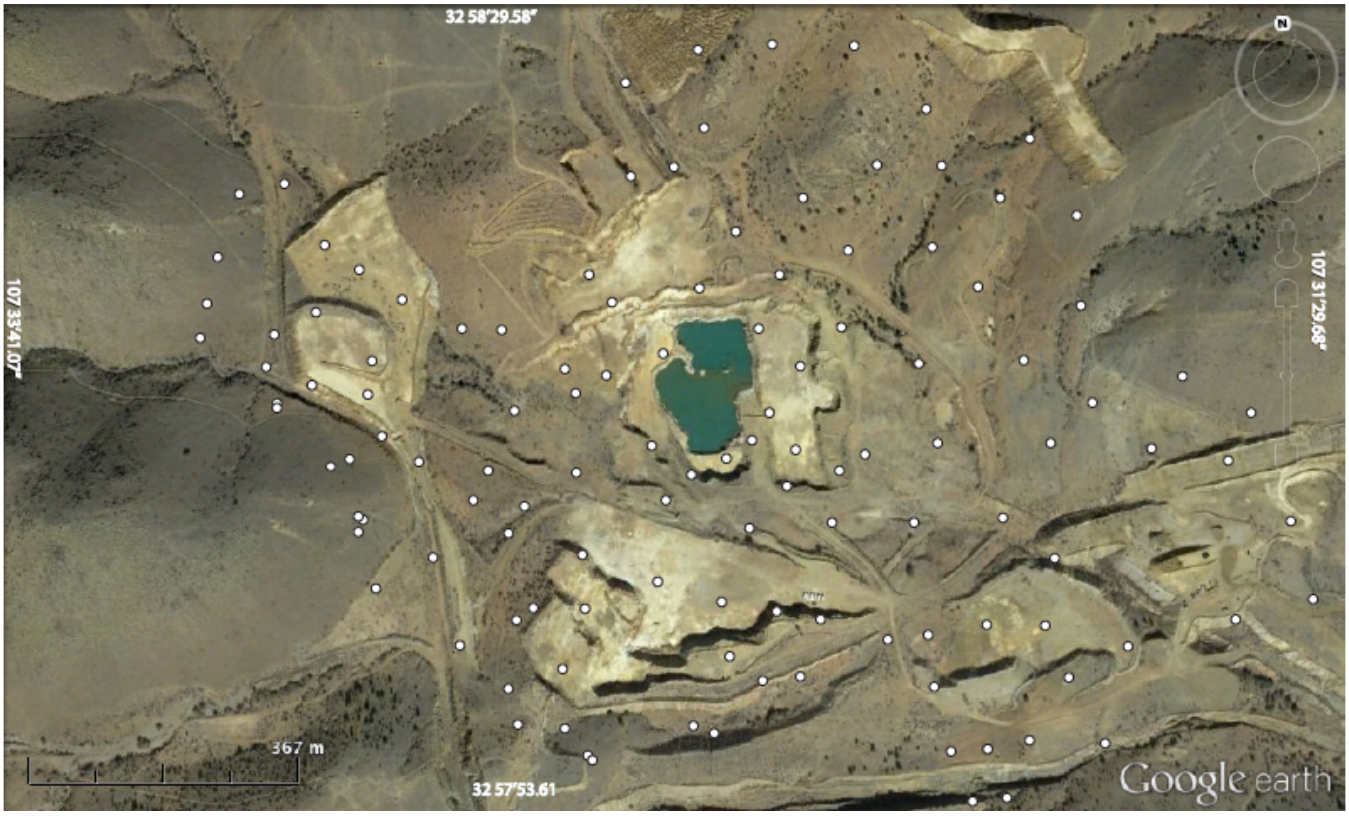

Figure 5.1: Locations of gravity readings on a Google Earth image.

5.1 DATA PROCESSING

Following the data collection, the gravity readings were processed to determine the distribution of mass in the subsurface of the study area. The first steps in the data processing were the dial, drift, and base station corrections to obtain the absolute gravity. Corrections for changes in shape of the earth with latitude and elevation corrections including free air, Bouguer and terrain corrections were applied to obtain the complete Bouguer gravity with a reduction density of 2.67 g/cc. The software package used to process the data and map the Bouguer gravity values was Oasis Montaj ™ .

The Oasis Montaj software uses algorithms for gridding that are optimal for interpolating data to produce grids using different techniques as minimum curvature, bi-directional, trended, gradient, IDW, tinning, or kriging routines. These routines used by the Oasis Montaj algorithms are best suitable for well sampled data, the processing of the data can be slower depending on the assumptions taken into

account at the moment of processing the data. The data obtained during the survey is set on a set position (X and Y in a plan) and a geophysical reading that represents the Z value. The X,Y, Z structure is called Point data. Point data can be arrange in lines in order to take advantages of the characteristics of the survey layout during processing. After the data has been corrected for positioning and data integrity, it is processed to create a grid.

Gridding is the process of interpolating data values at the nodes of a two dimensional grid from either point or line data that is less regularly distributed (MacLeod et. al., 2009). The grid representations of data are used for a number of two-dimensional procedures such as contouring, imaging and two-dimensional filtering. There are many gridding methods available, each with different characteristics that can produce quite different results, and it is important to choose the method that best matches the data. This thesis usea three different gridding processes.

The complete Bouguer gravity map (Figure 5.1) was produced using a minimum curvature gridding method to produce a uniform grid from unequal spacing of the acquired data that could also be used for further analysis such as filtering studies. Three gridding techniques were used produce maps to try to understand the relationship between the anomalies previously found by Quantec geophysics and the gravity survey performed in 2012. The comparison is made in order to understand what is causing the MT and IP anomalies found by Quantec. The different models where filtered in some cases to try to define the known faults at the deposit and eliminate the possibilities of this faults resulting in a misinterpretation of the anomalies at Copper Flat.

5.2 FILTERING

The next step in the process was to apply derivative filters. These filters enhance anomalies from small and near-surface geological features (Sharma, 1997). The derivative filter was used in this study to highlight the structures that cross-cut the deposit (Figure 5.3). Also, the residual gravity was calculated as part of this process. The residual gravity has been shown to be very useful for detecting and locating weak anomalies against a strong regional back round (Skeels, 1966). Taking into consideration the

advantages of the residual gravity, it was calculated to see if there were any different anomalies at Copper Flat displayed in the models of residual gravity.

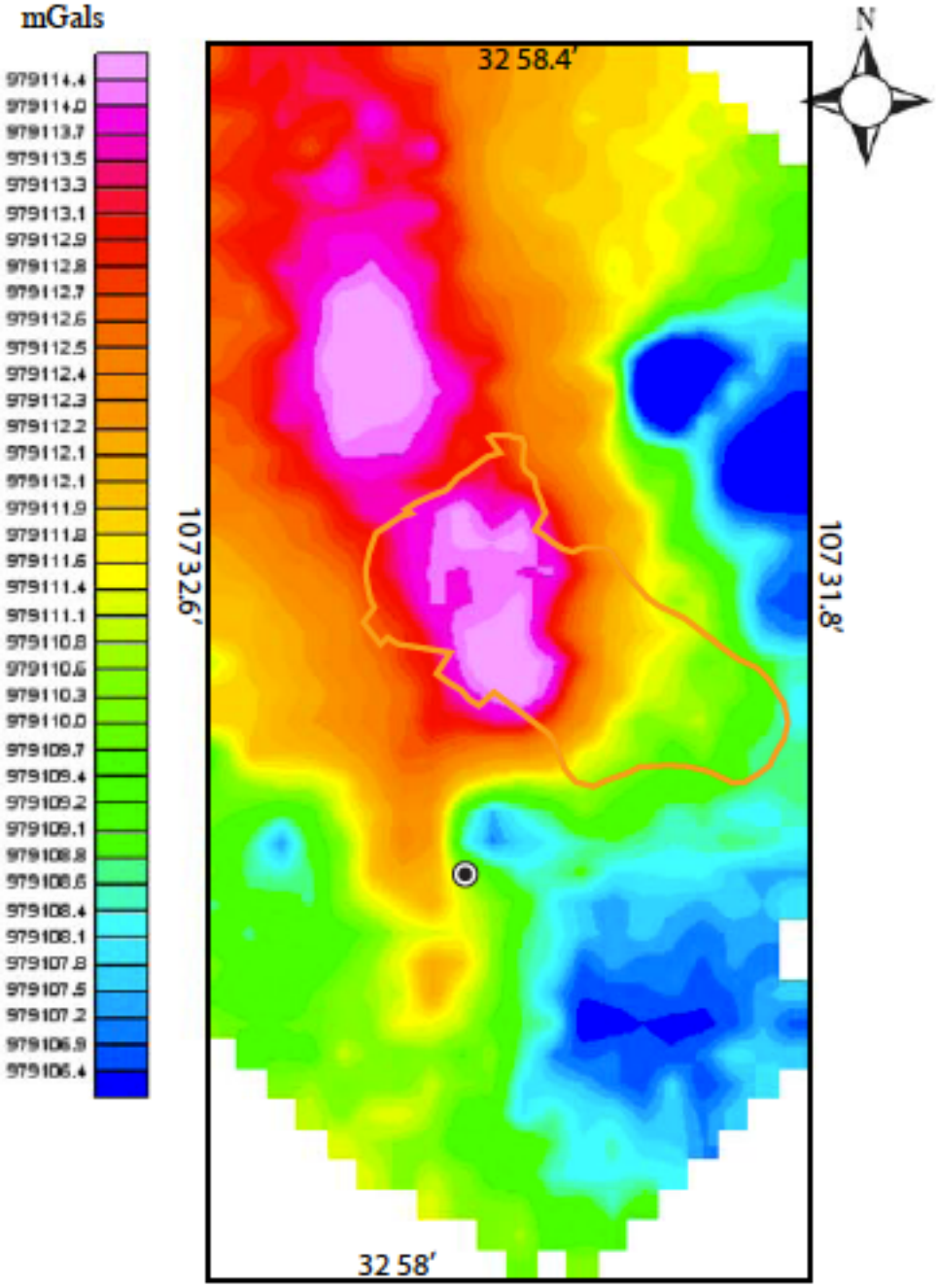

Figure 5.2: Absolute gravity model. The orange line is the mineralized body and the black dot is the base station of the survey.

Chapter 6: Interpretation

The complete Bouguer anomaly map (Figure 5.2) presents variations in the gravity field due to the subsurface geology of the area associated to the Black Range as well as the Animas Peak geology. The high values for the gravity are around the mountains made mostly of andesite. The low values are around the mineralized body at Copper Flat. Note that the low anomaly values to the southeast of the figures below suggest an alteration zone that also appears on the Quantec surveys, IP-1, in Figure 4.3. The gravity lows are related primarily to the mineralized zone at Copper Flat with a sharp gradient surrounding the mineralized zone where the Hunter, Patten and Aker faults are located. The gradient continues towards the Animas Peak area, western edge of the map. Unfortunately, no data was obtained beyond this point because the old mine dumpsite material was placed in this zone after the closing in 1985.

Because the main objective of this study was to locate the two anomalies found by previous electrical studies to determine the cause of the anomalies, regional and local geology maps (discussed in Chapter 2) were examined to determine whether the anomalies were cause by mapped geological features. These maps were compared with the gravity maps (shown below) enhanced for relief using Oasis Montaj. All of the available data was then used to construct surface maps as well as 2D and 3D models of the geology that could explain both the geophysical measurements and the surface geology.

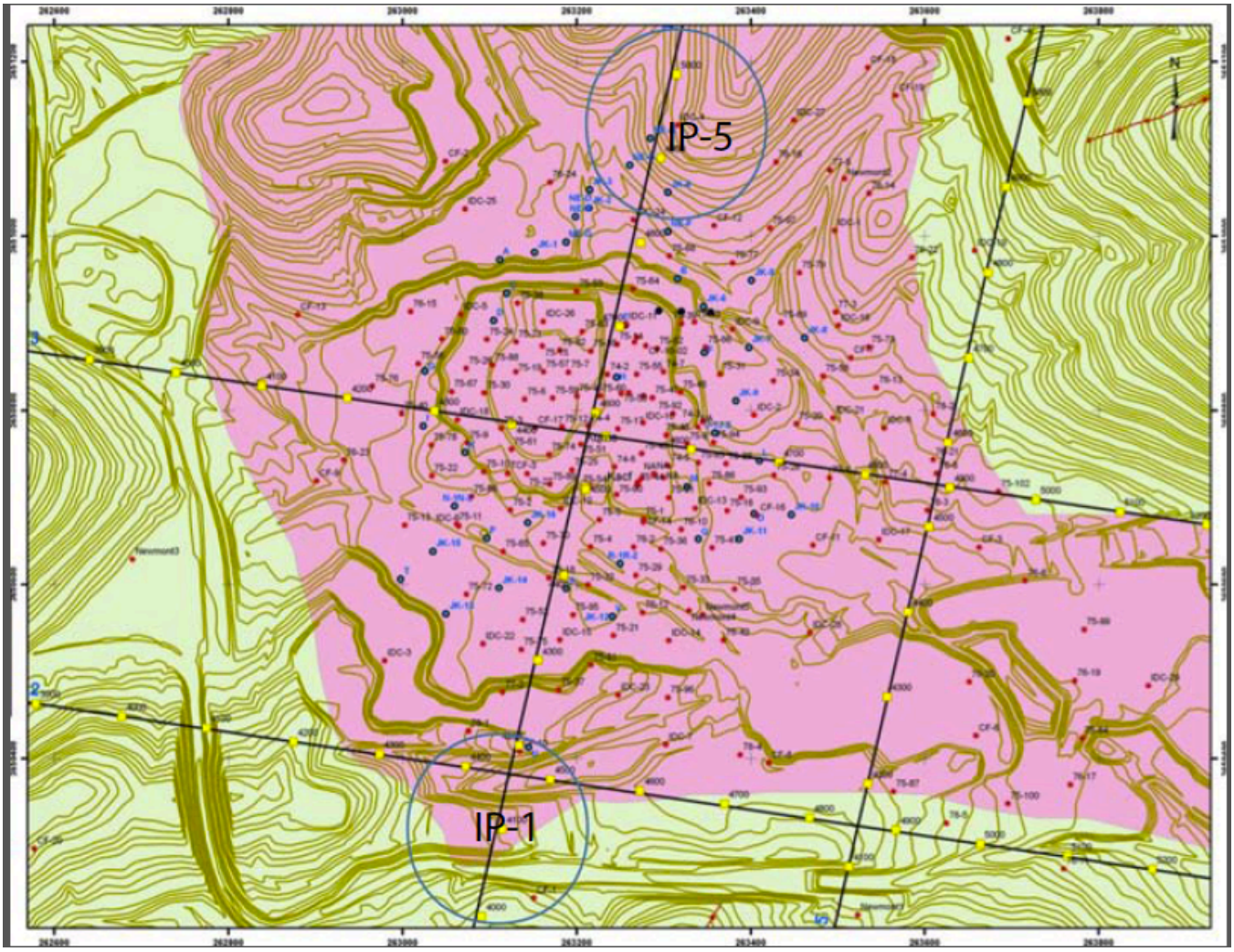

Figure 6.1: Location of the Quantec anomalies. The two blue circles represent the location of the anomalies. The black lines with yellow dots represent the lines done by Quantec during their survey. The dots in blue and red are the different drill holes performed at Copper Flat in different stages.

6.1 GRIDDING THE DATA

There were three types of gravity maps used to create the models for the Copper Flat area. These included the complete Bouguer anomaly, the free air anomaly, and residual gravity anomaly maps. The formulas and explanations for the different anomaly types can be found in Appendix II. Each of the anomaly map types was gridded with different gridding techniques in order to examine the different features that each of the gridding techniques has to offer. The three-gridding techniques use for the model generation was minimum curvature, kriging, and tinning.

The two anomalies found during the Quantec survey at copper flat are at the south (IP-1) and north (IP-5) end of the current pit at Copper Flat (Figure 6.1) The gridding were intended to maximize the identification of the same anomalies with different methods.

6.2 MINIMUM CURVATURE GRIDDING

The Minimum Curvature method, as its name suggests, generates a grid with the smoothest surface possible that fits the data values provided. The minimum curvature surface has the least curvature of all twice-differentiable surfaces that interpolate the data (Briggs, 1974). The method first estimates grid values at the nodes of a coarse grid (usually 8 times the final grid cell size) based on the inverse distance average of the actual data within a specified search radius (Geosoft, 2011). If there is no data within that radius, the average of all data points in the grid is used. An iterative method is used to adjust and determine the best fit for the grid being created according to the available dataset, once a fit is accomplished the process is repeated until the fittest surface is obtained according to the algorithm.

6.3 TRIANGULAR IRREGULAR NETWORK

The Triangular Irregular Network Gridding (TIN) is a method that applies the natural neighbor algorithm to interpolate the data using the closet data point to create a cell. Each cell is unique and can

be defined similarly in any dimension (Sambridge et. al., 1995). In the case of this survey, this gridding method expanded the maps further south and generated a longer map in all cases. The reason behind the extension of the maps towards the South is produced by the TIN interpolation producing a series of triangulates going to the south of the grid using the gravity data at the edges of the survey area. The anomalies produce by the TIN method were similar to the ones produced by the minimum curvature method with the exception that all south anomalies were projected further south and increased in size. The grid generated for the TIN method could not be considered reliable in the southern part of the map because there were no gravity stations in that area.

6.4 KRIGING

The last method used to generate grids was the kriging method which generates a grid based on statistical analysis of the data. Kriging is a geostatistical method that determines the most probable value at each grid node based on a statistical analysis of the entire dataset (Geosoft, 2011). Because this method is based on a maximum probability, the margin of error it produces is minimal therefore generating more reliable grids than the other techniques discussed above. The other techniques were gridded to see if there were any major changes in the predicted anomalies. There is minimum variation in the anomaly locations and sizes compared the previous gridding methods (TIN and Minimum Curvature). The main difference in this method is that the kriging map has smoother contour lines that define more gradually than the other methods (Akima, 1970). The main mineral deposit is the lowest complete Bouguer value on the map and it varies in size depending on the grid being produced for the gravity anomaly used.

6.5 GRID MAPS

The anomalies present on this grid for the Complete Bouguer values (Figure 6.2) show three anomalies. Two of them coincide with the ones previously found by Quantec Geophysics (IP-1 and IP-5) and one to the west of the property. Figure 6.5 is the Free Air Anomaly map gridded with minimum curvature that shows only two anomalies, one to the northeast of the property (A) and one two the southwest (C). The position where the anomalies were previously found has shifted from southwest to the sides southeast locating these anomalies in the southwest and northeast sections of the model for the free air anomaly grid. If you compare Figures 6.2 and 6.5 you can easily me change in position of the anomaly at the south (C) of the map. The residual gravity gridded map (Figure 6.8) shows the same anomalies as the free air map. In addition, there is a high anomaly to the southeast of the map that is separated by a gravity low from its counterpart in the southwest. Table 7.1 helps understand the difference between the 9 gravity maps.

Table 7.1: Guide to gravity maps.

Figure (Map)	Main Goal	Gridding Technique	Gravity Correction
6.2	Find anomalies with a correction in the terrain.	Minimum Curvature	Complete Bouguer
6.3	Find anomalies with a correction in the terrain.	TIN	Complete Bouguer
6.4	Find anomalies with a correction in the terrain.	Kriging	Complete Bouguer
6.5	Find anomalies with a correction based	Minimum Curvature	Free Air

	on height.		
6.6	Find anomalies with a correction based on height.	TIN	Free Air
6,7	Find anomalies with a correction based on height.	Kriging	Free Air
6.8	Find if anomalies are cause by deep structures.	Minimum Curvature	Residual Gravity
6.9	Find if anomalies are cause by deep structures.	TIN	Residual Gravity
6.10	Find if anomalies are cause by deep structures.	Kriging	Residual Gravity

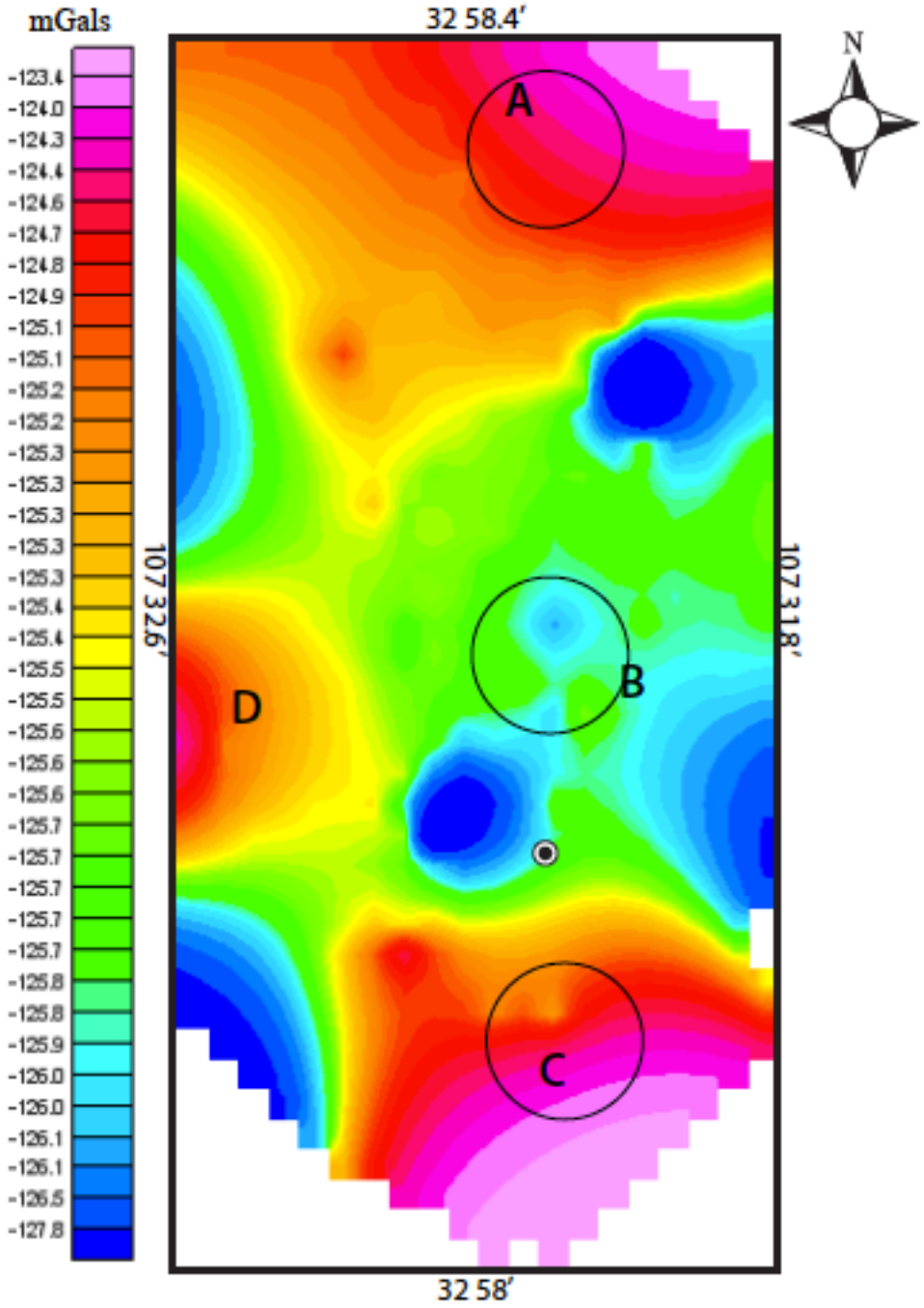

Figure 6.2: Minimum Curvature Model of the Complete Bouguer. A) is the anomaly found at the north of the deposit. B) represents the location of the mineral deposit. C) is the anomaly at the south of the deposit. D) is an anomaly normally seen at the west of the deposit. The circles represent the approximate location of the mineralized body and the anomalies. The black dot is the base station of the survey.

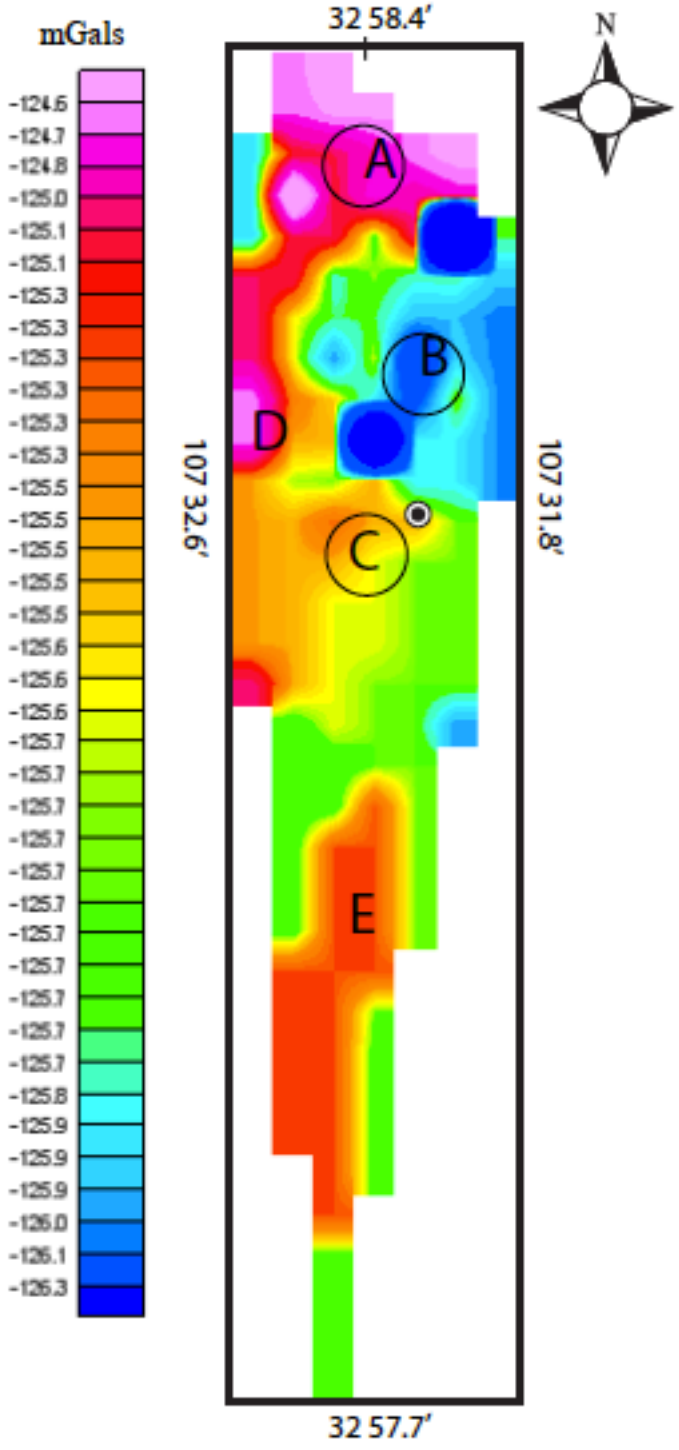

Figure 6.3: Complete Bouguer TIN gridded map. The complete Bouguer map has A) as a representation of the north anomaly, B) as the mineral deposit, C) as the anomaly found on the south, D) as the west anomaly and E) as a anomaly further south at Copper Flat. The circles represent the approximate location of the mineralized body and the anomlaies. The black dot is the base station of the survey.

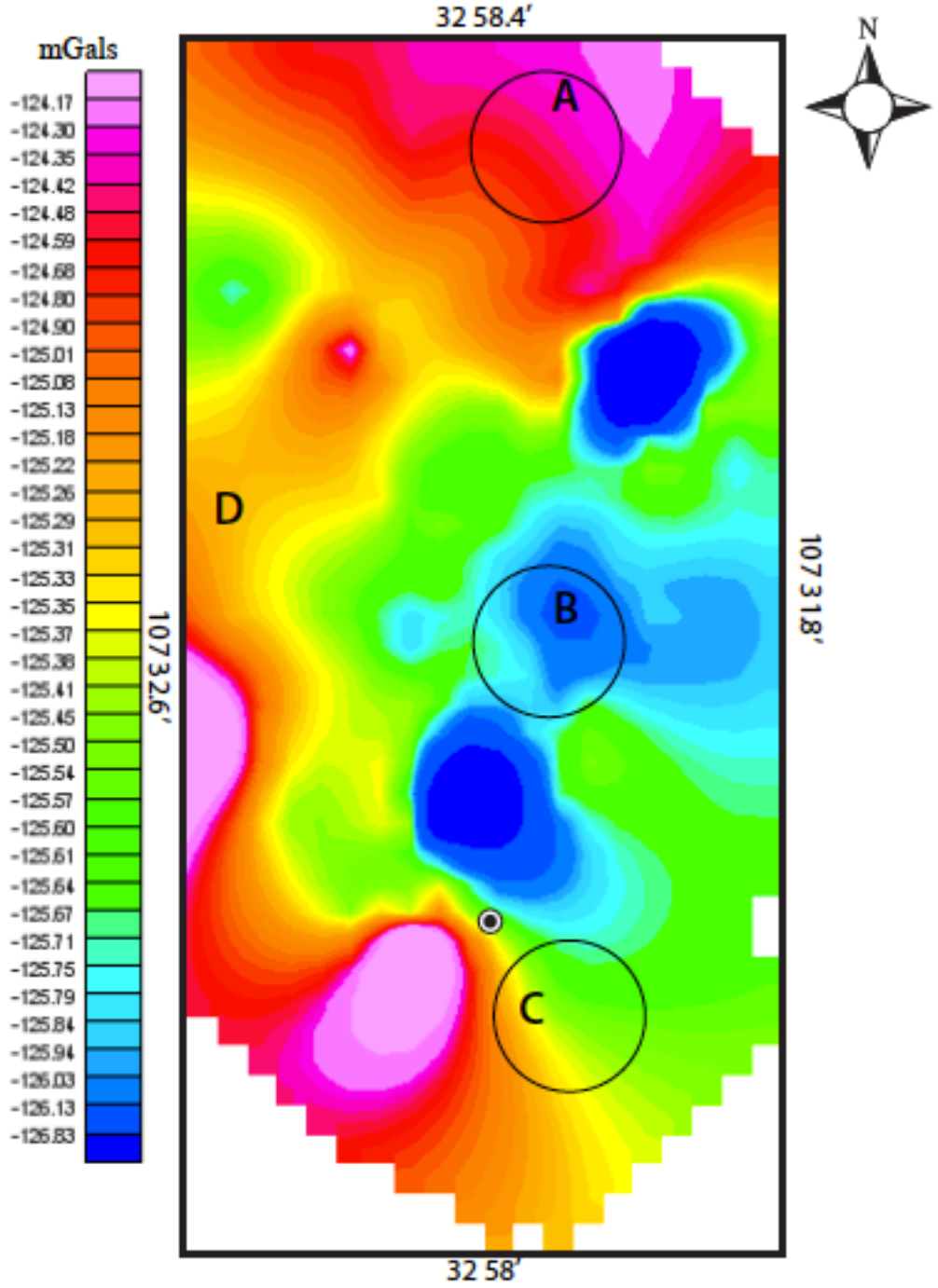

Figure 6.4: Complete Bouguer map using the Kriging Model. The north anomaly is represented by A), the mineral deposit is B), the south anomaly is C) and the anomaly at the west of the deposit is denoted by D). The circles represent the approximate location of the mineralized body and the anomalies. The black dot is the base station of the survey.

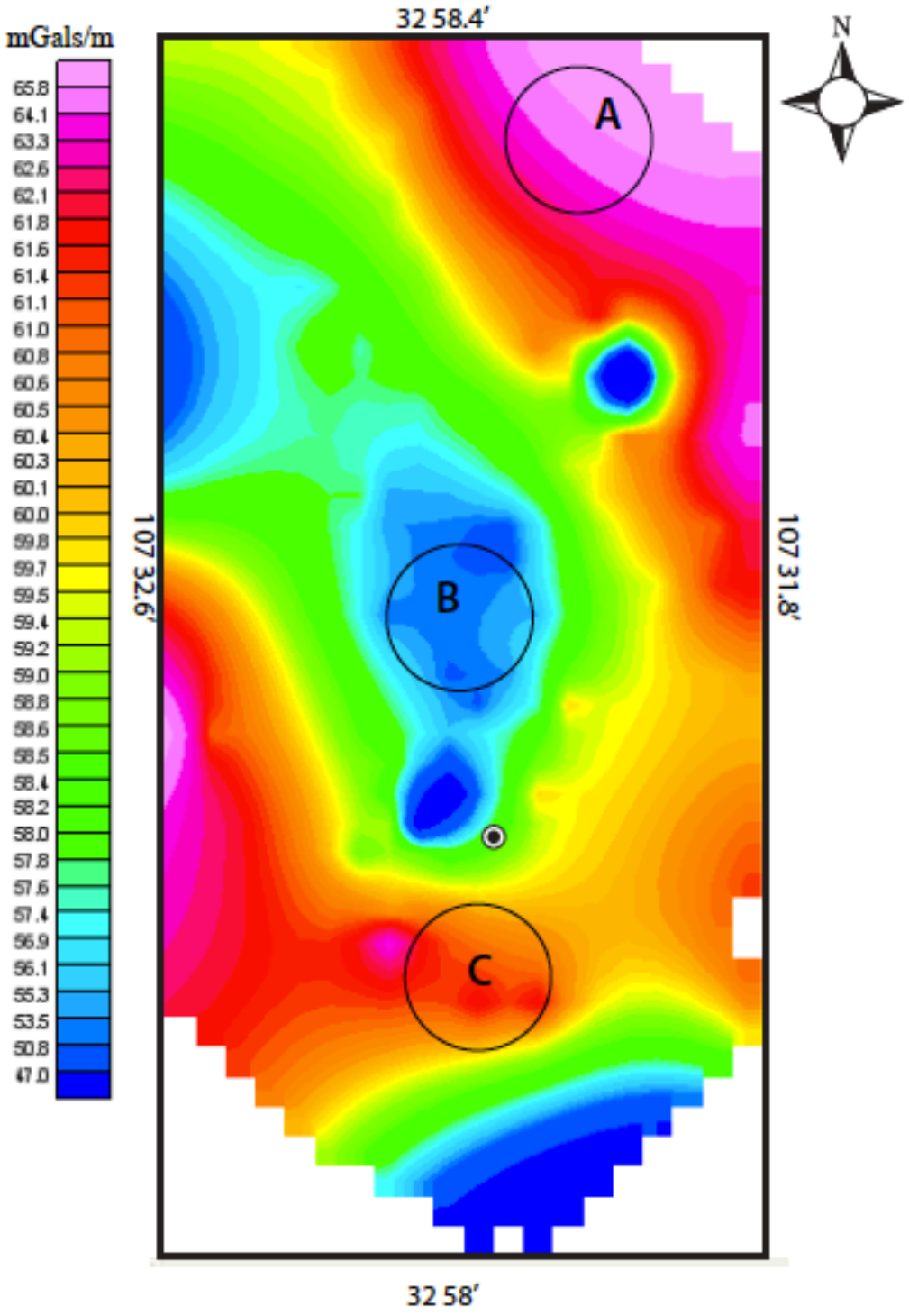

Figure 6.5: Minimum Curvature Free Air Model. A) is the anomaly at the north of the deposit. B) is the mineral deposit. C) The south anomaly that has shifted toward the southwest. The circles represent the approximate location of the mineralized body and the anomalies. The black dot is the base station of the survey.

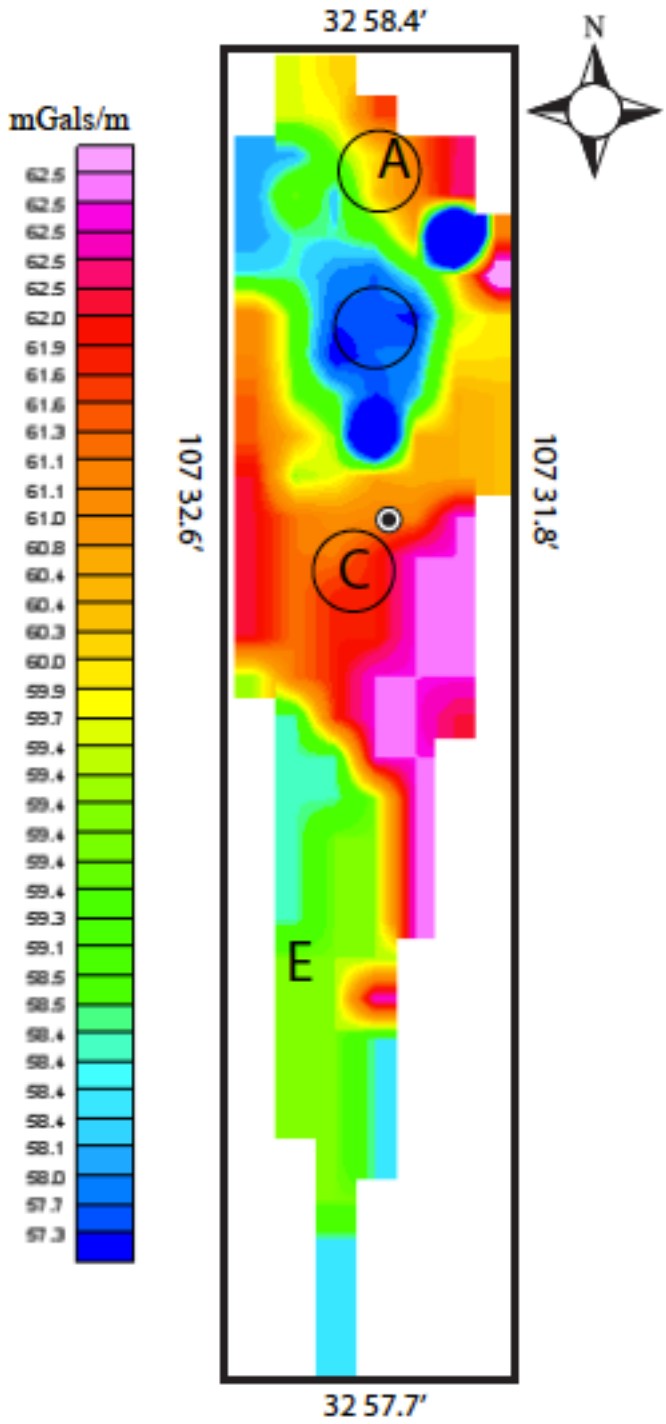

Figure 6.6: Free Air TIN Model. A) is interpreted as the north anomaly in this Free Air anomaly map. B) Is the south anomaly in this case the size of the anomaly has increase considerably towards the west of the map. E) is the extension of the map that is presenting a low gravity reading in this map. The circles represent the approximate location of the mineralized body and the anomalies. The black dot is the base station of the survey.

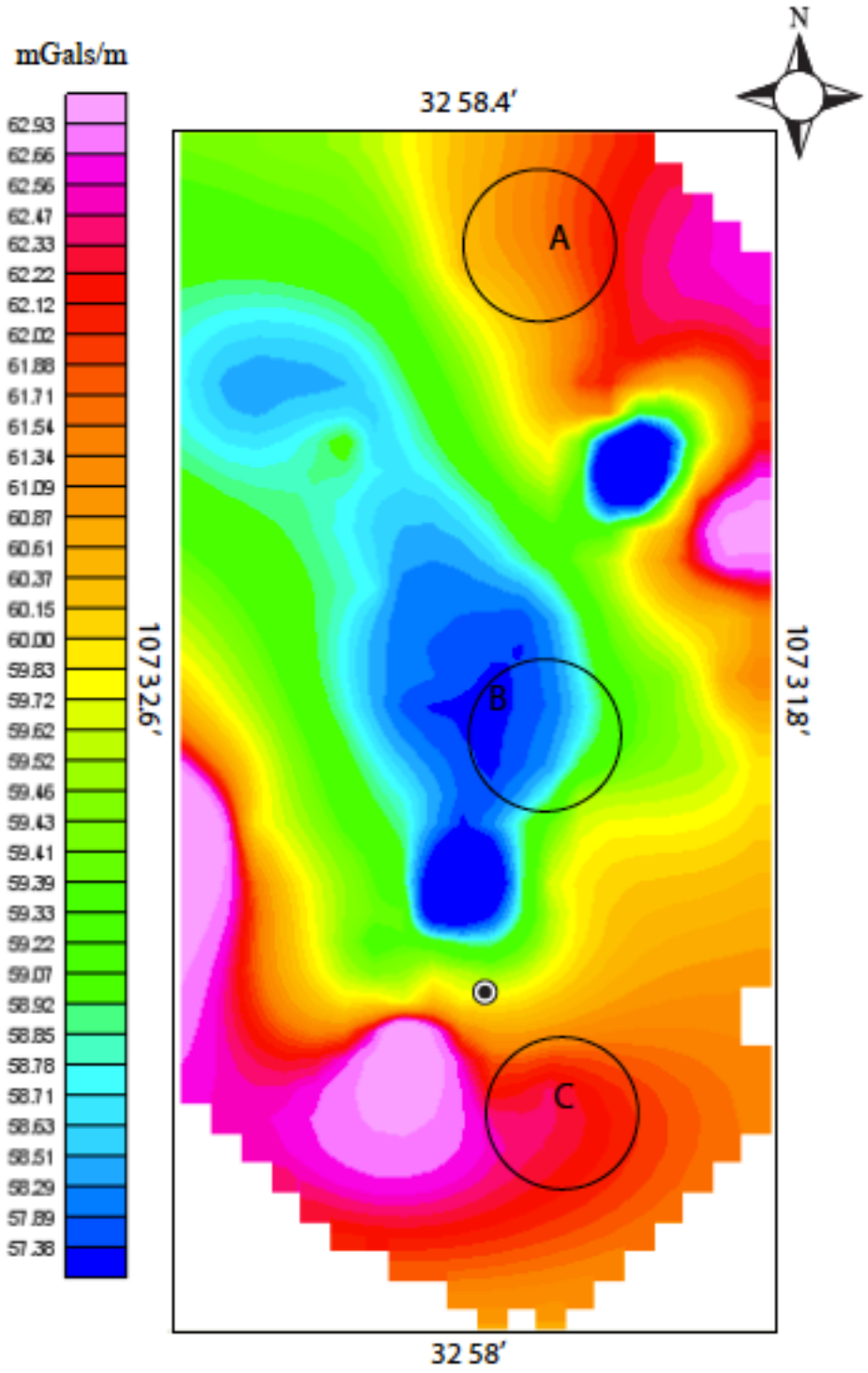

Figure 6.7: Free Air map using the Kriging method. The Free Air anomaly map has A) as the north anomaly, B) as the mineral deposit and C) as the south anomaly. The circles represent the approximate location of the mineralized body and the anomlaies. The black dot is the base station of the survey.

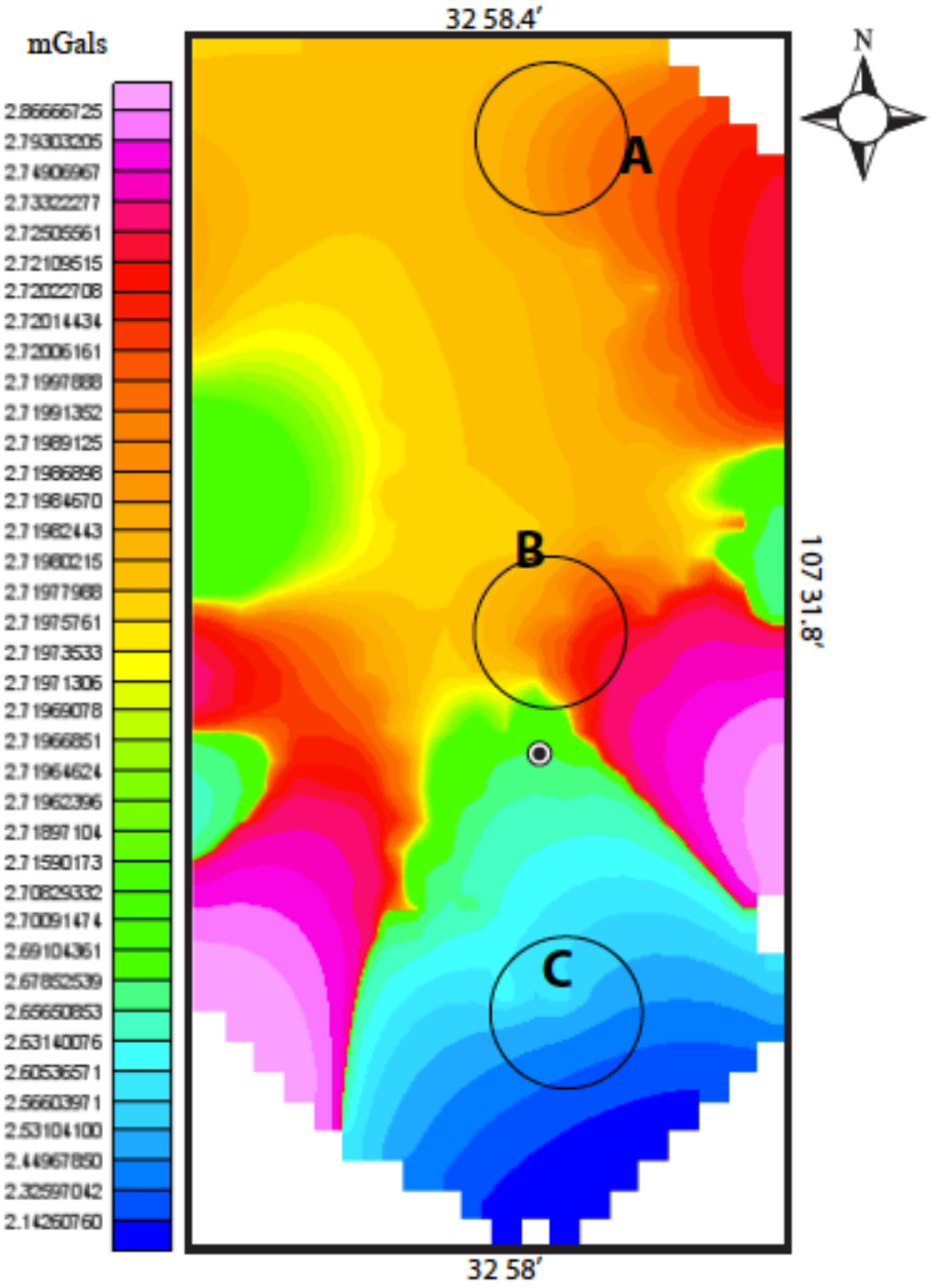

Figure 6.8: Residual Gravity Minimum Curvature Model. This map shows the residual gravity in the area A,B, and C show the location of the north anomaly, mineral deposit and south anomaly respectably. The circles represent the approximate location of the mineralized body and the anomalies. The black dot is the base station of the survey.

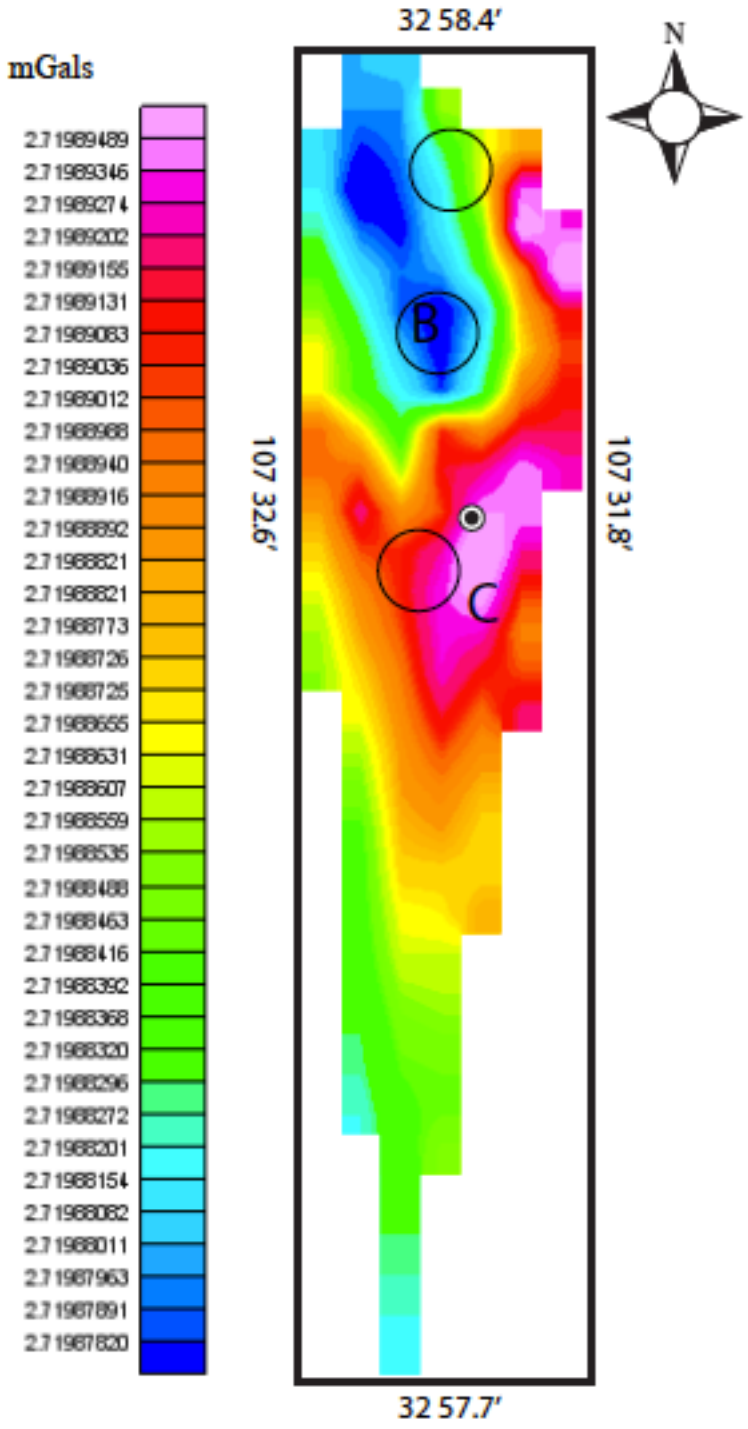

Figure 6.9: Residual Gravity TIN Model. In this residual gravity map there are only two important features: A) the mineral body at depth and B) the south anomaly with increased sized compared to, the minimum curvature maps, towards the eats boundary of the map. The circles represent the approximate location of the mineralized body and the anomalies. The black dot is the base station of the survey.

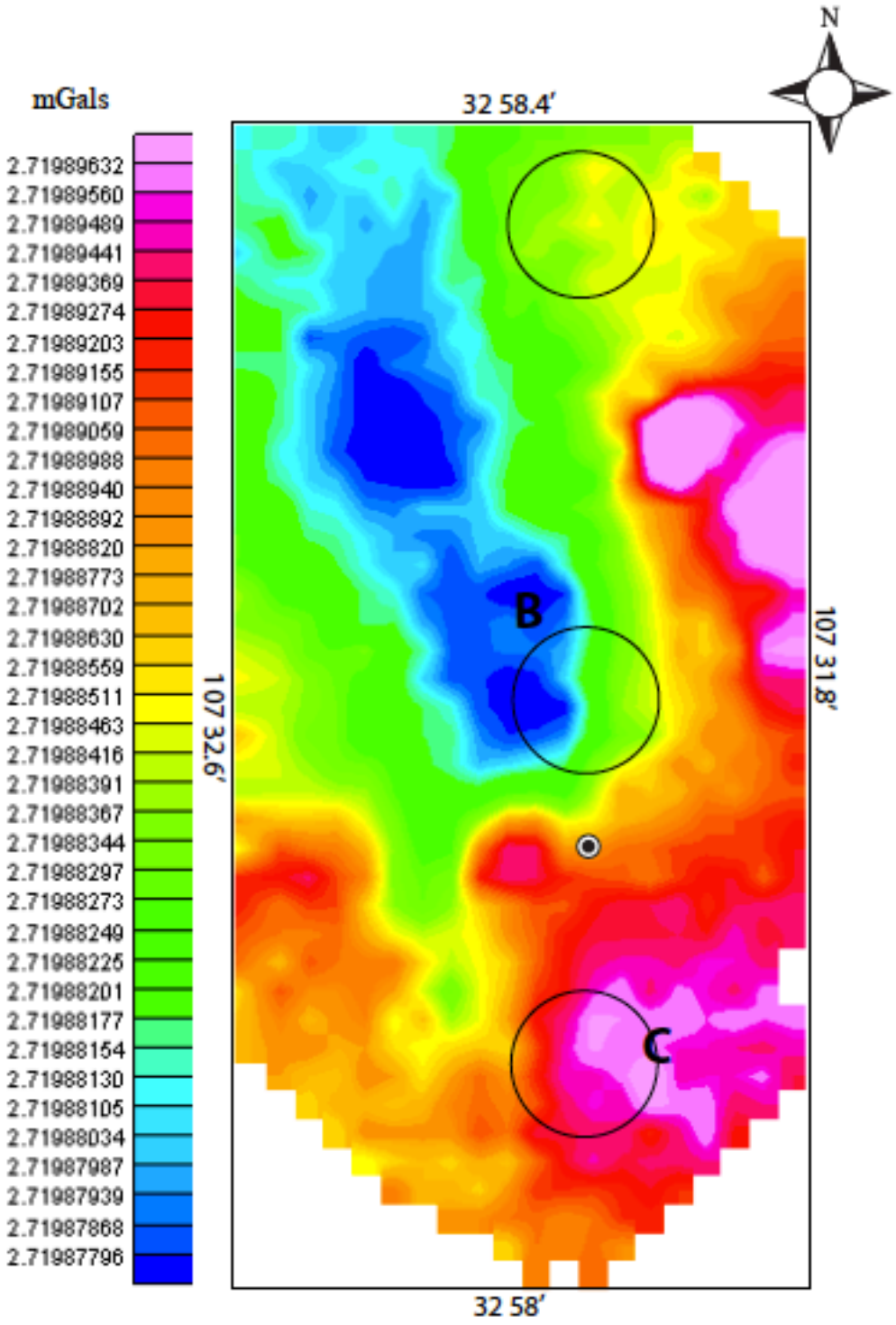

Figure 6.10: Residual Gravity anomaly map using Kriging method. The Residual Gravity model has two main features: A) represents the mineral body location and B) represents the south anomaly. The circles represent the approximate location of the mineralized body and the anomalies. The black is the base station of the survey.

Chapter 7: Interpretation and Results

The two anomalies found by the Quantec surveys, IP-1 and IP-5, were drilled during the campaigns in 2011 and 2012 (Figure 6.1). No apparent change in the copper grade was found in either of the two drill holes made in the north anomaly IP-5 or A. The south side anomaly, IP-1 or C, drilling was suspended due to the unsuccessful results on the previous drilling. The northern anomaly was not caused by an increase in mineralization of the deposit so there must be another change in density causing the anomaly in the northern part of Copper Flat. The southern anomaly, C, was not drilled but was assumed to be similar geology of near by drilled holes in the area. The geophysical methods and geological interpretation used to understand and to define the cause of the anomalies are explained below.

7.1 ANOMALIES

The anomaly in the northern part, A or IP-5, of the deposit is located within an area where there is an abrupt transition between the biotite breccia, quartz breccia, feldspar breccia to quartz monzonite and finally to the andesite near to the deposit (Figure 6.1). The quartz monzonite is crosscut by a series of dikes, including a quartz latite dike that intruded during the mineralization stage of the deposit and a basalt dike that intruded the area post mineralization. There is a fault junction between the Mims and Aker faults (Figure 3.4) and there is syenite in this area of Copper Flat both of which could indicate mineralization in the area. The core interpretation of the geologist on site during the drilling campaign in 2011 concluded that there were traces of a syenite porphyry rock with limited copper mineralization and quartz veining with pyrite. The change in density at this portion of the deposit could be the cause of the anomaly at this part of the deposit. The density difference between syenite and quartz monzonite is between .62-.14 g/cc (Guilbert et. al., 1986) with syenite denser than the quartz monzonite.

The south anomaly, C or IP-1, is located within the quartz monzonite part of the deposit. There are some latite dikes, plugs, and basalt dikes in the area but these bodies are not as dense as the ones

found in the northern area. The latite dikes intruded before mineralization of the deposit and the basalt dikes were post-mineralization. There are three faults in the area (Figure 3.4): the Geer, Hunter and Mims Faults. The Hunter and Mims fault trend parallel to each other while the Hunter and Geer fault join further south where the transition from quartz monzonite to andesite is located.

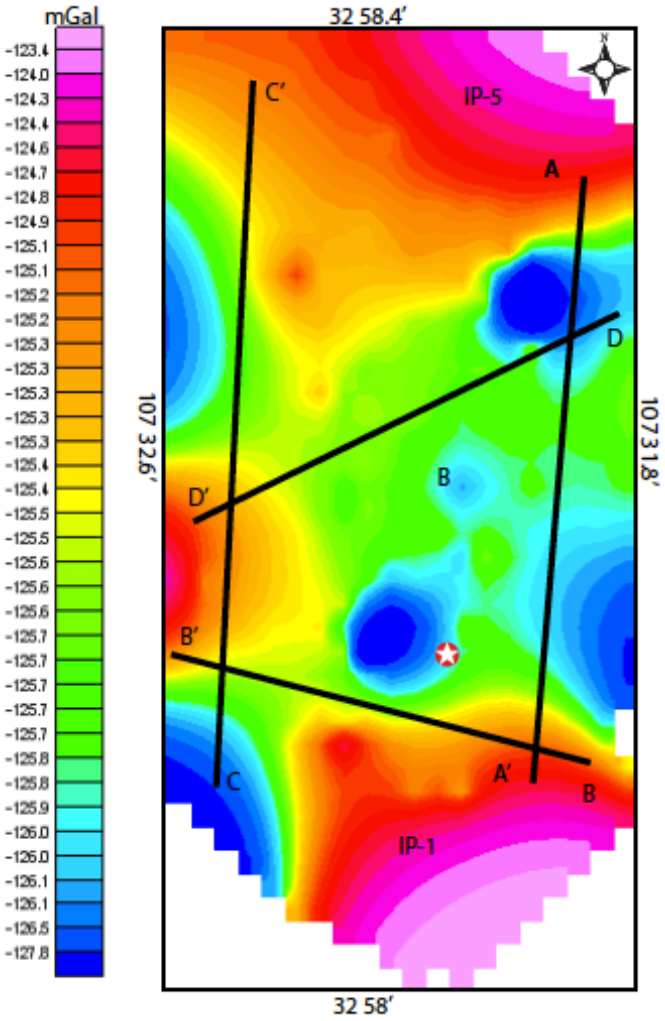

Figure 7.1: Location map of profiles. The star is the base station.

Figure 7.1 shows the location of four profiles that were constructed from the Complete Bouguer Anomaly data to analyze the effect of the faulting on the deposit. The profiles A-A' and D-D' cross the main mineral deposit, seen as gravity low in Figure 7.1, and the anomalies, A and D, at the sides of the deposit. The profiles B-B' and C-C' cross the south anomaly, C or IP-1, and the structures locate as the SW of the deposit. The distances in meters between each coordinate point used in the profiles were calculated from the latitude and longitude at each point. Since the most important cause of the anomalies is likely to be the fault junction, the use of a Talwani base software was the optimal option for the first set of profiles. The Talwani program allows creating different subsurface bodies based on the geology of the deposit in order to match the gravity anomaly pattern that is based on the gravity surface readings. There are an infinite number of mass distribution and body geometries that affects the gravitational attraction. The anomaly is calculated for specified polygon based method (Talwani et. al., 1959).

The Talwani models have numerical integration approaches that were used to divide every model into polygons. Each model has a depth of one kilometer and width depending on the length of each of the lines created. The profiles were sectioned into polygons, each polygon was assigned an specific density depending on the body being drawn. The elements of the models are bounded by known structures to be able to create polygonal sections for further modeling.

Due to the nature of the polygon prism program, there is some discrepancy between the color scales of the gravity maps and the polygon models. Figure 7.2 relates this two color scale in order to cross reference the gravity maps with the polygon models in this section.

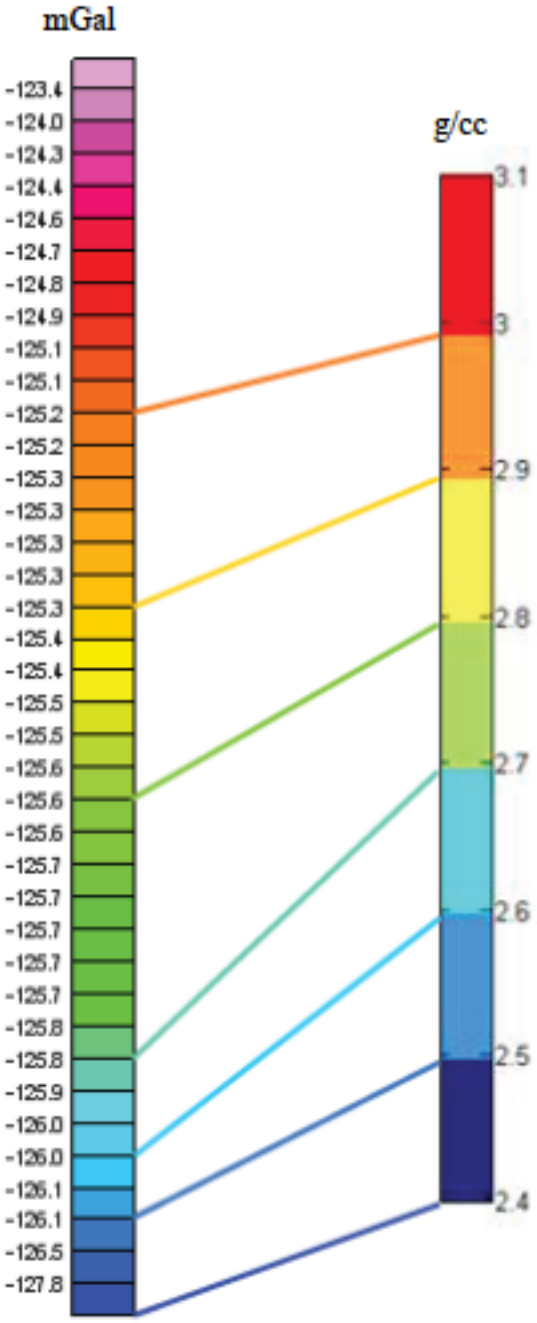

Figure 7.2: Color scale range between maps and polygon model.

7.2 SECTION A-A'

The A-A' profile below has a north-south direction it depicts the mineralize body in the middle of the profile. The south anomaly, C or IP-1, is shown in its entirety on profile. The rest of the anomalies are partially shown due to the lack of gravity readings further north. Taking into consideration that this anomaly is present, the fitting of the profile was modified accordingly. The modification in the profile explains that there is a structural change in this part of the profile. Given this, it can be said that the anomaly found at the south end of the model may be cause by the junction of the Geer and Hunter fault meet. There is no major change in the lithology that can explain the south anomaly since the density values are very similar at this zone. In Figure 7.3, the minimal change of densities could be seen more clearly pass the 0.8 kilometer mark of the profile. Figure 7.4 is the polygonal grid made with the different rock densities based on the geologic cross-section and assumed density for each polygon. The color scales goes from 2.5 mGals to 2.7 mGals with 5 major body types present in the model. The gravity high that represents the south anomaly can be seen at the transition from low to high gravity shown on the profile below. Figure 7.3 also supports the idea that there is no other geological body that could cause the change in gravity after the 0.8 kilometers mark in the profile. The biotite breccia with a density of 2.4 g/cc is very narrow at this area as seen in the figure below.

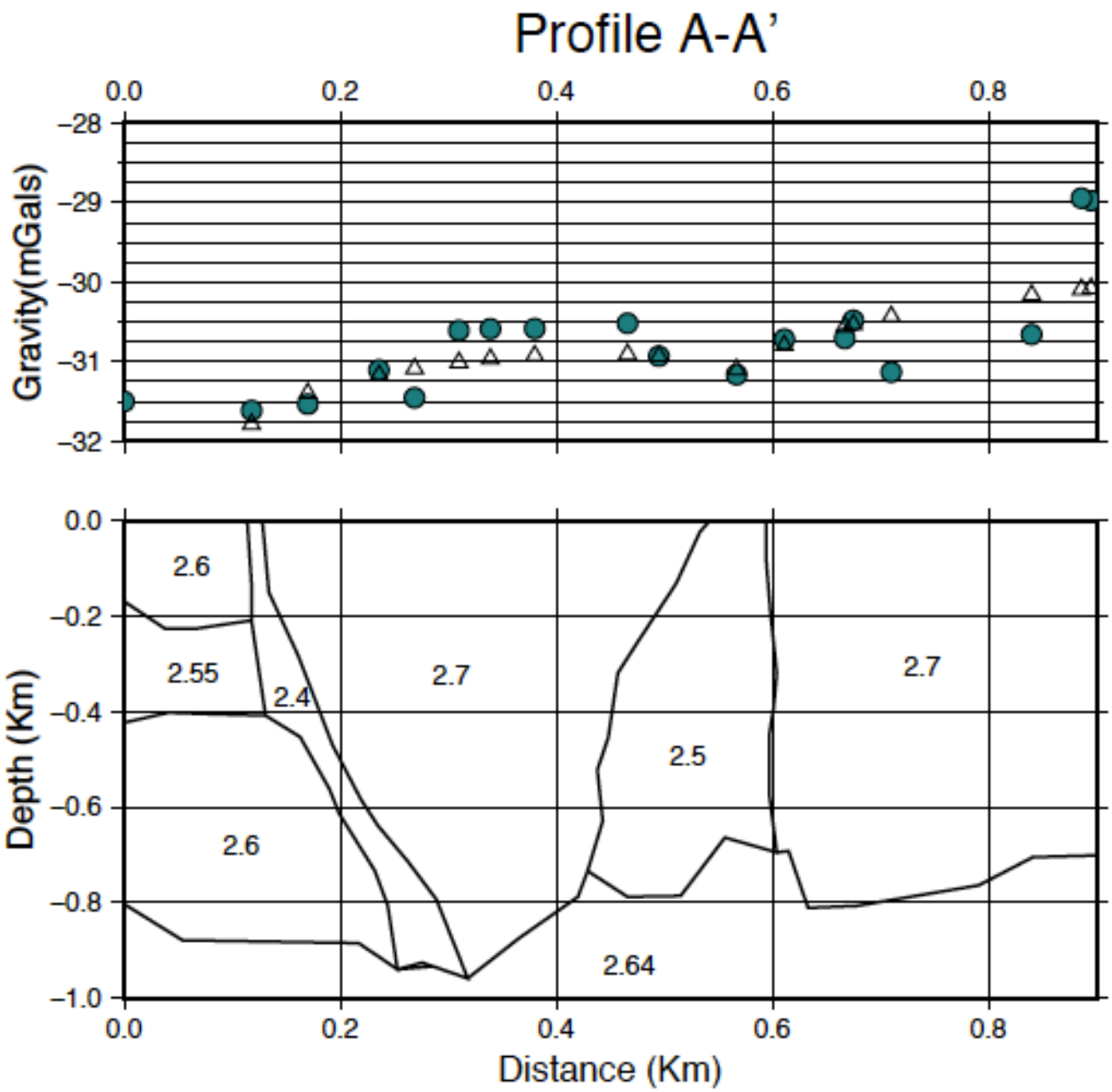

Figure 7.3: A-A' profile of the Complete Bouguer Anomaly. The exes are the observe readings and the triangles are the calculated values.

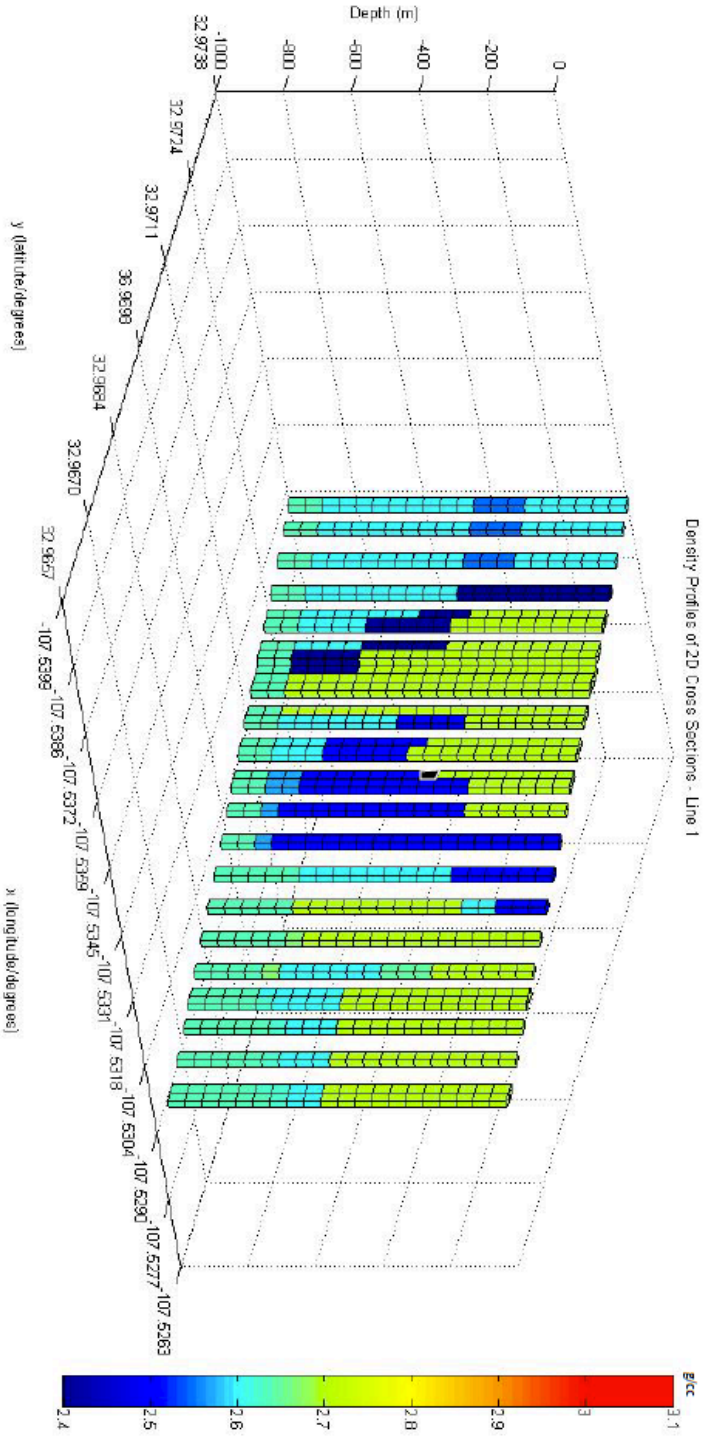

Figure 7.4: Polygon profile of line A-A'.

7.3 SECTION B-B'

The B-B' profile below has an east-west direction and it depicts, C or IP-1, the anomaly body in the south of Copper Flat. The gravity high causing the south anomaly can be seen between the 0.6-0.8 kilometer mark in gravity profile below. There is no major structure or body at this profile other than the Greer Fault. The anomaly is believed to be caused by dissemination of pyritze and chalcopyrite at this area.

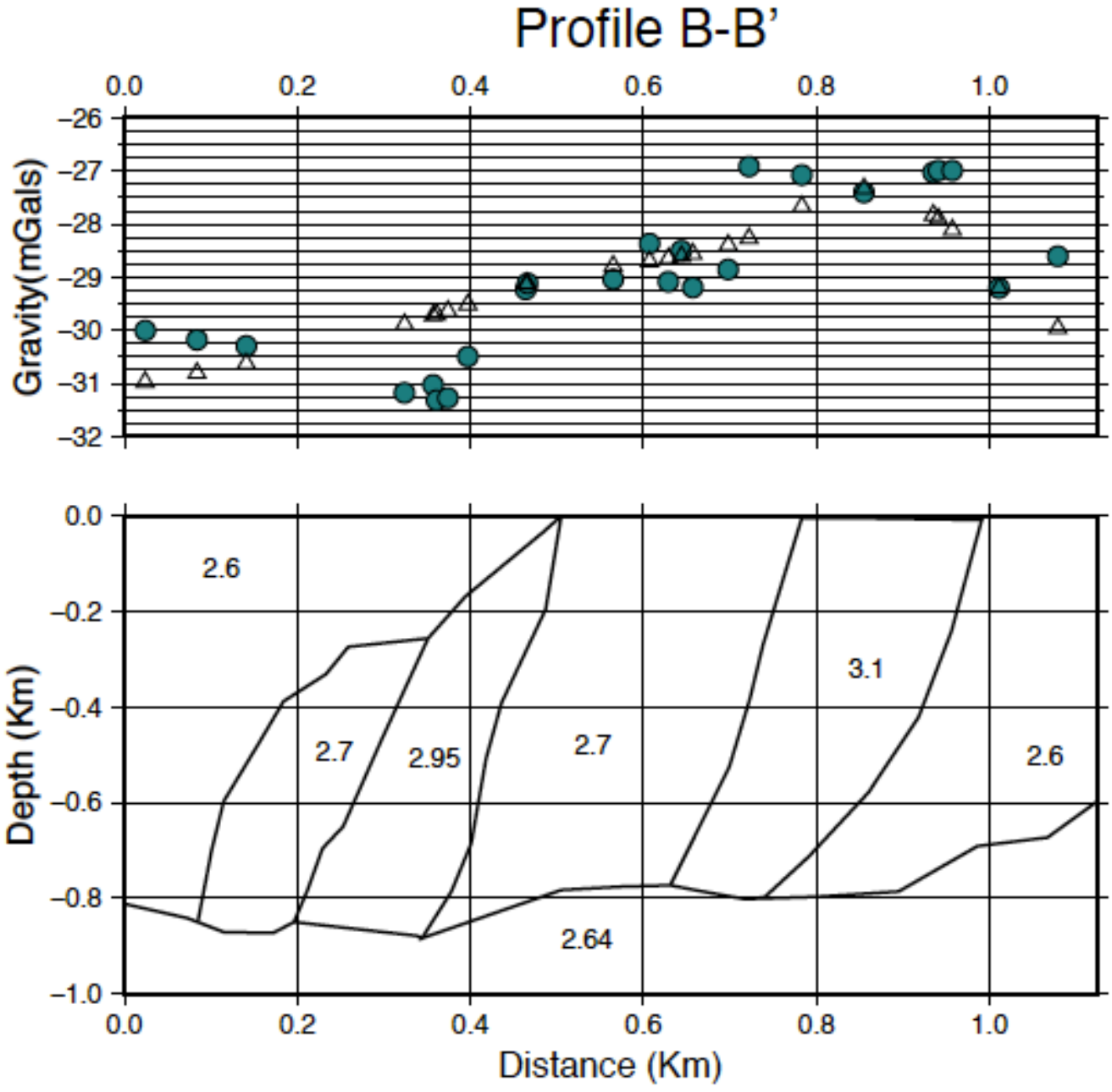

Figure 7.5: B-B' profile of the Complete Bouguer anomaly. The direction of the profile is east-west.

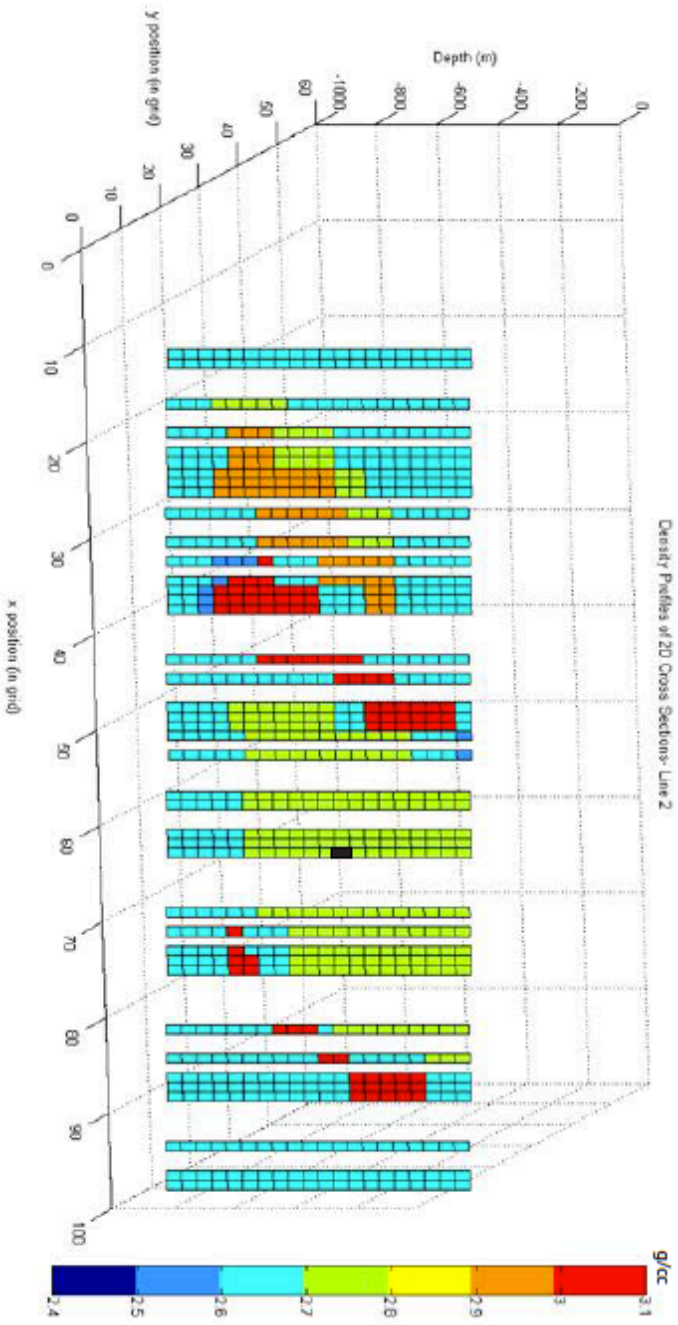

Figure 7.6: B-B' profile of the polygon grid to be used with Pluff approach. The profile has a East and West direction.

7.4 SECTION C-C'

The C-C' profile below has a north-south direction it is located on the west boundary of the deposit. The profile is set close to the contact between andesite and quartz monzonite. This transition does not affect the profile significantly to cause the smaller anomaly seen at the center of the profile. thiThe difference between the calculated and the observed gravity at the beginning of this profile (0.2 kilometers mark) is caused the junction of the Hunter and Greer Faults. The major issue with the calculations and discrepancy approximately at 0.25 kilometers on the profiles see Figure 7.7, this part of the model is that there is not enough gravity reading at this area since it is outside property of Copper Flat. Towards the end of the profile is a gravity low where the breccia was crosscut by the Hungerfold, Bowden, and Hunter Fault. The displacement of the quartz-feldspar breccia and biotite breccia can be seen in Figure 7.8 at the 0.4 kilometer mark. The polygonal grid for this profile section is more complex compare to the previous two profiles discussed. The change on densities for each of the polygons is more scattered, and this is due to the number of fault crossing this area. The scattering of the polygons is more noticeable on the x-axis from the 10 to 20 mark. Most of the anomalies at these profiles are caused by faulting and latite dikes in the area. The latite dikes were not included as part of the bodies on the profile since the size of the dikes is too small compared to the scale of the profile.

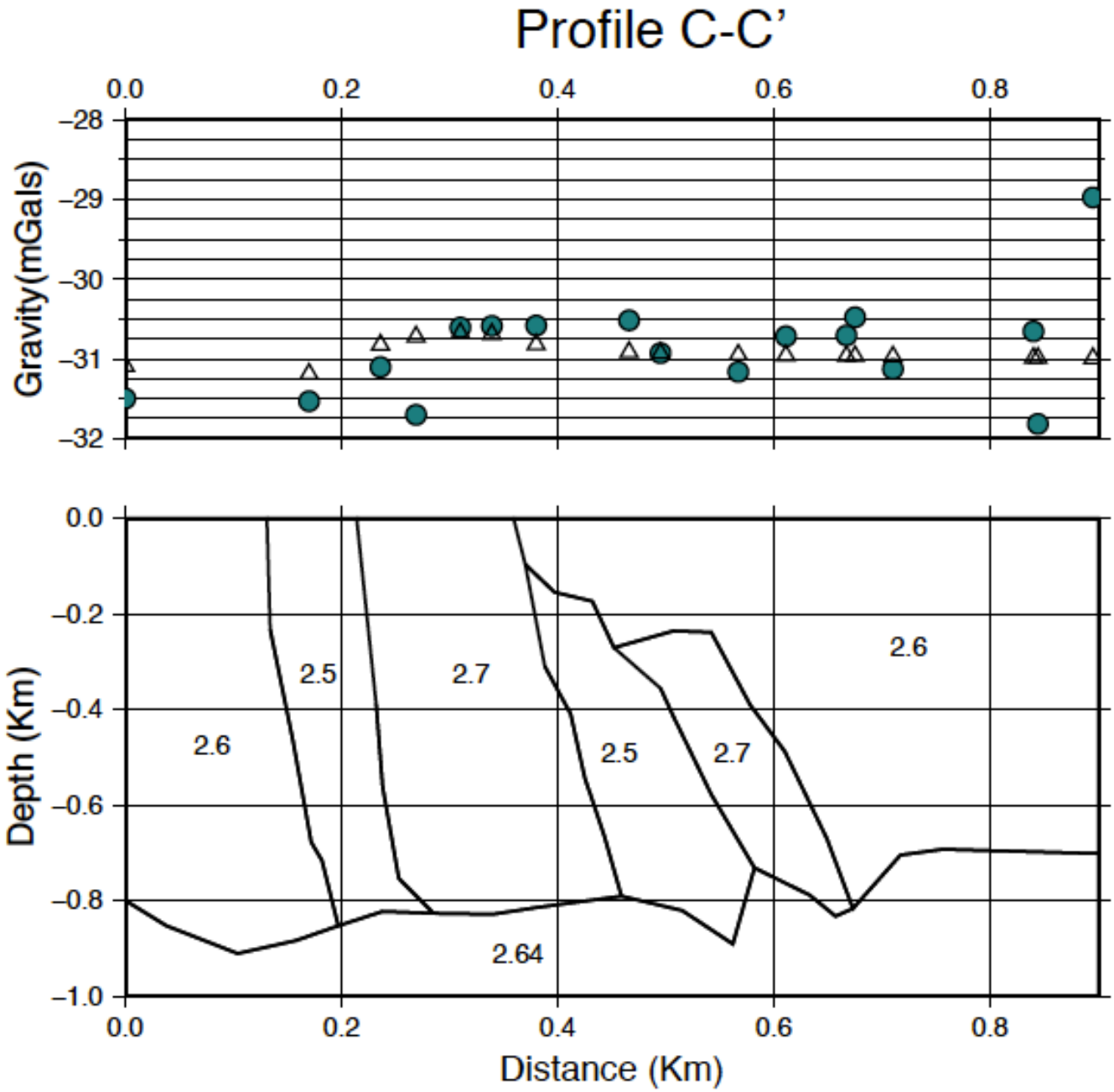

Figure 7.7: C-C’ profile of Bouguer Anomaly. The profile has a south and north direction.

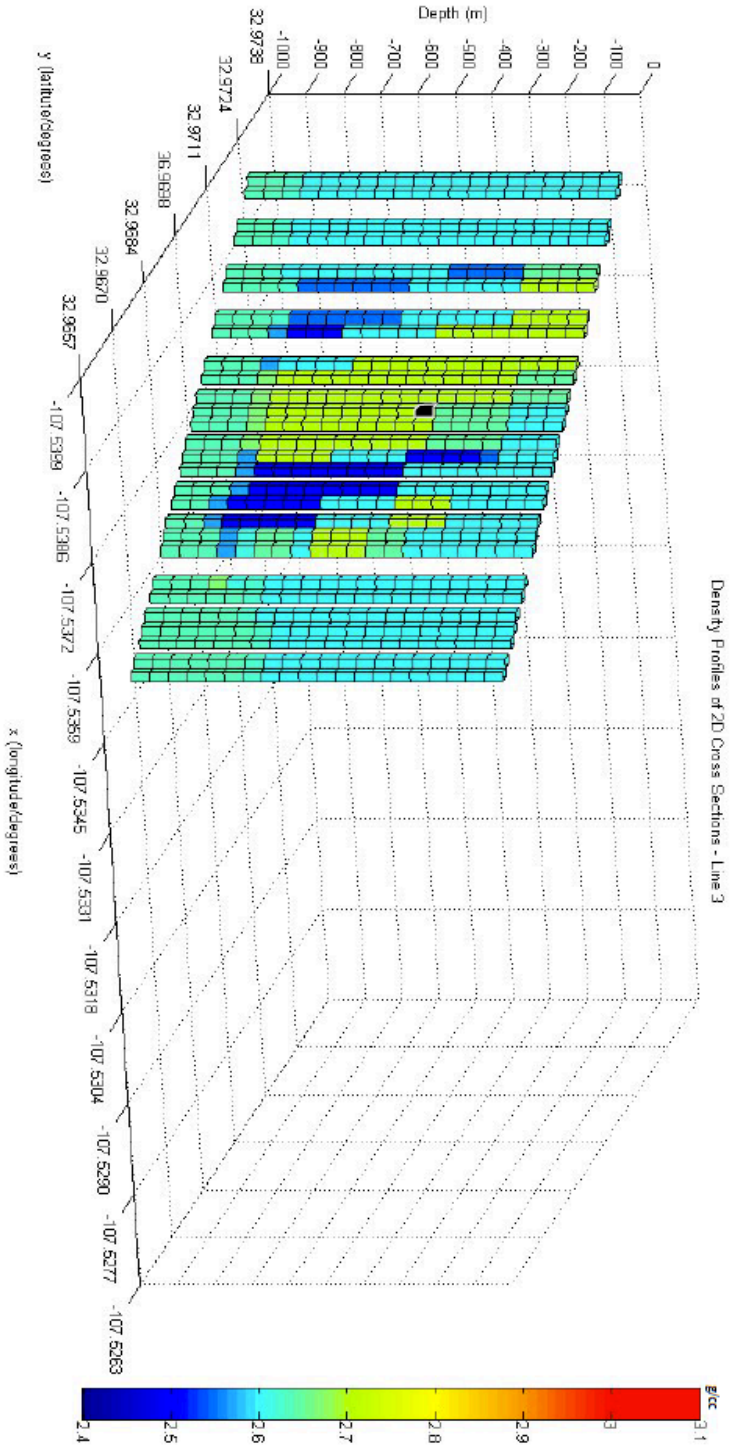

Figure 7.8: C-C’ profile of the polygon grid.

7.5 SECTION D-D'

The second profile D-D' (Figure 7.9) is located mostly at the middle of the map zone and has a northeast-southwest direction. The profile in relation with the other profiles has an almost smooth vertical slope due the gradual change in density in this profile. The importance of this profile was to test the western boundary of the model where some minor anomaly was found while producing the gravity maps. This anomaly, D, was not present or at least was not part of the anomalies emphasized by Quantec. There is a fault junction near this site where the Bowden and Patten fault cross each other. Although, it is more reliable to say that this sudden change in the profile is the expression of the Bowden fault cutting the breccia at Copper Flat. The presence of a syenite body at the 0.7 kilometers mark on Figure 7.8 also affects the model especially after the middle of the section but the difference in density is not as influent as expected.

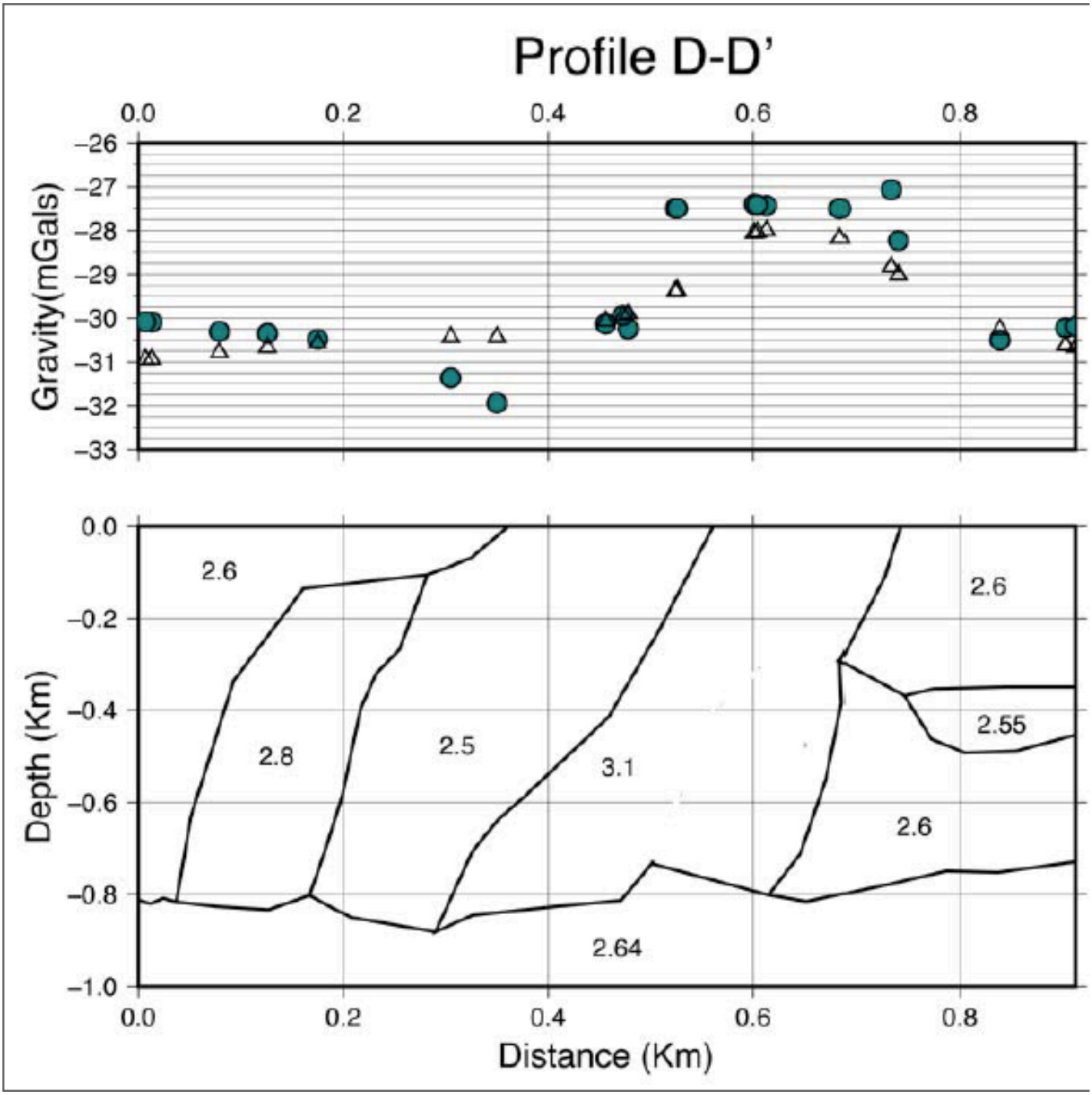

Figure 7.9: D-D' profile of Bouguer Anomaly. The profile has a north and south direction.

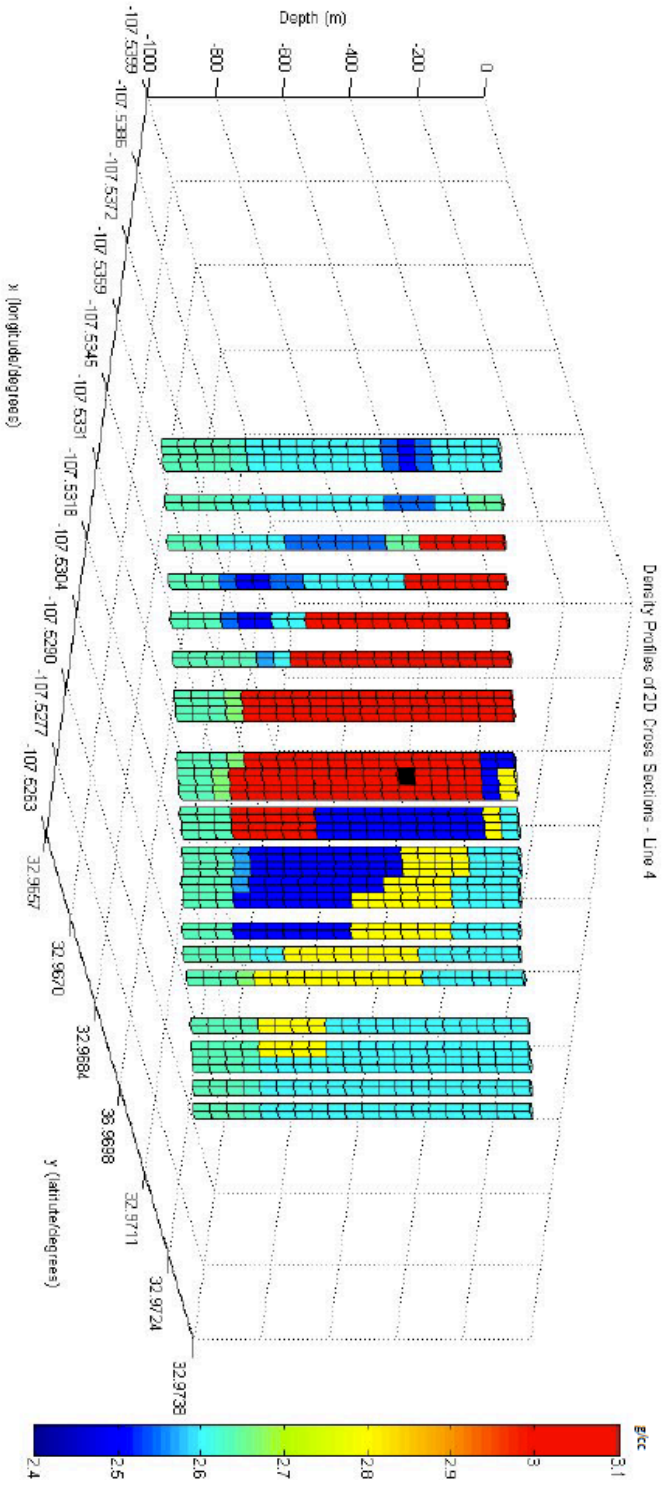

Figure 7.10: D-D’ profile of the polygon grid.

7.6 3D MODELS

The 3D models were created with an input of x, y, and z coordinates of polygon corners. Each of the four profiles previously made are the main planes to produce the modeling as seen in Figure 7.10. The program calculates the gravity effect of three-dimensional models that consist of elements that form polygons in plan view (Plouff, 1976). The calculation of the polygons used an exact formula instead of the numerical integration of the profile made with a Talwani approach. A least-squared comparison between the calculated and observed gravity is used to determine the best fitting gravity vectors and the best susceptibility for the assemblage of polygonal prisms (Godson, 1983).

The models are bounded by horizontal planes (previous polygon grid profiles) and have series of intercepting vertical planes. The 4 profiles are interpolated for each of the layers created in order to fill the gaps between the profiles. The interpolation of the model can be seen in Figure 7.12. The interpolation of the profile has a main problem, it does not fill the calculated block for the Copper Flat area especially at the edge of the block creating an incomplete model; it makes the interpretation hard at the edges. Extrapolation was use to fill the edges of the block, but the color scale of the extrapolation model do not change in comparison of the one use for interpolation due to the changes on the code to produce the extrapolation model in the transition between geologic bodies. The extrapolation model can be seen in Figure 7.13. Figure 7.14 shows the middle of the 3D model with the location of the center of the ore body and the position of anomalies A and C. The position of the anomalies as well the main mineralized body is important. It helps cross-reference the information with the model made by Quantec as well as the models done in this research.

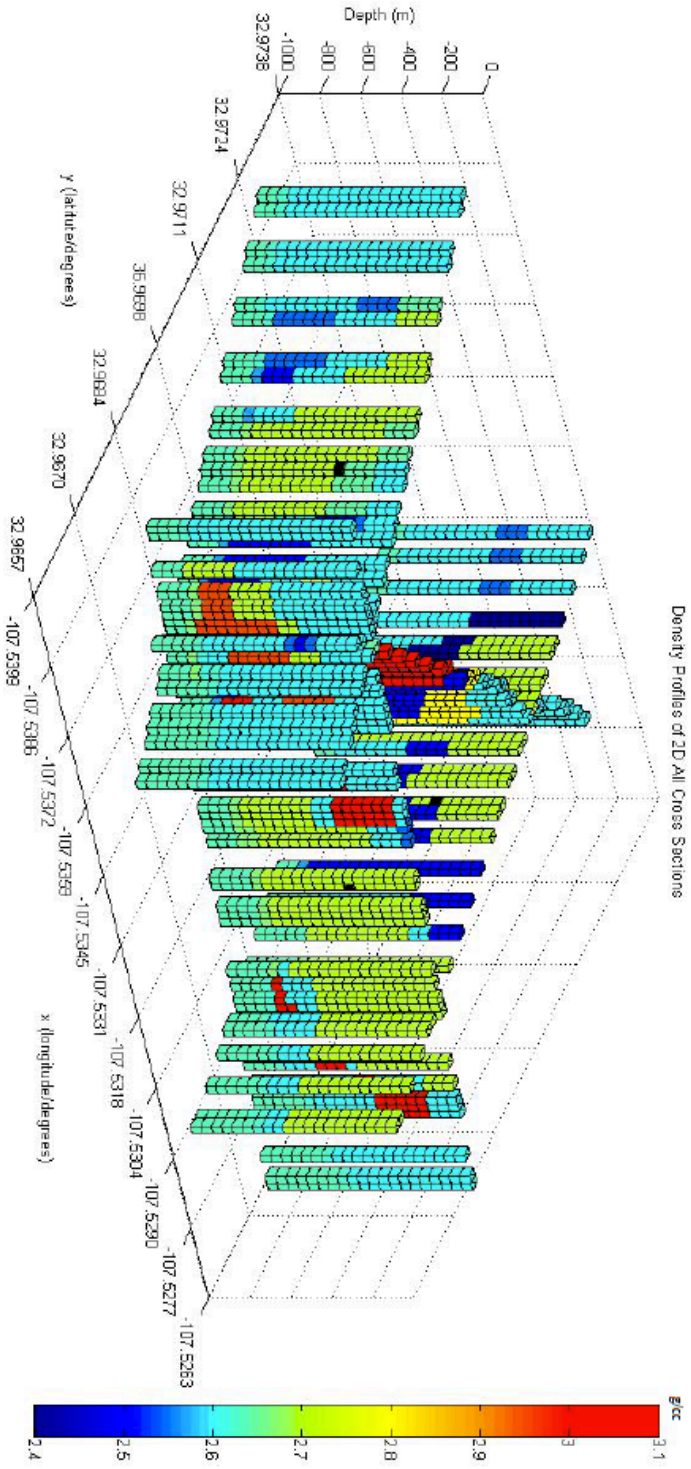

Figure 7.11: The four profiles of the polygon grids prior to interpolation.

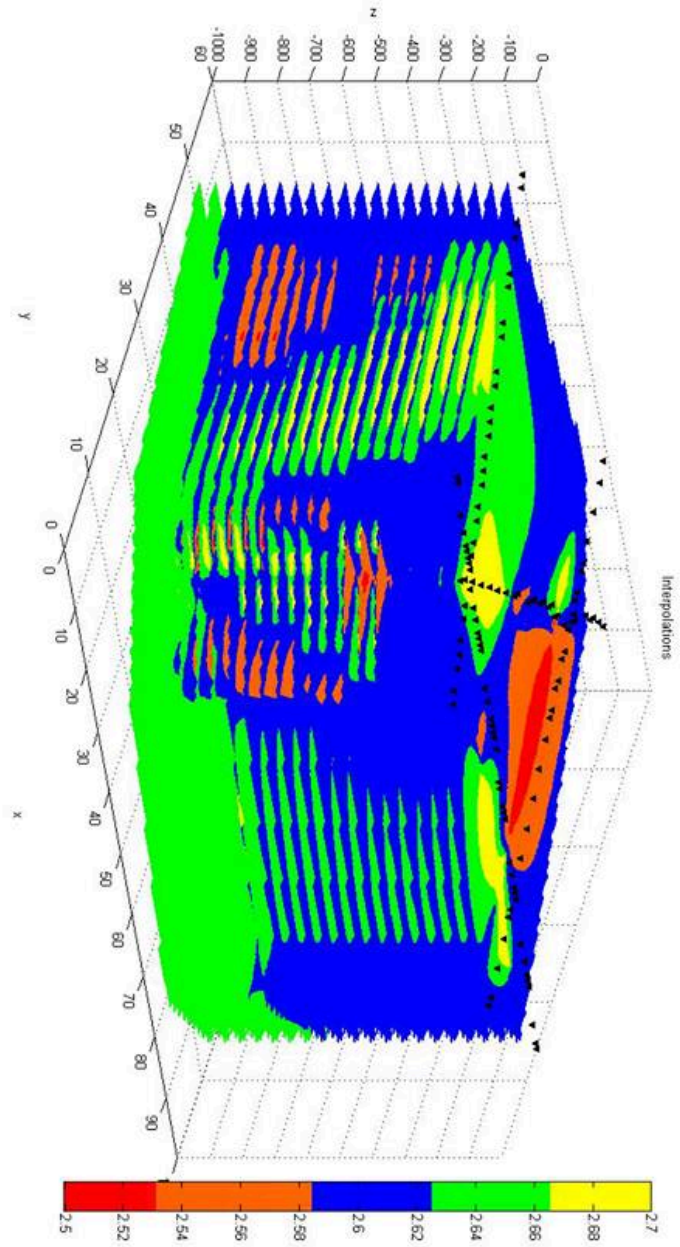

Figure 7.12: Interpolation 3D model.

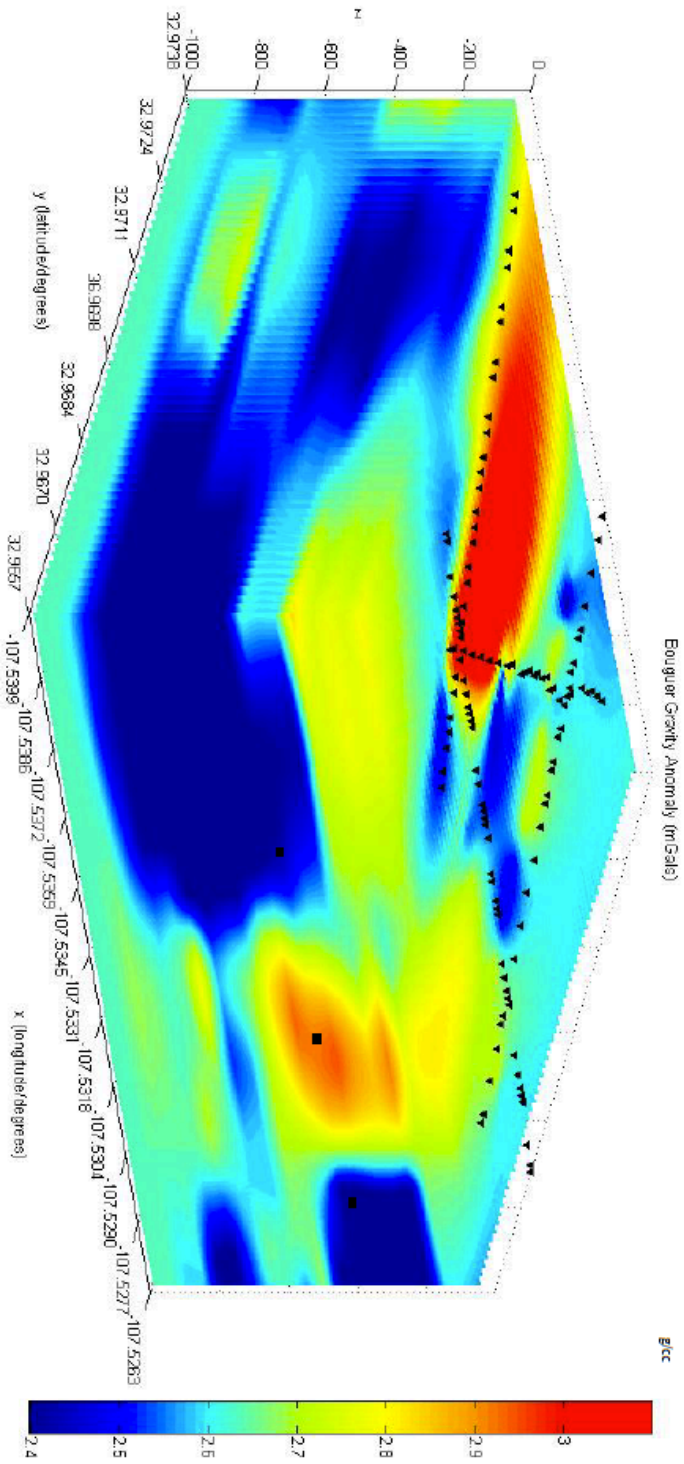

Figure 7.13: Extrapolation 3D model.

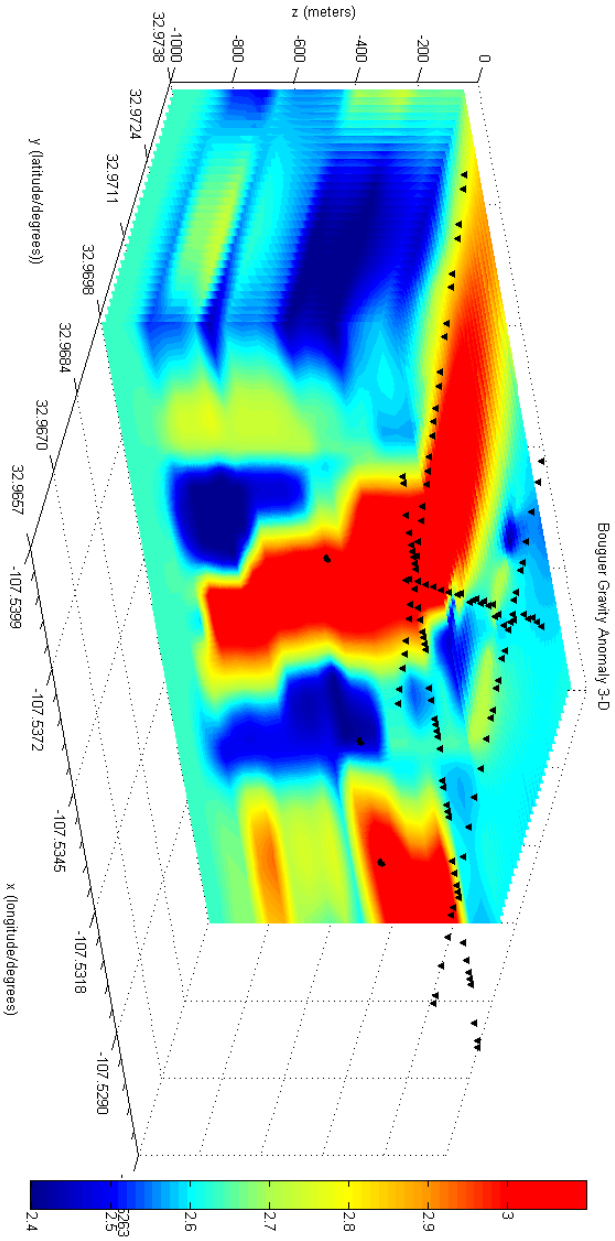

Figure 7.14: 3D model section with projected location points. From left to right the squares represent: A refers to the north anomaly, B is the mineral deposit and C is south anomaly.

The interpretation of the north anomaly, A or IP-5, as previously discussed in other chapters has several factors that could explain the change in density. The profile A-A' could not explain this due to insufficient data there is a drop on the density seen in Figure 6.2. The syenite rock found while drilling the north anomaly could be the major factor in the change in density at this part of Copper Flat. The effect of the syenite body on both the 2D and 3D models is weighted on the modeling. It was a common belief that the syenite segment at Copper Flat was removed by erosion but this section of rock found could mean that the northeast part of the deposit at Copper Flat was not eroded and there is still traces of this part of the alteration in the deposit. The difference in density between (0.2-0.4 mGals) the quartz monzonite and the syenite body is sufficient to cause these high anomalies. The only problem is that there is no proof or solid evidence that can prove that there is a continuous body of syenite at the deposit and it was not a unique finding at the drill hole in this area.

Chapter 8: Discussion

After modeling the Copper Flat area some conclusions were made about the two main anomalies found in the area (IP-1 and IP-5). The first thing to address is that during the survey there were more anomalies found. This anomalies were not taken into consideration during this study, since the main purpose was to focus in the anomalies found at the north and south side of the mine. These anomalies were mainly found on the west side of the mine and are related to a gravity high. The anomalies previously found during the Quantec survey were found during the modeling of the gravity data as seen in Figure 8.1 (below).

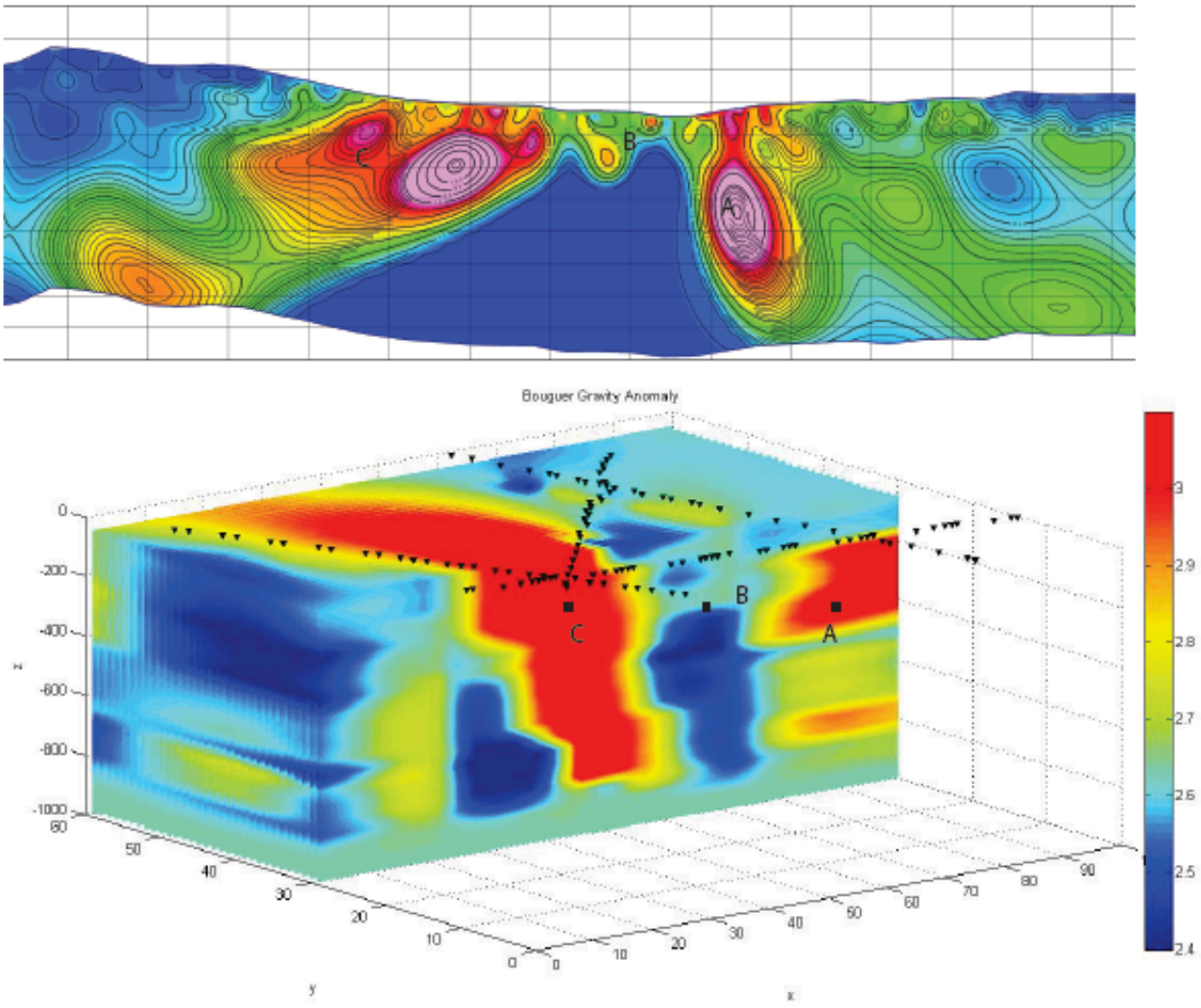

Figure 8.1 Comparison of the IP profile and the 3D profile showing the same anomalies.

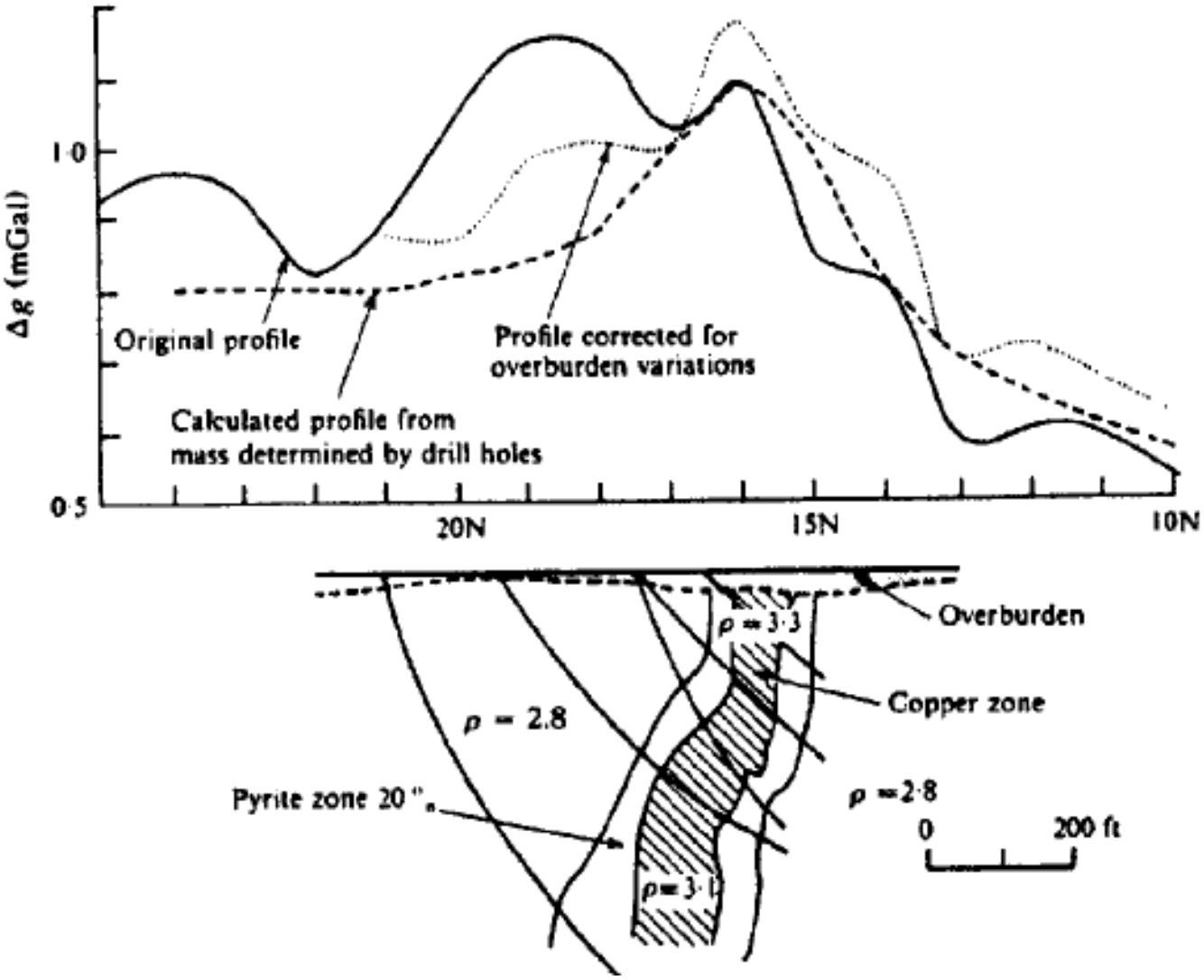

Figure 8.2 Val d'Or Mine gravity model (Musset et. al., 1992)

The decisions made to interpret the geology of the deposit were based on several information about copper porphyry deposits and its behavior in gravity surveys. Porphyry copper deposits almost always appear as moderate gravity lows, especially if the host rock is igneous or metamorphic (Oldenburg et.al., 1997). Taking this statement we know the mineralized area is in fact the gravity low shown in the previous models. Figure 8.2 is an example of the Val d'Or copper deposit in Quebec, Canada. This deposit has a gravity high where the pyrite concentration similar to the one at Copper Flat. Also, according to Musset et. al., (1992) The model is favorable in large areas with low-grade disseminated mineralization just like Copper Flat.

The north anomaly or IP-5 has two major factors affecting it: the presence of a syenite body and a major increase of pyrite in the area. These two factors create a gravity high on the area. The syenite body was thought to have eroded over time as most of the upper part of the porphyry complex at Copper Flat, but the presence of this rock on the area has a significant effect on the area. The second factor creating the gravity high in the area is the increase of pyrite in the area. During the modeling using the Talwani method the crease on pyrite was crucial in being able to match the calculated and observed gravity readings. The density of the pyrite was added to the density of the biotite and quartz/feldspar breccia in order to have a more realistic density of the area.

The south anomaly or IP-1, is located near the junction of the Geer and Hunter Fault as seen in Figure 8.2. This south anomaly has no major lithology changes to cause the increase in density at this zone. The drill hole information was to confirm that no mayor changes in the geology were present in the area. Also, the amount of pyrite or chalcopyrite the area has no significant change. Unlike the north anomaly the geology at IP-1 is as expected. During the modeling of this area, there was no problem matching the observed and calculated gravity using the known densities of the area. The only difference in this area is the fault junction as well as that this anomaly is in the same direction of the Greer Fault strike. During the residual gravity mapping of this area it was notice that there is a big structure underneath the deposit seen with this method. This deep structure located with residual gravity need to be study to understand if it is the cause of the gravity high at this area. In order to understand this zone the regional geology of the deposit has to be studied and a structural study has to be performed.

Future work on the north anomaly has to be done as well as identifying the syenite body and the geology of the northeast side of the deposit was less erosion of the complex and it could have more mineralization in the area that previously was not recognize. This would help to know if this syenite body was only displaced in the area due to the faulting in the region. Additional studies on the west side of the deposit need to be performed where a relevant gravity high was found.

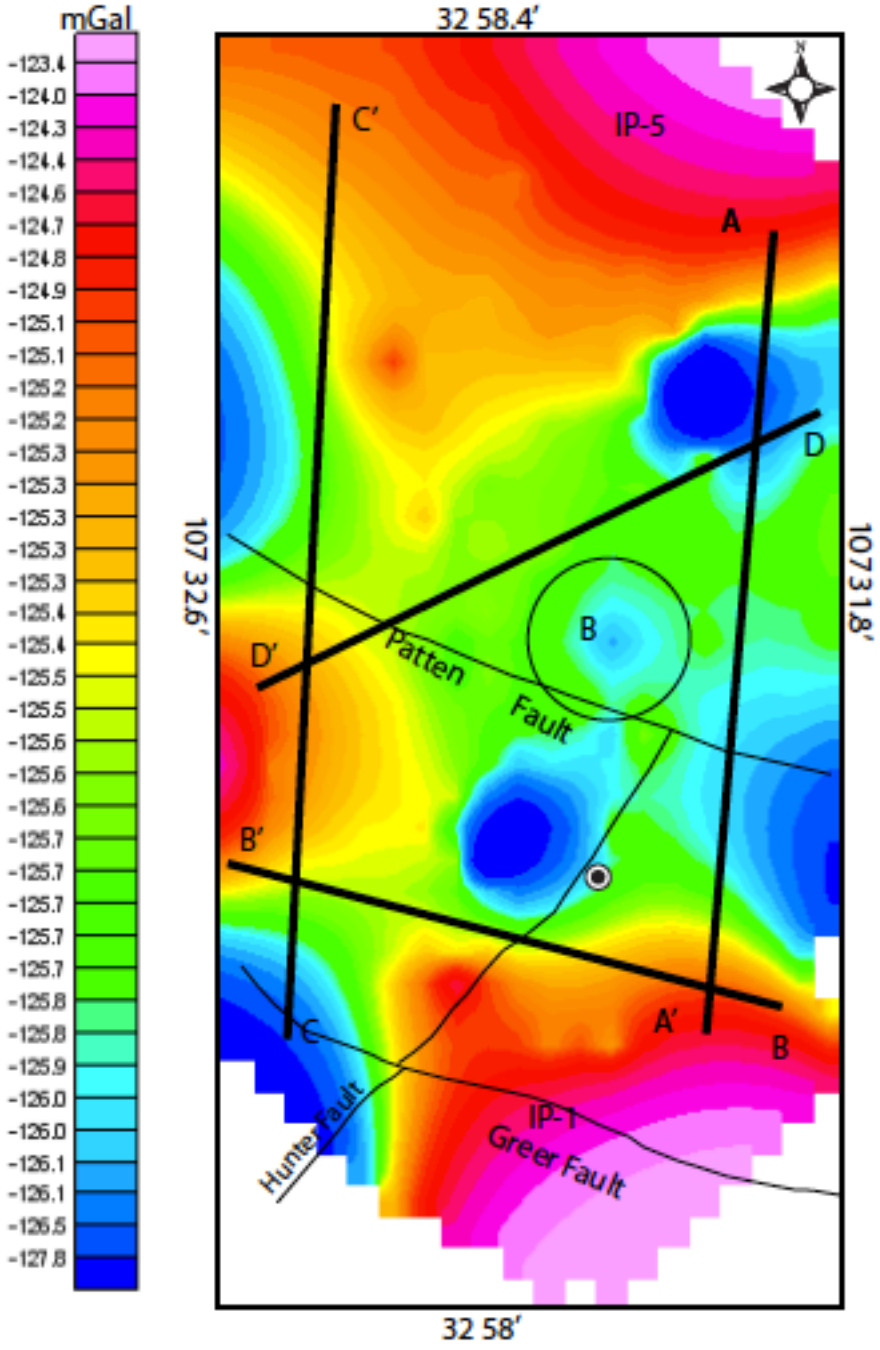

Figure 8.3 Profile line map major faults of Copper Flat.

Chapter 9: Conclusions

The gravity survey and the results obtained with the data processing done in this project resulted in a viable form to recreate the previous geophysical models at Copper Flat. The main mineralized body was defined as a gravity low in all the models produced for this study. There were no changes or extension in the previously mapped area for the breccia stock. The two main anomalies found could be reproduced with the gravity data and an interpretation is provided for each of them on the previous chapters.

The south anomaly, C, is defined as the Geer and Hunter Fault junction. Although there could be some other explanations for this anomaly such as the dissemination of pyrite in the area, the fault junction was selected since the anomaly was reproduced using the layering of the 3D models. The north anomaly, A, is believed to be a body of syenite due to the changes in density with respect to the quartz monzonite in addition to the increase on pyrite on this part of the deposit. Although there is another possibility, such as structural changes, there is not enough evidence to support that theory. The extrapolation 3D model helps in the interpretation of the north anomalies but additional gravity surveys on the north site of Copper Flat is required to have a better model to help understand this part of the deposit.

References

American Geological Institute (AGI), 1987, Glossary of Geologic terms, American Geological Institute, 3rd edition.

Akima, H.,1970: A new method of interpolation and smooth curve fitting based on local procedures. Journal of Association for Computing Machinery, v. 17, no. 4 pp. 589-602.

Briggs, Ian C. "Machine contouring using minimum curvature." *Geophysics* 39, no. 1 (1974): 39-48.

Clarkson, Gerry W 1984, Analysis of Terrestrial Heat-Flow Profiles Across the Rio Grande Rift and Southern Rocky Mountains in Northen New Mexico, in: Rio Grande Rift-- Northern New Mexico, New Mexico Geological Society, Guidebook, 35th Field Conference, pp. 39-44.

Dunn, Peter 1982, Geology of the Copper Flat Porphyry Copper Deposit, Advances in Geology of the Porphyry Copper Deposits, editor S.R. Titley.

Dunn, Peter 1984, Geologic Studies During the Development of the Copper Flat Porphyry Deposit, Minining Engineering, February, 1984, pg. 151

Dunn, Peter, Birak, D.J., Doe, T.C., Stevens, D.L., Mateer, R.G., and Mercier, J.M. 1992, Development Geology of the Copper Flat Porphyry Copper Deposit, SME Minning Engineering Handbook, 2nd Edition, Vol. 1

Dunn-Behre, Dolbear, 1993, Due Diligence Study of the Copper Flat Porphyry Copper Project, New Mexico. Unpublished Report for Golde Express Corp. 1993.

Fowler, L.L. 1982, Brecciation, Alteration, and Mineralization at the Copper Flat Porphyry-Copper Deposit, Hillsboro, New Mexico. M.S. Thesis, Univ. of Arizona, Tucson, 133p.

Geosoft, 2011, Topics in Gridding, On-line resource through Geosoft Inc.

Godson, Richard H. 1983, Magpoly: A Modification f a Three-Dimentional Magnetic Modeling Program, United States Department of the Interior Geological Survey , open-File Report 83-345

Guilbert, J.M., Park, C.F., Jr., 1986, The Geology of Ore Deposits Freeman, New York, 985pp.

Harley, G.T., 1934, The Geology and Ore Deposits of Sierra County, New Mexico, N.M. Bur. Mines, Resources Bulletin 10, 220 pp.

Hedlund, D.C. 1974, Age and Structural Settings of Base Metal Mineralization in the Hillsboro San Lorenzo Area, Southwestern New Mexico.

Hedlund, D., 1985, Economic Geology of Some Selected Mines in the Hillsboro and San Lorenzo Quadrangles, Grant and Sierra Counties, New Mexico, Open File Report, 85-0456,United States Department of the Interior, Geological Survey, Denver, Colorado.

Keith, S.B. and Swan, M.M. 1995, Tectonic Setting Petrology, and Genis of the Laramide Porphyry Copper Cluster of Arizona, Sonora, and New Mexico: Arizona Geological Society Digest, v.20, pp. 127-155

MacLeod, Ian N., and Dobush, Tim M., 2009 Geophysics - More Than NumbersProcessing and Presentation of Geophysical Data, http://www.geosoft.com/media/uploads/resources/technical-papers/geophysicsmorethannumbers.pdf

McLemore, V.T., Munroe, E.A., Heizler, M.T., and McKee, C. 1999, Geochemistry of the Copper Flat Porphyry and Associated Deposits in the Hillsboro Mining District, Sierra County, New Mexico, USA, in: Journal of Geochemical Exploration 67, pp. 167–189.

McLemore, V.T., Munroe, E.A., Heizler, M.T., and McKee, C. 2000, Geology and Evolution of the Mineral Deposits in the Hillsboro District, Sierra County, New Mexico, Geology and Ore Deposits 2000: in The Great Basin and Beyond, proceedings Volume One, 17p.

McLemore, V. T., Munroe, E. A., Heizler, M. T. and McKee, C., 2000, Geology and evolution of the Copper Flat Porphyry-Copper and associated mineral deposits in the Hillsboro mining district, Sierra County, New Mexico; in Cluer, J. K., Price, J. G., Struhsacker, E. M., Hardyman, R. F. and Morris, C. L. eds., Geology and Ore Deposits 2000, The Great Basin and Beyond: Geological Society of Nevada, Symposium Proceedings, pp. 643-659.

McLemore, V.T., 2001, Geology and Evolution of the Copper Flat Porphyry System, Sierra County, New Mexico, on-line resource though New Mexico Tech.

Mussett, A. E., W. M. Telford, L. P. Geldart and R. E. Sheriff, 1992, Applied Geophysics (2nd edition) , Cambridge University Press.

New Mexico Bureau of Geology and Mineral Resources 2003, Geologic Map of New Mexico, 1:500,000: New Mexico Buruau of Geology and Mineral Resources.\

LaFehr, Thomas R., Nabighian, Misac N., 2012, Geophysical Monograph Series: Fundamentals f Gravity Exploration, Society of Exploration Geophysics.

Oldenburg, D.W., Li, Y., and Ellis, R.G., 1997, Inversion of Geophysical Data Over a Gold Porphyry Desposit- A Case History of Mt. Milligan, Geophysics, v.62 p 1419-1431.

Plouff, D. 1976, Gravity and Magnetic Fields of Polygonal Prisms and Application to Magnetic Terrain Corrections, Geophysics, 41: 727-741.

Quantec Geoscience LTD. 2011, Titan-24 DC/IP/MT Survey Geophysical Report Copper Flats New Mexico, USA on Behalf of New Mexico Copper Corporations, unpublished.

Quintana Minerals Corporation 1980, Hillsboro-Copper Flat Project: Fesibility Report, unpublished.

Raugust, J. S., 2003, The Natural Defenses of Copper Flat, Sierra County, New Mexico, New Mexico Bureau of Geology and Mineral Resources, Open File Report, NMBGMR OFR- 475, 485p.

Reeves, C.C. Jr., 1963, Economic Geology of a Part of the Hillsboro, New Mexico, Mining District, Economic Geology, vol.58, pg 1278-1284.

Richards, J.P. 2003, Tectono-Magnetic Precursors for Geophysical Data Over a Copper Gold Porphyry Cu-(Mo-Au) Deposit Formation, Journal of Economic Geology, V.96 pp. 419-1431

Sambridge, M., Braun, J., and McQueen, H., 1995, Geophysical Parameterization and Interpolation of Irregular Data Using Natural Neighbours, Geophysical Journal International, 122 837-857.

Segerstrom, K., and Antweiler, J.C., III, 1975, Placer-Gold Deposits of the Las Animas District, Sierra County, New Mexico, Sierra County, New Mexico, U.S. Geological Survey Open-File Report 75-206, 38p.

Sharma, P.V. 1997, Enviromental and Engineering Geophysics, 1st Edition, Cambridge university Press.

Siemers, C.T., Woodward, L/A., and Callender, J.F. (eds.), Ghost Ranch, central-northern New Mexico: New Mexico Geological Society, Guidebok 25 and San Lorenzo quadrangles, Sierra and Grand Counties, New Mexico; with sections on geochemistry and geophysics. U.S. Geological Surveys , Circular 808, iv, 26

Skeels, D.C., 1966, What is Residual Gravity?, 36th Annueal International SEG Meeting in Houston, Texas, 10 November 1966.

SRK Consulting 2001, NI 43-101 Preliminary Assesment THEMAC Resources Group Limited Copper Flat Project, Sierra County, New Mexico.

Talwani, M., Worzel, J.L., Landisman, M., 1959, Rapid Gravity Comunications of Two-Dimentional Bodies with the Application to the Mendocino Submarine Frecture Zone, Journal of Geophysical Research, 64:49-59.

Themac Resources 2012, On-line resource through New Mexico Copper Corporation.

Themac Resources 2013, On-line resource through New Mexico Copper Corporation.

Titley, S.R., 1982, Geology Setting of Porphyry Copper Deposits, Southeastern Arizona, Advances i Geology of the Porphyry Copper Deposits, editor S.R. Titley, pp. 37-58.

Titley, S.R. 1994, An Abridged Overview of Some Features of Porphyry Copper Deposits in the American Southwest, McKelvey Forum 1994, Guidebook for Field Trips.

USGS, 1974, New Mexico Gravity Base Station Catalog, www.usgs.gov

Verdel S.C., Knepper D., Livo K.E., McLemore V.T., Penn B., and Keller R. 2001, Mapping Minerals at the Copper Flat Porphyry, New Mexico, Using AVIRIS Data, AVIRIS Airborne Geoscience Workshop.

Appendix I

The gravity base station used to close the gravity reading loops used during this survey is located in Truth or Consequences, New Mexico. The exact location is on the latitude of 33 07.80'N and a Longitude of 107 15.16'W with and elevation of 1296.9 meters over see level. The adopted gravity value at this point is 979,168.06 mGals with an estimated accuracy of +/- 0.1 mGals. Other related information about this gravity base station can be found in the USGS 1974 New Mexico Gravity Base Station Catalog. The map of the gravity base station is below:

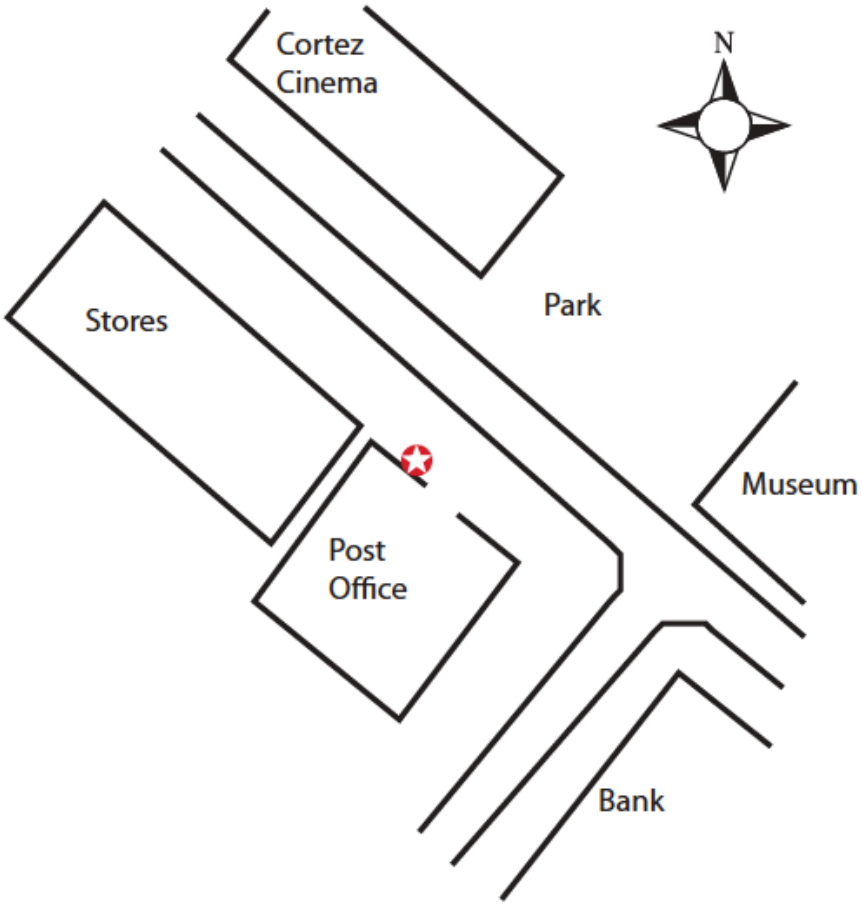

Figure Appendix 1: Locations of Gravity Base Station.

Appendix II

The different formulas used for the calculation mentioned in the thesis are below. The formulas were taken from LaFehr et. al., 2012.

Complete Bouguer Anomaly

$$\Delta g_{cb} = g_{obs} - g_{fa} - g_{sb} - g_t - g_0$$

Where:

$\Delta g_{cb} = complete\ Bouguer\ anomaly$

$g_{obs} = Observed\ Gravity$

$g_{fa} = Free\ Air\ Anomaly$

$g_{sb} = Boguer\ Correction$

$g_{gt} = terrain\ Correction$

$g_0 = theoretical\ gravity$

Residual Gravity:

$$g_{res} = \left(g_{obs} / g_t\right) \bullet \left(g_{fa} / g_{cb}\right)$$

Free Air Correction:

$$C_F = 3.086h$$

Bouguer Correction:

$$C_B = 0.000419\Delta h\rho$$

Appendix III

The following table is all the data points collected with the different corrections and calculations; some of the gravity reading points are excluded from this table due to filtering of data.

Table appendix III, geophysical survey data

Station (CF - CFR)	Grv_(DD)	Lat	Long	Ele _N ED 83	mea _gr v	driff _co r	Tim e(hr)	absol ute	Fre eair	Bou gue r	latitu de	BA	FA	Residu al
300	2598. 38	32. 967 495 89	- 107. 5304 925	166 9.2 65	263 6.97 8	263 6.97 8	8.21	9792 06.32 8	515 .13 5	186. 624	9795 62.67 5	- 27. 83 5	158 .78 9	2.719 88316 3
301	2598. 95	32. 967 495 87	- 107. 5304 926	166 9.2 67	263 7.55 8	263 7.55 4	8.2 7	9792 06.90 4	515 .13 6	186. 624	9795 62.67 5	- 27. 25 9	159 .36 5	2.719 88179 7
302	2599. 04	32. 967 442 42	- 107. 5312 382	167 2.1 32	263 7.65 0	263 7.64 2	8.3 1	9792 06.99 2	516 .02 0	186. 944	9795 62.67 0	- 26. 60 2	160 .34 2	2.719 88158 1
303	2598. 61	32. 967 450 45	- 107. 5317 581	167 3.7 05	263 7.21 2	263 7.20 0	8.3 8	9792 06.55 0	516 .50 5	187. 120	9795 62.67 1	- 26. 73 6	160 .38 4	2.719 88261 2
304	2598. 59	32. 967 689 92	- 107. 5325 436	167 3.6 69	263 7.19 2	263 7.17 6	8.4 3	9792 06.52 6	516 .49 4	187. 116	9795 62.69 1	- 26. 78 7	160 .32 9	2.719 88266
305	2598. 47	32. 967 823 59	- 107. 5330 79	167 4.1 08	263 7.07 0	263 7.05 0	8.4 9	9792 06.40 0	516 .63 0	187. 165	9795 62.70 2	- 26. 83 8	160 .32 8	2.719 88294 8
306	2598. 24	32. 967 983 56	- 107. 5337 405	167 3.9 73	263 6.83 6	263 6.81 2	8.5 4	9792 06.16 2	516 .58 8	187. 150	9795 62.71 5	- 27. 11 5	160 .03 5	2.719 88349 9
307	2598. 45	32. 968 246 94	- 107. 5345 517	167 3.8 64	263 7.04 9	263 6.99 3	9	9792 06.34 3	516 .55 4	187. 138	9795 62.73 7	- 26. 97 8	160 .16 0	2.719 88299 5
308	2598. 39	32. 968 568 41	- 107. 5354 541	167 4.0 29	263 6.98 8	263 6.92 8	9.0 5	9792 06.27 8	516 .60 5	187. 156	9795 62.76 3	- 27. 03 6	160 .12 0	2.719 88313 9
309	2598. 17	32. 968 859 79	- 107. 5363 241	167 5.7 06	263 6.76 5	263 6.69 6	9.1 7	9792 06.04 6	517 .12 3	187. 344	9795 62.78 7	- 26. 96 3	160 .38 1	2.719 88366 7
310	2597. 71	32. 968 691 41	- 107. 5372 805	167 6.6 81	263 6.29 7	263 6.22 2	9.2 5	9792 05.57 2	517 .42 4	187. 453	9795 62.77 3	- 27. 23 0	160 .22 2	2.719 88477 1
311	2595. 97	32. 969 141 06	- 107. 5380 538	168 7.3 02	263 4.52 7	263 4.44 0	9.4 2	9792 03.79 0	520 .70 1	188. 640	9795 62.81 1	- 26. 95 9	161 .68 1	2.719 88894 9
400	2595. 66	32. 969	- 107.	168 9.1	263 4.21 1	263 4.11 9	9.5	9792 03.46 9	521 .25 8	188. 842	9795 62.86 1	- 26. 97	161 .86 7	2.719 88969

		74906	5381512	07								5		4
401	2596.18	32.96968318	-107.5373189	1685.777	2634.740	2634.642	9.58	979203.992	520.231	188.470	979562.855	-27.102	161.368	2.7888
402	2597.07	32.96926795	-107.5367104	1680.085	2635.646	2635.515	10.03	979204.865	518.474	187.834	979562.821	-27.315	160.518	2.7886
403	2598.15	32.96913457	-107.5361439	1675.325	2636.744	2636.608	10.11	979205.958	517.005	187.301	979562.810	-27.148	160.153	2.7883
404	2599.28	32.96941081	-107.5354107	1669.361	2637.894	2637.752	10.19	979207.102	515.165	186.635	979562.833	-27.201	159.434	2.7881
405	2598.94	32.96905294	-107.5343729	1668.71	2637.548	2637.401	10.26	979206.751	514.964	186.562	979562.803	-27.650	158.912	2.7881
406	2599.15	32.96872833	-107.5333117	1668.873	2637.761	2637.604	10.41	979206.954	515.014	186.580	979562.776	-27.389	159.191	2.7881
407	2599.94	32.96868453	-107.5322779	1645.43	2638.565	2638.404	10.45	979207.754	507.780	183.959	979562.773	-31.198	152.761	2.7879
408	2600.68	32.96861028	-107.5312142	1642.041	2639.318	2639.154	10.49	979208.504	506.734	183.580	979562.767	-31.109	152.471	2.7877
409	2601.99	32.96838817	-107.5302246	1640.633	2640.650	2640.484	10.53	979209.834	506.299	183.423	979562.748	-30.038	153.385	2.7874
410	2600.94	32.96809957	-107.529504	1639.969	2639.582	2639.412	10.59	979208.762	506.094	183.349	979562.725	-31.217	152.131	2.777
411	2599.78	32.96920229	-107.5281662	1649.5	2638.402	2638.199	11.04	979207.549	509.036	184.414	979562.816	-30.645	153.770	2.7879
500	2600.46	32.97080376	-107.5325389	1662.058	2639.094	2638.888	11.09	979208.238	512.911	185.818	979562.948	-27.617	158.201	2.7878
501	2600.74	32.97077601	-107.5330448	1661.927	2639.379	2639.169	11.14	979208.519	512.871	185.803	979562.945	-27.359	158.444	2.7877
502	2600.56	32.97035251	-107.5330145	1662.034	2639.196	2638.982	11.19	979208.332	512.904	185.815	979562.910	-27.490	158.325	2.7877
503	2600.69	32.96989422	-107.5329845	1661.961	2639.328	2639.104	11.34	979208.454	512.881	185.807	979562.873	-27.345	158.462	2.7877
504	2600.7	32.96961558	-107.5332122	1662.196	2639.338	2639.108	11.42	979208.458	512.954	185.834	979562.850	-27.271	158.562	2.7877
505	2600.	32.	-	166	2639.09	2638.86	11.	979208.21	512.82	185.786	979562.83	-27.	158.19	2.7

	46	96946601	107.5335806	1.769	4	0	47	0	2		7	591	5	8789
506	2600.35	32.96931358	-107.5340222	1660.752	2638.9822	2638.745	11.52	979208.095	512.508	185.672	979562.825	-27.894	157.778	2.7878 2
507	2600.38	32.9696396	-107.534503	1661.789	2639.013	2638.772	11.57	979208.122	512.828	185.788	979562.852	-27.690	158.098	2.7878
508	2600.55	32.96996949	-107.5348782	1661.597	2639.185	2638.912	12.03	979208.262	512.769	185.767	979562.879	-27.615	158.152	2.7877 3
510	2600.43	32.97043205	-107.5350281	1661.297	2639.063	2638.833	11.42	979208.183	512.676	185.733	979562.917	-27.790	157.943	2.7878 1
511	2600.67	32.97070111	-107.5345947	1661.415	2639.308	2639.074	11.47	979208.424	512.713	185.746	979562.939	-27.549	158.197	2.7877 6
512	2600.39	32.97063148	-107.5342583	1660.747	2639.023	2638.786	11.52	979208.136	512.507	185.672	979562.933	-27.963	157.709	2.7878 6
513	2600.65	32.96996949	-107.5348782	1661.597	2639.287	2639.046	11.57	979208.396	512.769	185.767	979562.879	-27.480	158.286	2.7877 4
514	2600.48	32.97043205	-107.5350281	1661.297	2639.114	2638.841	12.03	979208.191	512.676	185.733	979562.917	-27.783	157.950	2.7878 1
515	2600.44	32.97070111	-107.5345947	1661.415	2639.074	2638.796	12.08	979208.146	512.713	185.746	979562.939	-27.826	157.920	2.7878 7
516	2600.67	32.97063148	-107.5342583	1660.747	2639.308	2639.027	12.12	979208.377	512.507	185.672	979562.933	-27.721	157.950	2.7877 6
517	2599.04	32.96749589	-107.5304925	1669.265	2637.650	2636.978	17.58	979206.328	515.135	186.624	979562.675	-27.835	158.789	2.7881 1
600	2598.4	32.96749589	-107.5304925	1669.265	2636.999	2636.974	18.04	979206.629	515.135	186.624	979562.675	-27.535	159.089	2.7883 5
601	2597.11	32.96994233	-107.5277551	1663.801	2635.686	2635.661	18.1	979205.316	513.449	186.013	979562.877	-30.124	155.889	2.7886 1
602	2598.32	32.96948179	-107.5268759	1658.436	2636.917	2636.892	18.15	979206.547	511.793	185.413	979562.839	-29.911	155.502	2.7883 7
603	2600.07	32.96902357	107.52723	1649.363	2638.697	2638.672	18.28	979208.327	508.993	184.399	979562.801	-29.879	154.519	2.7879 3
604	2599.63	32.96821044	-107.5275319	1649.268	2638.250	2638.224	18.38	979207.879	508.964	184.388	979562.734	-30.279	154.109	2.7880 7

605	2599.51	32.967322 98	-107.5272719	1649.336	2638.128	2638.102	18.47	979207.757	508.985	184.396	979562.661	-30.3144	154.081	2.7880 4
606	2599.73	32.967473 72	-107.5263144	1649.881	2638.351	2638.325	18.53	979207.980	509.153	184.457	979562.673	-29.9966	154.461	2.7879 7
607	2599.72	32.968308 71	-107.5264927	1650.168	2638.341	2638.315	18.59	979207.970	509.242	184.489	979562.742	-30.0199	154.470	2.7879 1
608	2598.73	32.969740 51	-107.5288831	1653.817	2637.334	2637.307	19.04	979206.962	510.368	184.897	979562.860	-30.4277	154.470	2.7882 4
609	2597.42	32.970743 7	-107.5289372	1662.063	2636.002	2635.974	19.08	979205.629	512.913	185.819	979562.943	-30.2199	155.599	2.7885 7
610	2596.45	32.971698 44	-107.5288783	1668.243	2635.015	2634.987	19.16	979204.642	514.820	186.510	979563.022	-30.0699	156.441	2.7887 6
611	2595.91	32.972556 13	-107.5294149	1670.124	2634.466	2634.438	19.27	979204.093	515.400	186.720	979563.092	-30.3199	156.401	2.7889 3
612	2595.48	32.971950 32	-107.5298 92	1671.814	2634.028	2634.000	19.37	979203.655	515.922	186.909	979563.042	-30.3744	156.535	2.7890 7
613	2585	32.972326 34	-107.5305607	1659.961	2623.368	2623.340	19.43	979192.995	512.264	185.584	979563.073	-43.3988	142.186	2.7915
614	2597.43	32.971516 52	-107.5307217	1660.204	2636.012	2635.983	19.5	979205.638	512.339	185.611	979563.007	-30.6400	154.971	2.7885 3
615	2596.98	32.971042 29	-107.5302479	1663.012	2635.554	2635.526	19.56	979205.181	513.206	185.925	979562.967	-30.5066	155.419	2.7886 3
616	2598.81	32.970237 93	-107.5296943	1654.22	2637.416	2637.386	20.04	979207.041	510.492	184.942	979562.901	-30.3100	154.632	2.7882 2
617	2599.33	32.969357 7	-107.5294349	1649.242	2637.944	2637.915	20.12	979207.570	508.956	184.385	979562.828	-30.6888	153.697	2.7880 6
618	2600.75	32.968498 83	-107.5292633	1641.588	2639.389	2639.359	20.17	979209.014	506.594	183.530	979562.758	-30.6799	152.850	2.7877 4
619	2600.83	32.968575 34	-107.5301298	1640.834	2639.470	2639.440	20.23	979209.095	506.361	183.445	979562.764	-30.7533	152.693	2.7877 3
620	2598.41	32.967495 89	-107.5304925	1669.265	2637.009	2636.978	20.33	979206.633	515.135	186.624	979562.675	-27.5300	159.094	2.7883 1
699	2598.44	32.967495	-107.5304	1669.265	2637.039	2637.008	20.41	979206.383	515.135	186.624	979562.675	-27.7800	158.844	2.7883 9

		89	925											
700	2600.12	32.96944843	-107.5309696	1644.072	2638.748	2637.567	20.48	979206.942	507.361	183.807	979562.836	-32.341	151.466	2.7878 3
701	2598.68	32.97027854	-107.5320762	1650.343	2637.283	2637.387	7.13	979206.762	509.296	184.508	979562.904	-31.355	153.154	2.7882 4
702	2598.78	32.97075282	-107.5320762	1649.454	2637.385	2637.482	7.2	979206.857	509.022	184.409	979562.943	-31.474	152.935	2.7882 4
703	2598.28	32.97135578	-107.5327948	1650.435	2636.876	2636.966	7.28	979206.341	509.324	184.519	979562.993	-31.847	152.672	2.7883 3
704	2597.83	32.97127875	-107.5310636	1650.095	2636.419	2636.503	7.33	979205.878	509.219	184.481	979562.987	-32.370	152.111	2.7884 3
705	2598.04	32.97118687	-107.5321796	1650.701	2636.632	2636.711	7.39	979206.086	509.406	184.548	979562.979	-32.035	152.513	2.7883 9
706	2599.84	32.96937769	-107.5319519	1643.484	2638.463	2638.538	7.43	979207.913	507.179	183.742	979562.830	-31.479	152.262	2.7879 4
707	2600.55	32.96924967	-107.5322323	1639.984	2639.185	2639.246	7.58	979208.621	506.099	183.350	979562.819	-31.450	151.901	2.7877 3
708	2596.73	32.97154779	-107.5319215	1660.539	2635.300	2635.318	8.02	979204.693	512.442	185.648	979563.009	-31.522	154.126	2.7887 3
709	2594.82	32.97238238	-107.5314702	1670.401	2633.357	2633.363	8.15	979202.738	515.486	186.751	979563.078	-31.605	155.146	2.7891 3
710	2594.93	32.97294138	-107.5308186	1670.638	2633.469	2633.469	8.21	979202.844	515.559	186.777	979563.124	-31.499	155.279	2.7891 9
711	2590.17	32.97358394	-107.5316446	1694.188	2628.627	2628.618	8.3	979197.993	522.826	189.410	979563.177	-31.767	157.643	2.7902 7
712	2594.15	32.97375383	-107.5326884	1674.266	2632.675	2632.658	8.39	979202.033	516.678	187.183	979563.191	-31.662	155.521	2.7893 5
713	2592.49	32.97371782	-107.5335995	1681.737	2630.987	2630.959	8.5	979200.334	518.984	188.018	979563.188	-31.888	156.130	2.7897 2
714	2595.64	32.97293641	-107.5335989	1664.833	2634.191	2634.155	8.58	979203.530	513.767	186.128	979563.124	-31.954	154.174	2.7889 2
715	2595.79	32.97210954	-107.532435	1665.325	2634.344	2634.261	9.07	979203.636	513.919	186.183	979563.055	-31.684	154.500	2.7889 1
716	2596.81	32.971	-107.	1658	2635.38	2635.29	9.15	979204.66	511.95	185.471	979563.03	-31.	153.58	2.7886

		8457	533299	.957	1	1		6	4		4	885	6	1
717	2596.2	32.97257818	-107.534015	1662.774	2634.761	2634.662	9.24	979204.037	513.132	185.898	979563.094	-31.824	154.075	2.7888 6
719	2595.28	32.973485	-107.534539	1666.192	2633.825	2633.715	9.35	979203.090	514.187	186.280	979563.169	-32.172	154.108	2.7890 7
720	2595.62	32.97348474	-107.5345396	1666.195	2634.171	2634.051	9.45	979203.426	514.188	186.281	979563.169	-31.835	154.445	2.7889
721	2596.13	32.97249156	-107.5345518	1662.516	2634.690	2634.561	9.54	979203.936	513.052	185.869	979563.087	-31.967	153.902	2.7888 4
722	2595.51	32.97150222	-107.5351838	1662.638	2634.059	2633.886	10.01	979203.261	513.090	185.883	979563.005	-32.538	153.345	2.7890 4
723	2595.48	32.97098367	-107.5363035	1665.668	2634.028	2633.849	10.07	979203.224	514.025	186.222	979562.963	-31.935	154.287	2.7890 7
724	2594.04	32.9700105	-107.5379349	1665.827	2632.564	2632.371	10.21	979201.746	514.074	186.239	979562.882	-33.301	152.938	2.7893
725	2594.04	32.97113389	-107.5390983	1681.028	2632.564	2632.359	10.33	979201.734	518.765	187.939	979562.975	-30.414	157.525	2.7893
727	2592.43	32.97031725	-107.5391414	1673.843	2630.926	2630.712	10.43	979200.087	516.548	187.136	979562.908	-33.408	153.728	2.7897 7
728	2595.02	32.97031725	-107.5391414	1673.856	2633.560	2633.278	11.14	979202.653	516.552	187.137	979562.908	-30.839	156.298	2.7891 2
729	2595.05	32.96839918	-107.5381067	1668.195	2633.591	2633.302	11.21	979202.677	514.805	186.504	979562.749	-31.771	154.733	2.7891
730	2597.84	32.9691815	-107.5383314	1668.645	2636.429	2636.116	11.46	979205.491	514.944	186.555	979562.814	-28.934	157.621	2.7884 9
731	2597.89	32.97053096	-107.5355954	1651.23	2636.480	2636.163	11.5	979205.538	509.570	184.608	979562.925	-32.425	152.182	2.7884 9
732	2592.93	32.97013578	-107.536265	1652.627	2631.435	2631.113	11.55	979200.488	510.001	184.764	979562.893	-37.168	147.596	2.7896 2
733	2593.5	32.96953712	-107.53669	1653.64	2632.014	2631.633	12.17	979201.008	510.313	184.877	979562.843	-36.399	148.478	2.7894
734	2593.78	32.96724921	-107.5365956	1674.747	2632.299	2631.911	12.24	979201.286	516.827	187.237	979562.654	-31.778	155.459	2.7894 6
735	2596.	32.	-	16	2634.84	2634.44	12.	979203.82	516.89	187.263	979562.59	-29.	158.13	2.7

	28	96647414	107.5355953	74.98	2	6	32	1	9		1	133	0	8884
736	2596.39	32.96659968	-107.5340481	1663.84	2634.954	2634.551	12.4	979203.926	513.461	186.017	979562.601	-31.232	154.786	2.7887
737	2596.36	32.96809767	-107.5362368	1662.303	2634.923	2634.513	12.47	979203.888	512.987	185.845	979562.724	-31.695	154.151	2.78882
738	2596.99	32.96686714	-107.5355854	1663.273	2635.564	2635.146	12.55	979204.521	513.286	185.954	979562.623	-30.769	155.184	2.78869
739	2599.13	32.96710809	-107.5329639	1661.883	2637.741	2637.265	13.15	979206.640	512.857	185.799	979562.643	-28.944	156.855	2.78815
740	2599.1	32.96686251	-107.529552	1647.878	2637.711	2637.230	13.2	979206.605	508.535	184.233	979562.623	-31.715	152.518	2.78817
741	2598.87	32.96712143	-107.5287761	1648.349	2637.477	2636.991	13.25	979206.366	508.681	184.285	979562.644	-31.883	152.403	2.78818
742	2598.95	32.96742409	-107.5297879	1648.742	2637.558	2637.064	13.34	979206.439	508.802	184.329	979562.669	-31.757	152.572	2.78817
743	2598.53	32.9668668	-107.5312666	1649.876	2637.131	2636.625	13.46	979206.000	509.152	184.456	979562.623	-31.927	152.529	2.78824
744	2598.85	32.96716071	-107.5349168	1650.593	2637.456	2636.945	13.52	979206.320	509.373	184.536	979562.647	-31.491	153.046	2.78826
745	2598.93	32.96738969	-107.5338286	1650.5	2637.538	2636.978	14.02	979206.353	509.344	184.526	979562.666	-31.494	153.031	2.78815
901	2598.2	32.96802771	-107.5345868	1650.274	2636.795	2638.225	14.02	979209.005	509.275	184.501	979562.719	-28.940	155.561	2.78835
902	2594.04	32.96898495	-107.538217	1667.991	2632.564	2634.011	14.09	979204.791	514.742	186.481	979562.798	-29.747	156.735	2.7893
903	2594.04	32.96967494	-107.5384827	1668.718	2632.564	2634.018	14.12	979204.798	514.966	186.563	979562.855	-29.653	156.910	2.7893
904	2592.43	32.97023919	-107.5389871	1672.157	2630.926	2632.393	14.17	979203.173	516.028	186.947	979562.901	-30.648	156.299	2.78977
905	2595.02	32.97058189	-107.5396284	1677.746	2633.560	2635.034	14.2	979205.814	517.752	187.572	979562.929	-26.935	160.637	2.78912
906	2595.05	32.97113491	-107.5399433	1680.075	2633.591	2635.072	14.23	979205.852	518.471	187.832	979562.975	-26.484	161.348	2.7891

907	2595.08	32.97149364	-107.5397923	1681.31	2633.621	2635.113	14.27	979205.893	518.852	187.970	979563.005	-26.230	161.740	2.7891 8
908	2595.09	32.97118899	-107.5392786	1680.215	2633.632	2635.133	14.31	979205.913	518.514	187.848	979562.979	-26.400	161.448	2.7891 4
909	2592.23	32.97075856	-107.5391366	1679.656	2630.723	2632.238	14.37	979203.018	518.342	187.786	979562.944	-29.369	158.416	2.7897 9
910	2591.76	32.97054404	-107.5386171	1671.966	2630.244	2631.773	14.42	979202.553	515.969	186.926	979562.926	-31.331	155.595	2.7899 1
911	2591.85	32.97131081	-107.5385236	1673.968	2630.336	2631.874	14.46	979202.654	516.587	187.150	979562.990	-30.899	156.251	2.7898 4
912	2591.64	32.97166203	-107.5391018	1674.309	2630.122	2631.673	14.51	979202.453	516.692	187.188	979563.019	-31.062	156.126	2.7899 1
913	2591.78	32.97197099	-107.5396556	1676.537	2630.265	2631.827	14.56	979202.607	517.379	187.437	979563.044	-30.494	156.943	2.7899 3
914	2591.42	32.97261267	-107.5393361	1676.972	2629.899	2631.572	15.01	979202.352	517.514	187.485	979563.097	-30.717	156.769	2.7899 1
915	2591.55	32.97265316	-107.538724	1678.009	2630.031	2631.716	15.06	979202.496	517.834	187.601	979563.100	-30.372	157.230	2.7899 8
916	2592.32	32.97198239	-107.538293	1676.186	2630.814	2632.519	15.14	979203.299	517.271	187.398	979563.045	-29.872	157.525	2.7897 2
917	2593.41	32.97140346	-107.5374191	1672.477	2631.923	2633.643	15.2	979204.423	516.126	186.983	979562.997	-29.431	157.552	2.7895 6
918	2597	32.97103578	-107.5367145	1666.821	2635.574	2637.341	15.39	979208.121	514.381	186.351	979562.967	-26.815	159.535	2.7886 5
919	2596.59	32.96613054	-107.5290417	1651.587	2635.157	2636.937	15.44	979207.717	509.680	184.647	979562.562	-29.813	154.834	2.7887 9
920	2595.73	32.96605817	-107.5297244	1653.958	2634.283	2636.079	15.51	979206.859	510.411	184.913	979562.556	-30.198	154.714	2.7889 6
921	2595.73	32.96622531	-107.5300427	1656.142	2634.283	2636.089	15.55	979206.869	511.085	185.157	979562.570	-29.772	155.384	2.7889 6
922	2595.42	32.96621802	-107.5306028	1656.6	2633.967	2635.781	15.58	979206.561	511.227	185.208	979562.569	-29.990	155.218	2.7890 1
923	2595.43	32.966170	-107.5310	1657.1	2633.977	2635.897	16.01	979206.677	511.408	185.273	979562.565	-29.754	155.519	2.7890 7

		42	112	86										
924	2595.87	32.96566443	-107.5308383	1659.811	2634.425	2636.359	16.07	979207.139	512.218	185.567	979562.524	-28.734	156.833	2.7889
925	2594.65	32.96570899	-107.5303194	1658.468	2633.184	2635.158	16.23	979205.938	511.803	185.417	979562.527	-30.203	155.213	2.7892
926	2594.34	32.96791316	-107.5363492	1661.601	2632.869	2634.852	16.27	979205.632	512.770	185.767	979562.709	-30.074	155.693	2.7892
927	2593.83	32.96740932	-107.5358328	1662.026	2632.350	2634.587	17.3	979205.367	512.901	185.815	979562.668	-30.214	155.600	2.7894
928	2594	32.96677145	-107.535877	1663.085	2632.523	2634.523	16.34	979205.303	513.228	185.933	979562.615	-30.016	155.916	2.7893
929	2594.46	32.96674333	-107.5349869	1663.156	2632.991	2634.999	16.37	979205.779	513.250	185.941	979562.613	-29.525	156.416	2.7892
930	2592.34	32.96669423	-107.5342615	1662.921	2630.834	2632.857	16.43	979203.637	513.177	185.915	979562.609	-31.709	154.206	2.7897
931	2591.92	32.96685905	-107.5363901	1674.171	2630.407	2632.440	16.47	979203.220	516.649	187.172	979562.622	-29.926	157.247	2.7898
932	2594.35	32.96647783	-107.5355741	1674.091	2632.879	2634.921	16.51	979205.701	516.624	187.163	979562.591	-27.428	159.735	2.7892
933	2596.36	32.96709735	-107.5333452	1662.39	2634.923	2636.978	16.56	979207.758	513.014	185.855	979562.642	-27.725	158.130	2.7888

Curriculum Vita

Adrián Emmanuel Gutiérrez was born in September 19, 1985 in Ciudad Juárez México. The first child of Noemi Gutiérrez and Carlos Estrada. He obtained his Bachelors degree of Geological Sciences at UTEP (University of Texas at El Paso) in 2010. He worked in the mining industry for a year before he was accepted into the Geophysics graduate program in 2011 at UTEP were he obtained his MS in geophysics in June 2014.

Permanent address: Quinta San Antonio 1109, Quintas del Valle
Ciudad Juárez, Chihuahua, México CP 23545

This thesis was typed by Adrián E. Gutiérrez